

GEMS & GEMOLOGY

VOLUME XXX

SUMMER 1994



THE QUARTERLY JOURNAL OF THE GEMOLOGICAL INSTITUTE OF AMERICA

GEMS & GEMOLOGY

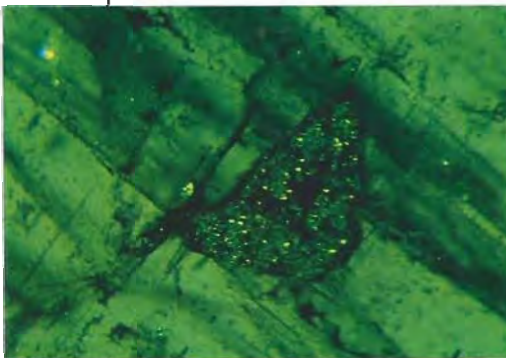
SUMMER 1994

VOLUME 30 NO. 2

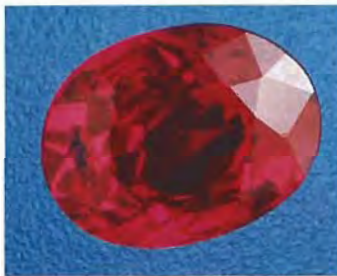
T A B L E O F C O N T E N T S



p. 74



p. 98



p. 114

p. 110



EDITORIAL

- 71 Thank You, Donors

FEATURE ARTICLES

- 72 Synthetic Rubies by Douros: A New Challenge for Gemologists
Henry A. Hänni, Karl Schmetzer, and Heinz-Jürgen Bernhardt
- 88 Emeralds from the Mananjary Region, Madagascar: Internal Features
Dietmar Schwarz

NOTES AND NEW TECHNIQUES

- 102 Synthetic Forsterite and Synthetic Peridot
Kurt Nassau
- 109 Update on Mining Rubies and Fancy Sapphires in Northern Vietnam
Robert C. Kammerling, Alice S. Keller, Kenneth V. Scarratt, and Saverio Repetto

REGULAR FEATURES

- 115 Gem Trade Lab Notes
- 122 Gem News
- 133 Book Reviews
- 135 Gemological Abstracts

ABOUT THE COVER: One of the most prized of colored gems, ruby is used in many forms of jewelry and decorative items. Because of its significance, the importance of differentiating between natural and synthetic material cannot be overemphasized. This issue's cover article deals with a new synthetic ruby—manufactured by Douros Created Gems in Piraeus, Greece—that may present an identification challenge for gemologists.

The fine natural rubies in the contemporary Buccellati chalice and necklace on the cover are integral to these two classic designs. The necklace contains 17 pear-shaped cabochon rubies, totaling 17.69 carats, accented by 34 emeralds and 375 rose-cut diamonds. Thirty-two rubies with a total weight of 9.92 carats adorn the rock-crystal chalice, which also uses 53 emeralds and 513 grams of gold. Courtesy of Buccellati of Beverly Hills, California. The chalice will be on display at the Natural History Museum of Los Angeles County from November 5, 1994 to January 8, 1995, as part of the "Buccellati—Artistry and Gemstones in Gold" exhibit.

Photo © Harold & Erica Van Pelt—Photographers, Los Angeles, CA.

Typesetting for Gems & Gemology is by Graphix Express, Santa Monica, CA. Color separations are by Effective Graphics, Compton, CA. Printing is by Cadmus Journal Services, Easton, MD.

© 1994 Gemological Institute of America All rights reserved ISSN 0016-626X

GEMS & GEMOLOGY

EDITORIAL STAFF

Editor-in-Chief
Richard T. Liddicoat

Associate Editors
William E. Boyajian
Robert C. Kammerling
D. Vincent Manson
John Sinkankas

Technical Editor
Carol M. Stockton

Assistant Editor
Irv Dierdorff

Editor
Alice S. Keller
1660 Stewart St.
Santa Monica, CA 90404
(800) 421-7250 x251

Subscriptions
Gail Young
Jin Lim
(800) 421-7250 x201
Fax: (310) 453-4478

Contributing Editor
John I. Koivula

Editors, Gem Trade Lab Notes
Robert C. Kammerling
C. W. Fryer

Editors, Gem News
John I. Koivula
Robert C. Kammerling
Emmanuel Fritsch

Editors, Book Reviews
Susan B. Johnson
Jana E. Miyahira

Editor, Gemological Abstracts
C. W. Fryer

PRODUCTION STAFF

Art Director
Lisa Joko-Gleeson

Production Assistant
Judith Lynch

Word Processor
Ruth Patchick

EDITORIAL REVIEW BOARD

Robert Crowningshield
New York, NY

Alan T. Collins
London, United Kingdom

Dennis Foltz
Santa Monica, CA

Emmanuel Fritsch
Santa Monica, CA

C. W. Fryer
Santa Monica, CA

Henry A. Hänni
Zurich, Switzerland

C. S. Hurlbut, Jr.
Cambridge, MA

Alan Jobbins
Caterham, United Kingdom

Robert C. Kammerling
Santa Monica, CA

Anthony R. Kampf
Los Angeles, CA

Robert E. Kane
Lake Tahoe, NV

John I. Koivula
Santa Monica, CA

Henry O. A. Meyer
West Lafayette, IN

Kurt Nassau
P.O. Lebanon, NJ

George Rossman
Pasadena, CA

Kenneth Scarratt
Bangkok, Thailand

Karl Schmetzer
Petershausen, Germany

James E. Shigley
Santa Monica, CA

SUBSCRIPTIONS

Subscriptions in the U.S.A. are priced as follows: \$54.95 for one year (4 issues), \$134.95 for three years (12 issues). Subscriptions sent elsewhere are \$65.00 for one year, \$165.00 for three years.

Special annual subscription rates are available for all students actively involved in a GIA program: \$44.95, U.S.A.; \$55.00, elsewhere. Your student number *must* be listed at the time your subscription is entered.

Single issues may be purchased for \$14.00 in the U.S.A., \$17.00 elsewhere. Discounts are given for bulk orders of 10 or more of any one issue. A limited number of back issues of *G&G* are also available for purchase.

Please address all inquiries regarding subscriptions and the purchase of single copies or back issues to the Subscriptions Department.

To obtain a Japanese translation of *Gems & Gemology*, contact the Association of Japan Gem Trust, Okachimachi Cy Bldg., 5-15-14 Ueno, Taito-ku, Tokyo 110, Japan. Our Canadian goods and service registration number is R126142892.

MANUSCRIPT SUBMISSIONS

Gems & Gemology welcomes the submission of articles on all aspects of the field. Please see the suggestions for authors in the Spring 1993 issue of the journal, or contact the editor for a copy. Letters on articles published in *Gems & Gemology* and other relevant matters are also welcome.

COPYRIGHT AND REPRINT PERMISSIONS

Abstracting is permitted with credit to the source. Libraries are permitted to photocopy beyond the limits of U.S. copyright law for private use of patrons. Instructors are permitted to photocopy isolated articles for noncommercial classroom use without fee. Copying of the photographs by any means other than traditional photocopying techniques (Xerox, etc.) is prohibited without the express permission of the photographer (where listed) or author of the article in which the photo appears (where no photographer is listed). For other copying, reprint, or republication permission please contact the editor.

Gems & Gemology is published quarterly by the Gemological Institute of America, a nonprofit educational organization for the jewelry industry, 1660 Stewart St., Santa Monica, CA 90404.

Postmaster: Return undeliverable copies of *Gems & Gemology* to 1660 Stewart St., Santa Monica, CA 90404.

Any opinions expressed in signed articles are understood to be the opinions of the authors and not of the publishers.

THANK YOU, DONORS

The Gemological Institute of America extends its sincerest appreciation to all of the people and firms in 1993 who helped the Institute fulfill its commitment to the industry through donations of "gifts-in-kind"—gems for reference, research, and classroom use, as well as written materials for the Richard T. Liddicoat Gemological Library and Information Center. We are pleased to acknowledge many of you below.*

Sue Adams	Gem Reflections of	New York Chapter, GIA
Adris Oriental Gems & Arts Corp.	California	Alumni Association
Michael Allbritton	The Getty Center for the	Officers
American Association of	History of Art and the	Kusum Naotunne
Crystal Growth	Humanities	Glenn R. Nord
American Pearl Company	Edward Gübelin	OroAmerica
Amsterdam Sauer	Taketoshi Hayakawa	C. M. Ou Yang
Aucoin-Hart Jewelers	Mark P. Herschede, Jr.	Pinky Trading Co.
Barzel Custom Gems & Lapidary	House of Diamonds	Platinum Guild
Wendy Beckerson	Durward Howes III	International (Italia)
G. S. Bhatnagar	Cornelius S. Hurlbut	.Pranda Intergems Co.
Borsheim's	Idaho Opal & Gem Corporation	Rainbow Mineral & Crystal Co.
William E. Boyajian	International Mines Outlet	Stephane Salerno
Bruce Chai	Craig Jackson	Rosa Santorroman
Tom Chatham	E. Alan Jobbins	Scheherazade
Santpal Singh Chawla	Johnson Gems	Service Merchandise
CISGEM	Jonz Jewels	James E. Shigley
Don Clark	Robert C. Kammerling	John Sinkankas
Don Clary	Robert E. Kane	Mauro Souja
Jo Ellen Cole	Christopher Keenan	T. L. C. Gems Company
Commercial Mineral Company	Kimberley Created Emeralds	Louise Thomas
Frances D'Angelo	John I. Koivula	Tuckman International U. S. A.
Frederick Darling	Lee Larson	Doug Turet
De Beers Central Selling Organisation	Lehrer Designs	Bill Underwood
R. Evans Jeweler	Jack Lowell	V.O.I.C.E. of Gold
Farrar Jewelers	Jurgen Maerz	West Coast Semi-Precious Stone
Emmanuel Fritsch	Manning Opal & Gem Co.	Ron Yehuda
C. W. Fryer	Marshall Martin	
	Kay Morrow	
	Pascal Mouawad	*Partial listing

For more information about GIA's Gift-In-Kind Program, please call (800) 421-7250, ext. 208, or from outside the U.S. (310) 829-2991, ext. 208.

SYNTHETIC RUBIES BY DOUROS: A NEW CHALLENGE FOR GEMOLOGISTS

By Henry A. Hänni, Karl Schmetzer, and Heinz-Jürgen Bernhardt

Greek manufacturer J. & A. Douros introduced a new flux synthetic ruby in early 1993. Grown by spontaneous nucleation in a lead-based solvent, the Douros synthetic ruby occurs as rhombohedral single crystals and twinned tabular crystals, as well as in clusters. The tabular crystals typically have intense red cores that gradually decrease in saturation to a near-colorless outermost layer; the rhombohedral crystals have a deep red body and a thin near-colorless layer on the rhombohedral faces, with umbrella-like growth patterns in some areas. Some samples contain distinctive inclusions of yellow residual flux with spherical bubbles. Chemically, the crystals are heavily zoned, and EDXRF analyses revealed variable trace amounts of Ti, Fe, Cr, and Ga, as well as some Pb. SEM-EDS identified the flux particles as lead bearing. Microprobe analyses showed high Cr values in the crystal cores; in certain growth zones, Fe replaces Cr in the outermost layers. If inclusions or typical growth structures are not present, chemical composition appears to be the best means of separating these Douros synthetic rubies from natural rubies.

ABOUT THE AUTHORS

Dr. Hänni is director of SSEF Swiss Gemological Institute, Zurich, and associate professor of gemology at Basel University, Switzerland. Dr. Schmetzer is a research scientist residing in Petershausen near Munich, Germany. Dr. Bernhardt is a research scientist at the Institute for Mineralogy of Ruhr-University, Bochum, Germany.

*Acknowledgements appear at end of article.
Gems & Gemology, Vol. 30, No. 2, pp. 72-86.
© 1994 Gemological Institute of America*

Recently, a new type of flux-grown synthetic ruby entered the gem market (figure 1). Manufactured by J. & A. Douros Created Gems in Piraeus, Greece, the Douros synthetic ruby poses new challenges for gemologists. Like the Ramaura flux-grown synthetic rubies introduced in 1982 (Bosshart, 1983; Kane, 1983), stones faceted from the Douros laboratory-grown crystals may create considerable difficulties for identification. Standard gemological tests are inadequate for clean or only slightly included samples. Even with advanced tests such as U.V.-visible spectrophotometry, EDXRF chemical analysis, or identification of growth planes, the present material may cause difficulties in identification (see, e.g., Hänni and Bosshart, 1993; Hänni and Schmetzer, 1993; and Smith and Bosshart, 1993).

This article reports on our examination of several crystals and faceted samples of the Douros material. To help establish criteria by which the Douros synthetic rubies can be separated from their natural counterparts, we will describe in detail the mineralogical, gemological, and chemical characteristics of this new flux-grown synthetic ruby.

PRODUCTION

Brothers John and Angelos Douros run a small family business that manufactures synthetic crystals. A physicist and an electrical engineer, respectively, they previously specialized in refining precious metals. With furnaces they built themselves, the Douros brothers use controlled spontaneous nucleation and slow cooling techniques to produce synthetic rubies by unseeded flux growth (J. Douros, pers. comm., 1993).

After some years of experimentation, in January 1993 they presented the material to the public for the first time, at the Athens Jewellery Fair. Simultaneously, they reported on their new synthetic ruby in the Greek jewelry magazine *Chrysotechni* (Douros and Douros, 1993).

At present, the Douros brothers use two furnaces in



Figure 1. This 44.74-ct rhombohedral crystal and the accompanying cut stones (from left to right—4.93, 2.55, 2.14, and 3.51 ct) are representative of some of the Douros flux-grown synthetic rubies that have been produced to date. Samples courtesy of John Douros, Piraeus, Greece; photo by Robert Weldon.

which exact temperature control permits very slow cooling and, thus, steady crystal growth that incorporates the chemical constituents needed to duplicate natural ruby as closely as possible (J. Douros, pers. comm., 1993). They dope the flux with various trace elements in their effort to reproduce the different shades of color and trace-element compositions encountered among natural rubies. As is typically the case with flux-grown synthetics, the production costs are significantly higher than for synthetic ruby crystals produced by the Verneuil or Czochralski methods. The Douros flux method typically yields crystals up to 20 to 50 ct; the largest crystal produced to date is 70 grams (350 ct) and the largest faceted stone, 8.5 ct. In June 1994, John Douros reported that they were producing approximately 2,000 ct per month, but expected this quantity to increase. The precise conditions of growth and composition of the flux are proprietary and were not revealed to the authors. The material is being sold through various channels.

MATERIALS AND METHODS

For this study, we obtained 12 synthetic ruby crystals (2–17 ct) and 10 faceted synthetic rubies (1–5 ct) directly from the Douros brothers. To best examine the inclusions, we polished one or two faces on some of the crystals.

For gemological testing, we used a Topcon refractometer with a sodium light source, a Mettler

balance with specific-gravity attachment, a Zeiss Jena 7° dispersion spectroscope with Eickhorst base, a standard ultraviolet lamp (long-wave and short-wave) with dark box, a Schneider immersion microscope with Zeiss optics, and a Wild Stereozoom microscope with Eickhorst Multiscope base. We used methylene iodide as the immersion liquid (with a special sample holder) for examination and photomicrography of the samples.

Polarized absorption spectra for the e- and o-vibrations were recorded on two crystals, one crystal slice, and one faceted sample. We used Hitachi 4001 and Pye-Unicam SP8-100 spectrophotometers with polarization filters, the crystals oriented with the c-axis perpendicular to the incident beam (see, e.g., Bosshart, 1982). Qualitative chemical investigations, by energy-dispersive X-ray fluorescence analysis (EDXRF; see, e.g., Stern and Hänni, 1982; Muhlmeister and Devouard, 1991), were performed on 13 samples (as well as, subsequently, on sections cut and polished from two of these samples) using a Philips PV 9500 X-ray generator and detectors with a Spectrace TX-6100 system and software package. Quantitative chemical analyses were performed on seven of the same samples with a CAMECA Camebax SX 50 electron microprobe. The electron microprobe analyses (EPMA) included 30 point analyses on table facets of three faceted synthetic rubies and on a rhombohedral face of one rhombohedral crystal, as well as 30 point analyses on the



Figure 2. The 10.37-ct tabular crystal (inset), two rhombohedral crystals (44.74 and 13.69 ct), and 167.97-ct crystal cluster shown here represent the Douros crystals observed thus far. Photo by Robert Weldon. Inset photo by Maha DeMaggio.



two new surfaces produced when an irregular intergrowth of two rhombohedral crystals (samples D1 and D2) of random mutual orientation was sawn and polished. For the microscopic examination of one of the tabular crystals (to obtain a cross-section between the two basal pinacoids), we had a slice cut perpendicular to the basal pinacoid *c*. Three microprobe scans of 50 point analyses each were performed on this 2.2-mm-thick polished slab on the surface at the cross-section.

A Philips scanning electron microscope (SEM 515) with a Tracor energy-dispersive X-ray spec-

trometer (EDS) system was used to investigate the surfaces of one rough and one cut Douros synthetic ruby in order to identify the chemical components of yellow material and metallic particles on those surfaces. We also submitted some of the yellow material removed from the surface of one of the crystals to X-ray powder diffraction analysis with a Gandolfi camera.

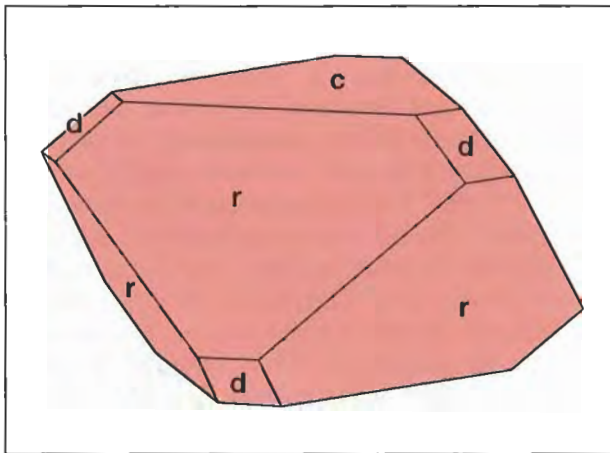
CRYSTALLOGRAPHY

The Douros flux-grown synthetic ruby crystals occur in two habits: rhombohedral (see, e.g., figures 1–3) and tabular (figures 2 and 4). There are also crystals intermediate between these two basic types as well as intergrown clusters (figure 2). In all the samples we examined, we noted that only three crystal faces are developed: the basal pinacoid *c* (0001), the positive rhombohedron *r* ($10\bar{1}1$), and the negative rhombohedron *d* ($01\bar{1}2$). Trigonal growth structures were typically seen on rhombohedral and tabular crystals alike (again, see figure 2).

As illustrated in figure 3, the rubies with tabular habit have a dominant basal plane *c*; the rhombohedral faces *r* and *d* are small. Occasionally, they also show small, colorless "satellite" corundum crystals that have intergrown with the main crystal; rarely, metallic flakes of platinum (from the crucible; figure 5) or a yellow material (figure 6) are found on the surface.

Most of the tabular crystals are penetration twins, with the two components symmetrically related by a 180° rotation about the *c*-axis. This twinning is identical to a reflection across one of

Figure 3. As is evident in this schematic drawing of a rhombohedral crystal of Douros synthetic ruby, three crystal faces are well developed: the dominant basal plane *c* (0001), the positive rhombohedron *r* ($10\bar{1}1$), and the subordinate negative rhombohedron *d* ($01\bar{1}2$).



the first-order hexagonal prism faces $(10\bar{1}0)$ or across the basal pinacoid (0001) . The two components of the twinned individuals are in contact along four twin boundaries, which are oriented parallel to the twin planes $(10\bar{1}0)$ and (0001) , respectively (figure 4; see, e.g., Schmetzer et al., 1994).

The rhombohedral crystals are more equidimensional and thus better suited for cutting. They are basically formed by dominant basal and rhombohedral faces, c and r , with somewhat smaller d faces (again, see figure 3). We did not see prism faces on any of our samples, but we did see small hexagonal dipyramids $n(22\bar{4}3)$ on one crystal. We did not observe twinning in any of the rhombohedral crystals.

These two habits of Douros synthetic rubies are similar to those described for Ramaura flux-grown synthetic rubies (Kane, 1983; Schmetzer, 1986a and b). The penetration twinning seen in the Douros synthetic rubies is identical to that commonly seen in Ramaura synthetic rubies (as described in Schmetzer et al., 1994), but different from twinning in other flux-grown synthetic rubies, such as those produced by Chatham Created Gems. However, whereas we observed twinning only in tabular Douros crystals, most twinned Ramaura synthetic ruby crystals observed up to now are of rhombohedral habit.

Figure 5. A small satellite crystal and a shiny grain of platinum (from the crucible) can be seen on the surface (basal face c) of this tabular crystal. The crazed orange area is enclosed flux that lies below the surface. Magnified 50 \times .

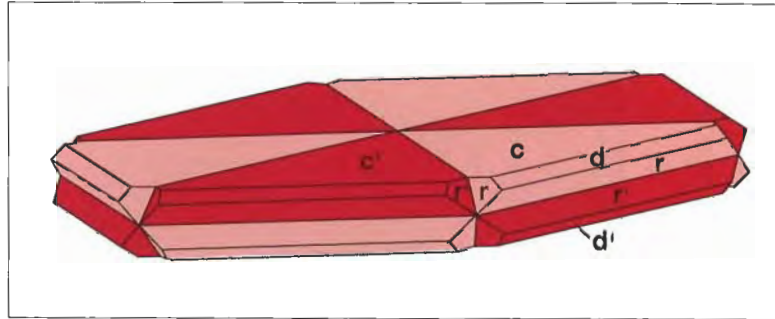
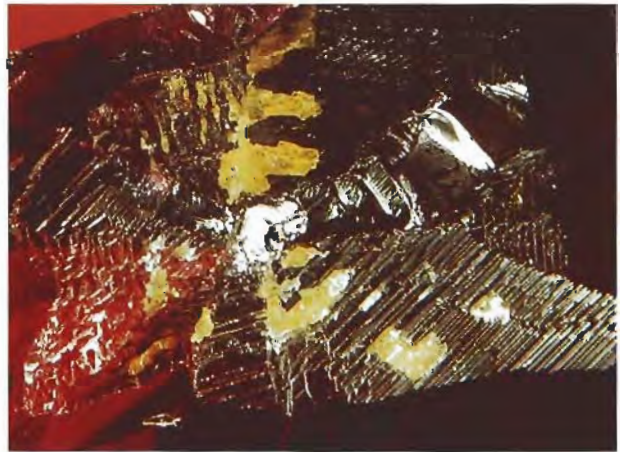


Figure 4. This schematic drawing of a tabular Douros synthetic ruby crystal shows the dominant c planes and the subordinate r and d faces. The sample illustrated is actually a penetration twin, which is frequently encountered in this material. The second crystal is denoted by the darker color and its relative faces marked c' , r' , and d' .

COLOR AND COLOR ZONING

The samples ranged from saturated red to purplish red and reddish purple (see, e.g., figures 1 and 2), depending on the amounts of chromium, titanium, and iron present in each. The different concentrations of color-causing trace elements also produced geometrically bounded color zoning within the crystals. In the tabular crystals only, we noted: (1) near-colorless to light red outermost zones confined to r and d faces (figure 7); (2) near-colorless to light red triangular growth sectors confined to twin boundaries (figure 8); and (3) purple to bluish purple color bands running parallel to both rhombohedral faces r and d (figure 9). In both the rhombohedral and tabu-

Figure 6. On the surfaces of some of the crystals, we saw pits filled with a yellow polycrystalline material. Magnified 6 \times .



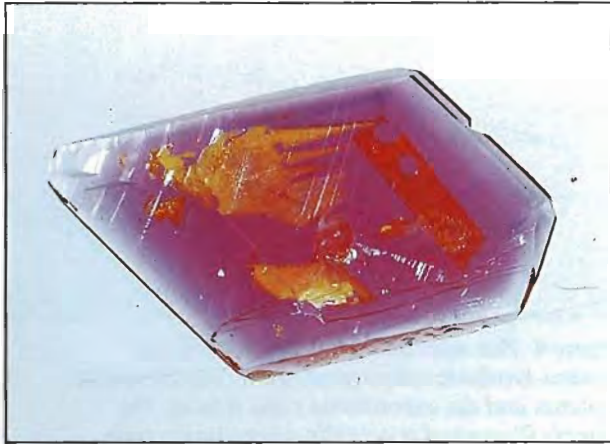


Figure 7. This 34-mm-diameter tabular Douros synthetic ruby crystal exhibits the near-colorless outermost zone typical of this form. Note also the large pieces of yellow flux that have been trapped in the crystal. The flux is typically oriented parallel to the basal face.

lar crystals, we saw purple to bluish purple intercalated acute-angle triangles (figures 9 and 10). The purple to bluish purple bands and triangular zones represent a distinct blue-sapphire component within the synthetic ruby (cf. Schmetzer and Bank, 1981).

GEMOLOGICAL PROPERTIES

Table 1 gives the gemological properties for the 10 faceted Douros synthetic rubies and 12 crystals (eight rhombohedral and four tabular). Because R.I.

Figure 9. Purple to bluish purple color bands (like the one shown here in the lower part of the photo) were occasionally seen in tabular Douros synthetic ruby crystals, as were acute-angle purple to bluish purple triangular growth zones (like the one seen here in the lower left). A distinct iron/titanium component, in addition to the chromium component of ruby, is responsible for this color zoning. The inclusions shown here are flux. Magnified 10 \times .

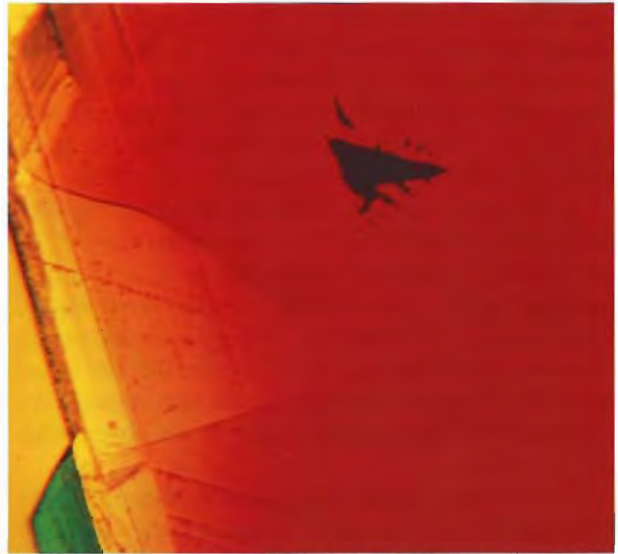


Figure 8. On the edge of a tabular crystal, a near-colorless to light red triangular growth sector is confined to twin boundaries. Immersion, magnified 25 \times .

and density readings overlap those of natural rubies, they are not useful in identifying this material as synthetic. Note, however, that the R.I.'s measured on the rhombohedral faces of rhombohedral crystals are somewhat lower than the values obtained from the basal pinacoids. The latter correspond to the R.I.'s of the faceted samples. The basal-pinacoid R.I.'s of the tabular crystals were similar to those from rhombohedral faces of the rhombohedral crystals. On a plane cut perpendicular through the basal pinacoids of a tabular crystal, no distinct readings could be obtained. These differences in R.I. are undoubtedly related to differences in chemical composition—especially the differential incorporation of chromium (which tends to increase R.I.)—between the body of the crystal and its outermost layers.

The strong red fluorescence to ultraviolet radiation (more pronounced to long-wave) of the faceted Douros synthetic rubies is characteristic for low iron-bearing rubies, so it cannot be used to identify the synthetic material. The absence of fluorescence in some of the outermost areas of the Douros crystals appears to be due to the selective chemistry on the faces (see below) and, again, to the lower chromium content in the outermost layers. The resulting appearance of the crystals has been described as a layer of yellowish orange fluorescence on some of the outside faces to long-wave U.V. radiation, or a moderate to strong whitish blue fluorescence to short-wave U.V. Because these inert to pale-colored



portions of the crystals are generally removed during cutting, the fluorescence of the faceted Douros synthetic rubies is typically a uniform red.

MICROSCOPIC CHARACTERISTICS

Structural Properties (Growth Features and Twinning). The internal growth features of both the rough and the faceted Douros samples correspond to the external morphology of the crystals. We identified internal growth planes parallel to all three macroscopically observed crystal faces *c*, *r*, and *d*. Although similar growth planes are also found in Ramaura and Chatham flux-grown synthetic rubies (Schmetzer, 1987), there are three types of growth patterns that appear to be most characteristic of rhombohedral Douros synthetic rubies (table 2).

In most of the rhombohedral crystals, we recognized a growth pattern that is evident as areas of different colors with sharply defined boundaries. The main body color between the basal planes is intense red, whereas the thin outermost layers confined to the *r* and *d* faces are near-colorless to light red (figure 11). These outer layers represent the latest growth stage.

All of the rhombohedral crystals showed faces parallel to the negative rhombohedron *d*. Such faces were prominent (although smaller than *c* and *r*) on the actual surface of the crystals, which represents the latest growth period. In earlier stages of growth (i.e., more toward the center of the crystal) the *d*



Figure 10. Acute-angle color zoning was also seen in rhombohedral Douros synthetic ruby crystals. Compare the appearance of the zone in this sample with that in the tabular Douros crystal in figure 9. Again, the bluish purple color is due to (Fe,Ti)-rich zones within the ruby crystal. Immersion, magnified 40 \times .

faces were smaller. In the earliest growth stage, in the center of the crystal, growth parallel to *d* was absent, and the surface of the crystal at that stage was defined just by *r* and *c* faces. When a rhombohedral Douros synthetic ruby crystal was viewed with immersion in the microscope, in most cases the area confined to *d* growth showed a distinct, curved, umbrella-like outline, because this part of the crystal has a higher saturation of red compared to neighboring zones (figure 12). In some cases, the

TABLE 1. Gemological properties of Douros synthetic rubies.^a

Property	Rhombohedral crystals	Faceted samples	Tabular crystals
Density (g/cm ³)	3.993 – 4.010	3.997 – 4.015	4.023 – 4.029
Refractive indices	Basal pinacoid <i>c</i> : <i>n</i> _o 1.771 – 1.773 <i>n</i> _e 1.763 – 1.765 Pos. rhombohedron <i>r</i> : <i>n</i> _o 1.768 – 1.770 <i>n</i> _e 1.760 – 1.762	<i>n</i> _o 1.772 – 1.774 <i>n</i> _e 1.762 – 1.764	Basal pinacoid <i>c</i> : <i>n</i> _o 1.768 – 1.771 <i>n</i> _e 1.760 – 1.763 Plane cut and polished perpendicular to <i>c</i> : no distinct reading
Pleochroism			
I _{lc}	Yellowish red to red	Yellowish red to red	Yellowish red to red
I _{lc}	Purplish red	Purplish red	Purplish red
Fluorescence			
LWUV	Intense orangy red, inert in the surface layer confined to <i>r</i> and <i>d</i>	Intense red	Intense orangy red, inert in the surface layer confined to <i>c</i> , <i>r</i> , and <i>d</i>
SWUV	Moderate red, inert in the surface layer confined to <i>r</i> and <i>d</i>	Moderate red	Moderate red, inert in the surface layer confined to <i>c</i> , <i>r</i> , and <i>d</i>

^aAs recorded for eight rhombohedral crystals, 10 faceted samples, and four tabular crystals.

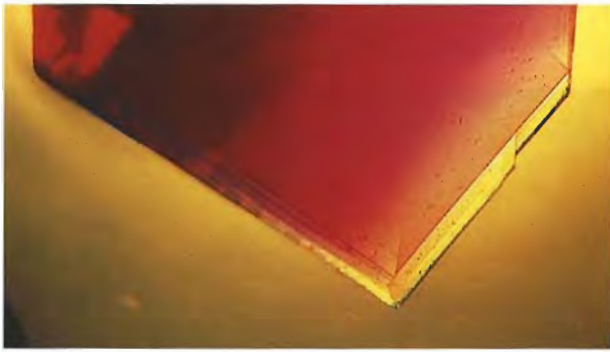


Figure 11. The thin outermost layers confined to the *r* and *d* faces that form the sharp edge of this rhombohedral crystal are near-colorless to light red. Note that there is no colorless layer on the basal faces (here, upper right and upper left). Immersion, magnified 25 \times .

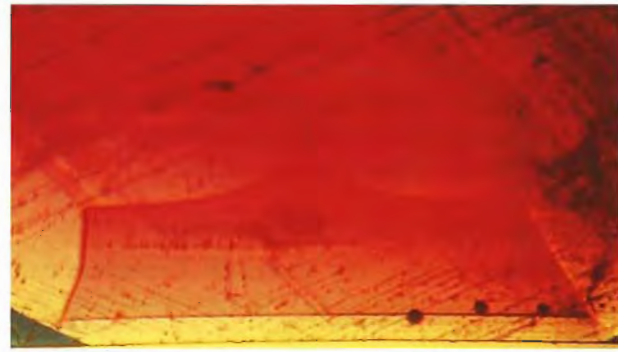


Figure 12. The growth sector formed by *d*-face growth (at the bottom of the picture) in this rhombohedral crystal is defined by a distinctive umbrella-like boundary toward the neighboring *r* and *r'* face growth areas. Immersion, magnified 40 \times .

d-face growth zones were confined to the outer areas of the crystal; the intermediate and central areas showed only growth parallel to *c* and *r* faces (figure 13).

Also in the rhombohedral crystals, as noted earlier, we occasionally saw acute-angle purple to

bluish purple triangles that lie in the red core (again, see figure 10). These areas undoubtedly contain a distinct blue sapphire (Fe, Ti) component in addition to the Cr content responsible for the ruby coloration.

In the tabular crystals, growth patterns includ-

TABLE 2. Crystallography, structural properties, and color zoning in Douros synthetic ruby crystals.^a

Property	Rhombohedral crystals	Tabular crystals
Faces		
Basal pinacoid <i>c</i> (0001)	Dominant	Dominant
Pos. rhombohedron <i>r</i> (10 $\bar{1}$ 1)	Dominant	Subordinate
Neg. rhombohedron <i>d</i> (01 $\bar{1}$ 2)	Subordinate	Subordinate
Hexagonal dipyramid (2243)	Extremely small (in one sample)	Not observed
Twinning	Not observed	Penetration twinning
Growth patterns, color, color zoning		
<i>c</i> faces	Growth patterns present from the center to the surface; red; no color zoning, no boundary	Growth patterns present from the center to the surface; red in the center, continuous decrease in saturation toward the surface, and almost colorless in the outermost layer
<i>r</i> faces	Growth patterns present from the center to the surface; red; no color zoning from the center to a distinct boundary near the surface, with the outermost zone almost colorless	Growth patterns present from the center to the surface; red in the center, continuous decrease in saturation toward the surface, and almost colorless in the outermost zone
<i>d</i> faces	Growth patterns not present in the center, but begin to develop toward the surface; darker red (umbrella-type) growth structure; no color zoning from the beginning to a distinct boundary near the surface, with the outermost zone almost colorless	Growth patterns present from the center to the surface; dark red in the center, with a continuous decrease in saturation toward the surface; almost colorless in the outermost zone
Undetermined faces	Intercalated acute-angle purple to bluish purple triangles present	Intercalated acute-angle purple to bluish purple triangles present

^aAs observed in eight rhombohedral and four tabular crystals examined.

ed both regular and irregular distributions of color (again, see table 2). As a rule, there was no color zoning in the cores, and the outermost areas tended to be light red or near-colorless (again, see figure 7). The slice cut parallel to the *c*-axis of a twinned tabular crystal (on which microprobe analysis was also done) exhibits a rather complex growth pattern (figure 14). From the upper to the lower surface (i.e., from the *c* to the *-c* face), growth zones parallel to *c*, *r*, *d*, and *-c* can be seen. Both of the growth zones parallel to *c* and *-c* are colorless or light red on the surface. The color saturation increases toward the center of the crystal, which is saturated red. Growth areas confined to faces *r* and *d* are intense red in the center of the crystal, but they decrease in saturation in a direction parallel to the length of the slab, that is, toward the surfaces formed by the *r* and *d* faces. The outer zones of these areas are light red, merging to near-colorless next to the surface of the crystal. In the slice examined, the *d* growth zones are a more intense red than the adjacent *r* zones. This feature was also found in the rhombohedral crystals examined.

Purple to bluish purple acute-angle zones were also observed in some of the tabular crystals; bands of similar color were seen in planes parallel to the rhombohedral faces (again, see figure 9). These represent areas rich in Fe and Ti.

Growth patterns of penetration twins on tabu-

Figure 13. This rhombohedral Douros synthetic ruby crystal also revealed an umbrella-like growth sector confined to *d* (intense red) as well as *r* and *r'* (light red), but the central part of the crystal shows only *r* and *r'* growth. Immersion, crossed polarizers; magnified 50 \times .

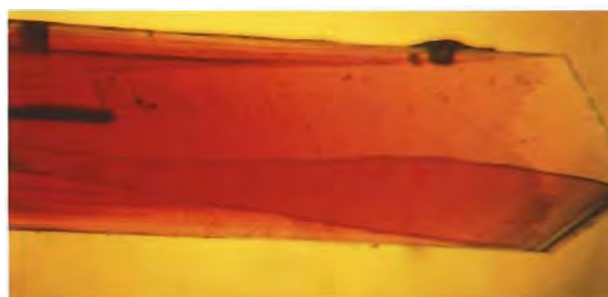
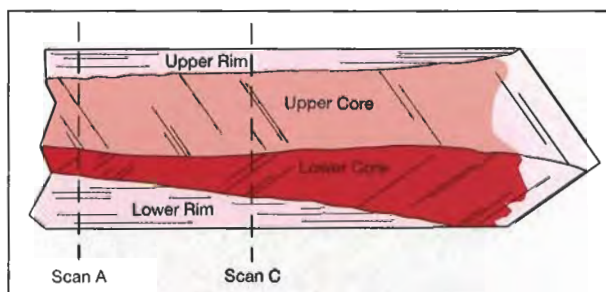
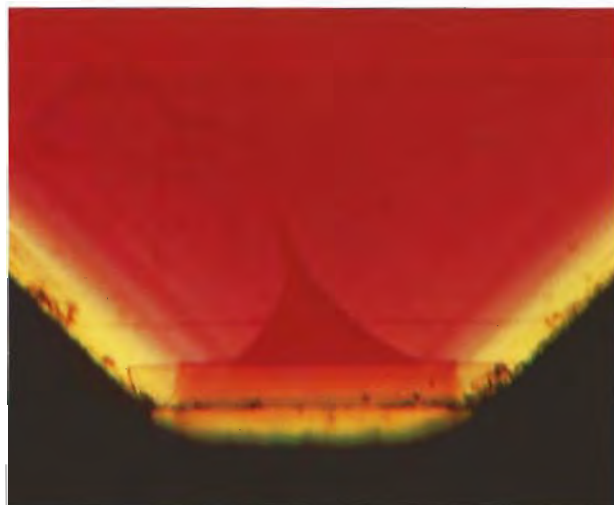


Figure 14. As illustrated in the line drawing, this slice from a tabular crystal cut parallel to the *c*-axis shows the large *c* (upper) and *-c* (lower) faces, as well as the *r* and *d* faces that form the edge of the crystal. Internal growth zoning is accentuated here due to differences in trace-element chemistry. The darkest red zone is confined to the *d*-growth area. Immersion, magnified 25 \times . The positions of the two paths of microprobe point analyses (A and C) are shown in the schematic drawing. (Path B was located between paths A and C.)

lar crystals may be extremely complex in areas confined to one of the four boundaries of the synthetic ruby. In general, the differences are so subtle that these patterns are not useful to discriminate between natural and synthetic rubies. Therefore, synthetic stones faceted from these areas cannot be separated from natural ruby on the basis of growth structures alone.

We did not see colorless outer zones in any faceted samples, which indicates that this characteristic growth feature is removed during cutting. In two or three faceted samples, we saw part of the umbrella-type growth pattern, which indicates that they had been cut from crystals with rhombohedral habit. In one case, we found an irregularly outlined *d* growth zone in a "distorted" umbrella pattern (figure 15). Note that these zones become smaller toward the interior of the crystal. Therefore, it is possible that some Douros synthetic rubies cut from the cores of rhombohedral crystals might also lack any distinctive structural patterns. See Schmetzer (1986a



Figure 15. Structural characteristics are not always easy to recognize. Note this "distorted" umbrella pattern found in a faceted Douros synthetic ruby. These peculiar growth structures, with r, d, and r' sectors, were observed in immersion at 50× magnification.

and b) and Kiefert and Schmetzer (1991) for more on the method to identify growth planes.

Inclusions. Although many of the faceted samples appeared to be free of distinctive inclusions even at 40× magnification, some showed evidence of residual flux similar to that seen in other flux-grown synthetic rubies. Such inclusions may occur as larger, individual pieces of flux or as "veils" formed by many tiny droplets of flux. The former actually consist of coarse, rounded to elongated cavities that have been filled with a typically yellow substance and contain one or more voids or bubbles. Note that, in small amounts, the flux appears near-colorless; when present in larger volumes, the flux not only looks yellow but also reveals a distinctive crazed appearance and forms a mosaic-like pattern (figure 16). Occasionally, the flux inclusions are oriented parallel to the basal pinacoids, especially in twinned tabular crystals. In rhombohedral crystals, we have seen flat flux-containing inclusions oriented parallel to the rhombohedral faces.

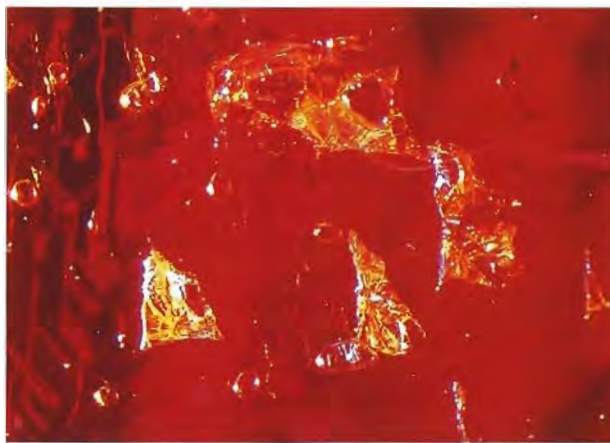


Figure 16. These pieces of yellow flux seen near the surface of a Douros synthetic ruby crystal are actually crazed residual fillings. Note the mosaic-like pattern of the flux, as well as the rounded voids or bubbles. Magnified 25×.

We saw rounded bubbles in nearly all of these flux inclusions (figure 17). Burch (1984) described similar two-phase inclusions for Kashan synthetic rubies. Most coarse flux is, as a rule, encountered near the surface of the crystals; that is, it was enclosed during the latest growth period.

The veil type of flux inclusion seen in the Douros synthetic rubies we examined (figure 18) looks very similar to patterns seen in heat- (and "borax-") treated natural ruby, which now represent most of the natural rubies encountered in the trade. Some of the flux particles are transparent, usually containing a bubble (figure 19).

Figure 17. This large piece of flux in a Douros synthetic ruby has a distinctive mosaic pattern and contains two bubbles. The fine lines—or "crazing"—in the solid part of the inclusion help distinguish such inclusions from two-phase inclusions that might be seen in a natural ruby. Immersion, magnified 25×.



For the most part, the Douros faceted synthetic rubies we examined were very clean, only slightly included, or the inclusions present resembled those seen in natural rubies (figure 20). They did not have platinum platelets or blades.

Optical Spectroscopy. The absorption spectra we observed with gemological desk-model spectrometers do not differ from those of natural or synthetic rubies that have no (or little) iron content. That is, the Douros synthetic rubies show the well-known absorption lines in the red and blue regions of the spectrum, as well as the typical red fluorescence lines due to chromium.

The spectrophotometer results in the ultraviolet-visible range are also characteristic for rubies with Cr-only spectra (figure 21). Absorption minima for a typical sample lie at 328 and 471 nm for the o-vibration and at 328 and 481 nm for the e-vibration. Absorption maxima (i.e., broad bands) are centered at 410 and 560 nm for the o-vibration and 400 and 545 nm for the e-vibration. General absorption in the ultraviolet region is at 290 (e) and 280 nm (o), respectively. There were no significant differences in spectra among the various crystals or faceted samples.

When we calculated the spectral characteristics as proposed by Bosshart (1982), we determined typical values of λ_o and λ/W as 328/6.5 for the o-vibration and 326/5.8 for the e-vibration. These values overlap those for both Knischka synthetic rubies

Figure 18. This veil-like inclusion in a faceted Douros synthetic ruby looks very similar to the networks of interconnecting channels seen in heat- (and "borax-") treated natural rubies. Magnified 50 \times .



Figure 19. These small flux inclusions, in parallel alignment, are transparent. Note that each contains a prominent bubble, which appears in high relief against the flux. The flux itself shows low relief against the ruby, which indicates that its refractive index is close to that of the ruby. Magnified 50 \times .

and natural rubies from Mogok. The minor spread of the plotting points within the Douros material is probably due to the trace-element variations encountered among different samples. Therefore, for the material examined so far, this method will not provide adequate distinction from natural rubies.

Chemistry. The EDXRF spectra showed the presence of chromium, titanium, and iron in varying

Figure 20. The presence of a fissure composed of tiny droplets, like that seen in this faceted Douros synthetic ruby, is of no help to a gemologist working only with a microscope. Such a pattern could also be seen in a natural ruby. Magnified 50 \times .



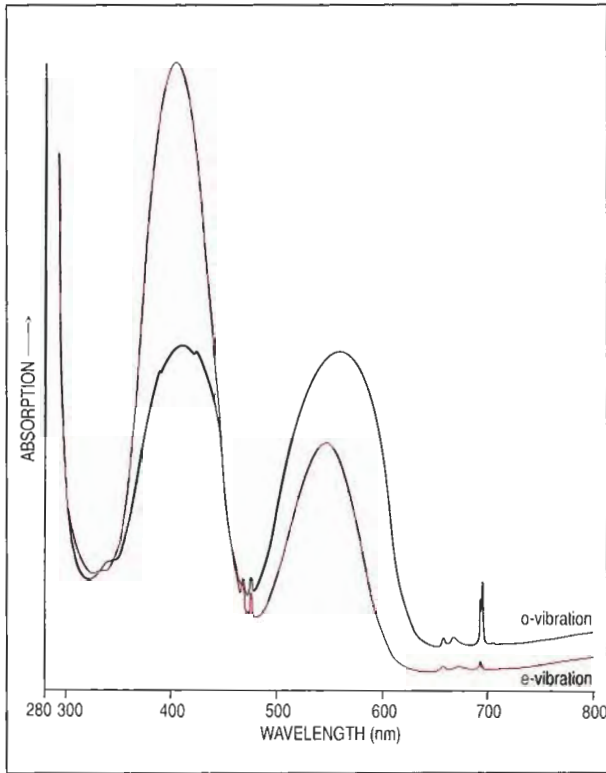


Figure 21. The U.V.-visible absorption spectra of the Douros synthetic rubies are similar to those of some natural rubies. These representative absorption spectra were taken with a Pye-Unicam SP8-100 spectrophotometer with polarization filter on a slice cut from a tabular Douros crystal. The sample was oriented with the *c*-axis perpendicular to the incident beam.

amounts (figure 22). In some cases, chromium peaks were dominant and only small amounts of iron were found. In other samples, distinct concentrations of both iron and chromium were observed. We noted the following variability in the peak heights for the prominent color-causing trace elements, iron and chromium (the letters in parentheses are keyed to the individual spectra in figure 22):

- Fe > Cr on *c* faces of tabular crystals (A)
- Fe > Cr on *r* faces of rhombohedral crystals (B)
- Fe < Cr on *c* faces of rhombohedral crystals (C)
- Fe < Cr on faceted stones (similar to C)

Titanium concentrations were always low, if present at all, and vanadium was at or below the detection limit of the instrument. Gallium signals were usually prominent.

The variability in, or absence of, certain color-causing elements (Ti, V, Cr, Fe) may be typical for Douros synthetic rubies. Most of the EDXRF spectra also indicated the presence of lead, which both

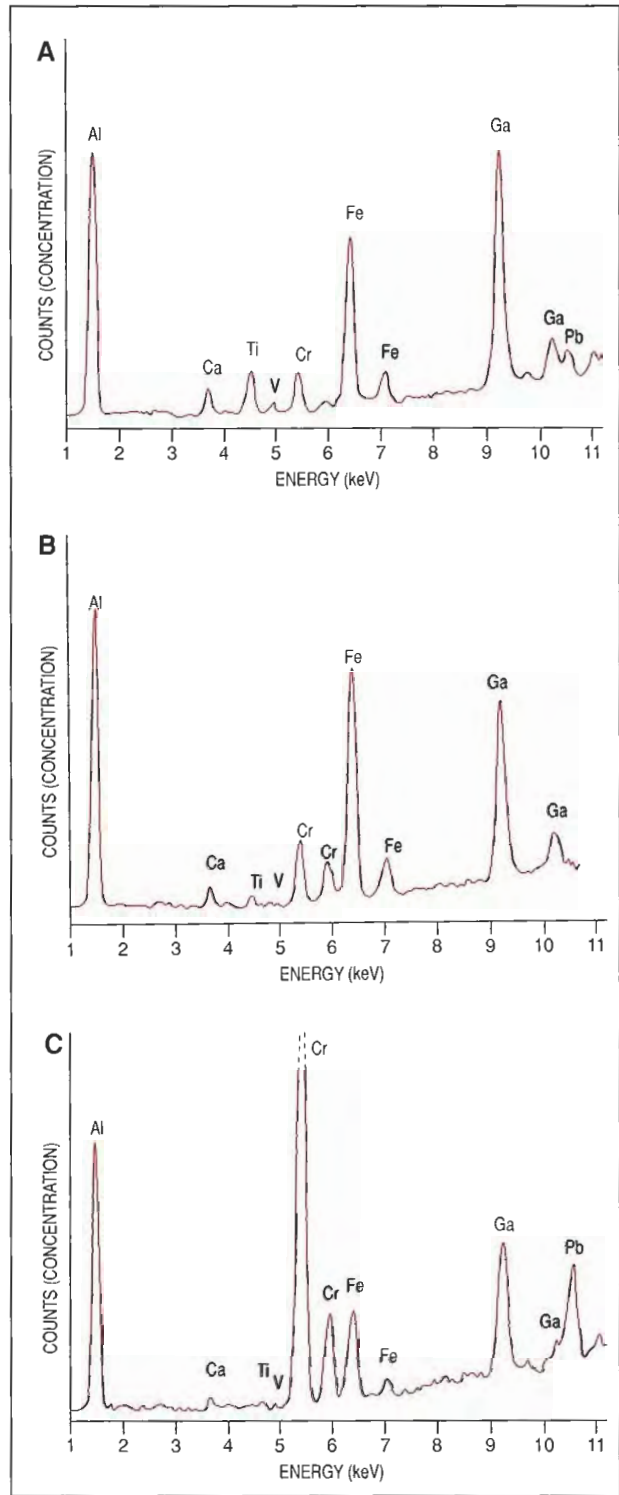


Figure 22. The variability in trace elements in the outermost layers of Douros crystals is evident in these EDXRF spectra of three samples: (A) a tabular crystal with Fe > Cr measured on the *c* face; (B) a rhombohedral crystal with Fe > Cr measured on the *r* face; and (C) a rhombohedral crystal with Fe < Cr measured on the *c* face. This last spectrum is also typical for faceted samples.

SEM-EDS and X-ray diffraction analyses (see below) showed to be a component of the flux used in the growth process. Even in those cases where flux inclusions cannot be seen with high magnification, EDXRF analysis sometimes reveals the presence of Pb peaks as evidence of submicroscopic particles of flux.

EDXRF analysis did not reveal traces of either platinum or iridium (from the crucible) or of lanthanum or bismuth. The latter are typical components of the flux used to grow Ramaura synthetic rubies (Schmetzer, 1986a; Schmetzer et al., 1994).

The quantitative data provided by the microprobe analyses (see Dunn, 1977) revealed only a limited chemical variation within each of five of the six rhombohedral rubies analyzed (three crystals and three faceted samples; table 3). The faceted samples (A, B, and C), as well as the intergrown crystals (D1 and D2), showed distinctly more chromium than iron. In contrast, iron was found to surpass chromium (present in very small amounts) on the rhombohedral face *r* of rough sample E, which was a typical "ruby" red color and had an ordinary chromium absorption spectrum. This indicates a selective compositional zoning with respect to different crystal faces, as well as between late-stage growth layers and the cores, in the rhombohedral crystals. It is consistent with the color zoning observed in the crystals.

Sample D1 showed a distinct zoning with respect to chromium, in the form of a compositional discontinuity between the two parts of the crystal. We recorded Cr₂O₃ values between 0.65 and

0.55 wt.% in the main part, and only 0.18 to 0.10 wt.% in the narrow outermost layer. There was no comparable zoning for iron. This zoning of chromium is consistent with the observation of dark red cores and lighter red or nearly colorless rims in the rhombohedral crystals (figure 11). Since the surface layers are typically thin, they are usually removed during cutting.

The results of microprobe analysis of the slice cut from a tabular crystal are given in table 4. The central part of the crystal (again, see figure 14) consists of two areas of different chromium content. In both areas, which are designated "upper core" and "lower core" in figure 14 and table 4, iron content is low. However, we found no distinct pattern to the distribution of iron and chromium within either core. In contrast, we measured a high variation in chromium and iron contents in the upper and lower surface layers: In both, chromium progressively decreased—and iron progressively increased—from the core side to the surface side. A substitutional exchange of Cr by Fe in these growth zones is evident. We could not detect a systematic variation of titanium in the same scans. We also found that the chromium content decreases from the center (scan A) to the outer zone (scan C) of the crystal (table 4). The data obtained from scan B are intermediate between those of scans A and C.

Scanning Electron Microscopy and X-Ray Diffraction Analysis. SEM-EDS analysis of the residual yellow flux exposed at the surface of some faceted samples showed characteristic X-ray fluo-

TABLE 3. Electron microprobe analyses of five Douros synthetic rubies.^a

Oxide	A		B		C		D			E
	Faceted (4.21 ct)		Faceted (1.31 ct)		Faceted (1.18 ct)		Intergrowth of two rhombohedral crystals (3.48 ct)			Rhombohedral crystal (7.57 ct) <i>r</i> face
							Crystal D1		Crystal D2	
							Core	Surface layer	Core	
Al ₂ O ₃	97.23–98.04	98.12–98.63	97.56–98.29	98.12–98.42	98.68–98.08	97.83–98.64	97.95–100.29			
TiO ₂	0.00–0.03	0.01–0.05	0.00–0.03	0.00–0.02	0.00–0.02	0.00–0.02	0.01–0.07			
Cr ₂ O ₃	0.79–0.96	0.60–0.70	0.77–0.99	0.55–0.65	0.10–0.18	0.47–0.75	0.01–0.04			
Fe ₂ O ₃	0.03–0.07	0.04–0.09	0.09–0.16	0.03–0.07	0.05–0.08	0.03–0.08	0.13–0.34			
MnO	0.00–0.02	0.00–0.02	0.00–0.01	0.00–0.02	0.00–0.01	0.00–0.02	0.00–0.01			

^aOxides in wt.%; ranges of 30 point analyses performed on each sample. Vanadium was below the detection limit; gallium was not measured.

rescence lines for lead (figure 23). A silvery metal grain on the surface of one crystal (again, see figure 5) proved to be platinum, probably from the crucible.

An X-ray powder diffraction pattern was prepared from some of the yellow material removed from the surface of one of the crystals (see, e.g., figure 6). The pattern revealed that the material was lead nitrate, $PbNO_3$, which undoubtedly formed from the lead-bearing flux on the surface of the crystal when it was separated from the flux in nitric acid, HNO_3 .

DISCUSSION

The present investigation indicates that the new Douros synthetic rubies occur in essentially two types of crystals—(1) rhombohedral and (2) tabular—which differ in habit, structural properties, and compositional characteristics. These two types probably result from the different temperature conditions that occur during the slow cooling that is part of the crystallization process from a flux. The ideal early growth conditions favor the formation of a rhombohedral crystal habit with c and r faces. When supersaturation decreases, and when the temperature starts to drop, new physical and chemical conditions favor the formation of d faces; the

development of tabular crystals seems to reflect these later formation conditions. Also, at the end of the growth period, there is less of the dominant color-causing element chromium and more iron, which leads to the formation of near-colorless surface layers.

EDXRF results support this scenario. Spectra taken on the basal plane of tabular Douros synthetic ruby crystals show small chromium peaks and high iron peaks. This agrees with the microprobe analyses taken on a cross-section, as shown in table 4. The complex chemical zoning observed across the tabular crystal is also responsible for the fact that no distinct reading could be taken on this plane with the refractometer. The low-chromium/high-iron content near the surfaces of tabular crystal faces not only explains the near-colorless to light red zones seen along the outermost layers, but also explains the lower intensity or even absence of U.V. fluorescence in these areas.

The EDXRF spectra of rhombohedral crystals revealed a difference in outer-layer composition between the intense red basal faces ($Cr > Fe$) and the almost-colorless to light red rhombohedral faces ($Fe > Cr$). Microprobe analyses of the outer layers of two rhombohedral samples (sample E and the surface layer of sample D1, in table 3) also revealed dis-

TABLE 4. Chemical zoning in a tabular crystal of Douros synthetic ruby.^a

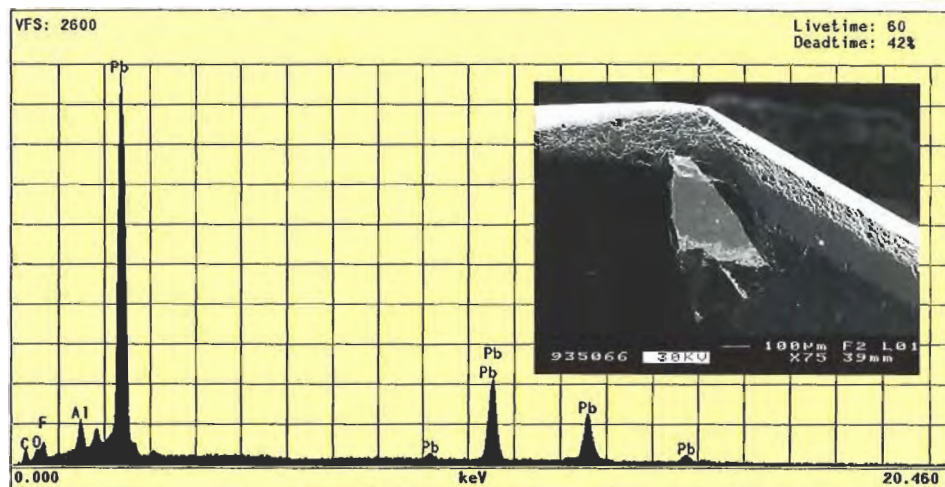
Oxide	Upper layer, confined to c	Upper core, confined to r	Lower core, confined to d	Lower layer, confined to $-c$
Scan A	12 point analyses	17 point analyses	8 point analyses	13 point analyses
Al_2O_3	100.21–99.72	98.66–99.55	98.36–99.73	98.55–99.93
TiO_2	0.00–0.02	0.00–0.02	0.00–0.02	0.00–0.02
Cr_2O_3	0.04–1.22 ^b surface → core	1.00–1.12	1.15–1.43	1.07–0.05 ^b core ← surface
Fe_2O_3	0.31–0.11 ^c surface ← core	0.09–0.15	0.08–0.14	0.15–0.32 ^c core → surface
MnO	0.00–0.01	0.00–0.02	0.00–0.02	0.00–0.02
Scan C	7 point analyses	23 point analyses	12 point analyses	8 point analyses
Al_2O_3	98.10–99.35	98.63–99.75	98.42–99.35	98.67–99.52
TiO_2	0.00–0.02	0.00–0.02	0.00–0.01	0.00–0.02
Cr_2O_3	0.04–0.90 ^b surface → core	0.67–0.81	0.92–1.03	0.88–0.02 ^b core ← surface
Fe_2O_3	0.23–0.11 ^c surface ← core	0.13–0.15	0.11–0.15	0.10–0.27 ^c core → surface
MnO	0.00–0.01	0.00–0.02	0.00–0.02	0.00–0.01

^aOxides in wt.%; ranges of electron microprobe analyses; scans along the c -axis between the upper and lower basal pinacoids; thickness of the tabular crystal is 2.2 mm (see text for further details of sample preparation). Vanadium was below detection limit; gallium was not measured.

^bContinuous decrease in chromium from core to surface layer in c face areas.

^cContinuous increase in iron from core to surface layer in c face areas.

Figure 23. This scanning electron micrograph shows the corner of a faceted ruby with a yellow material that was analyzed by SEM-EDS. The resulting spectrum indicates that lead (Pb) is the main component in this flux particle.



tinctly lower chromium and higher iron concentrations in these regions, as compared to sample D2 and analyses of the faceted samples. (Note that only the core area of D2 was analyzed, because the specimen had been cut such that there was no distinct outer layer on the new surface.)

Because EDXRF analyses were performed on the table facets of the faceted rubies, and there is no general rule for the crystallographic orientation of the tables, we also examined random orientations and cutting angles of the crystals. We found that the cut Douros synthetic rubies usually exhibited the same chemical characteristics as the cores (i.e., from which the colorless outer layers were removed) of rhombohedral material. This is consistent with our microscopic observations. Microprobe analyses of three faceted samples (A, B, and C of table 3), as compared to analyses of the core of rhombohedral crystal D1 and crystal D2, confirmed the high chromium and low iron concentrations.

With careful microscopic examination, we saw color zoning in all of the rhombohedral Douros crystals in the form of thin colorless outer layers on the *d* and *r* faces. R.I. differences between the *r* and *c* faces (table 1) and the different reactions to ultraviolet radiation of these external layers agree with the results of X-ray fluorescence and microprobe investigations. The zones with less-intense U.V. fluorescence were also mentioned by Smith and Bosshart (1993) for rhombohedral crystals.

SEPARATION OF DOUROS SYNTHETIC RUBY FROM NATURAL RUBY

Faceted Douros synthetic rubies may show a number of characteristic features that distinguish them from natural rubies if they are inspected carefully. Although yellow flux inclusions (e.g., figure 16) are probably the easiest means of identification, such

large flux inclusions were relatively rare in the faceted stones we examined. Because the flux consists of a lead compound, however, Pb may be identified by EDXRF as a trace element in the bulk composition. Lead is not found in natural rubies (except possibly in fissures or cavities; if a stone was polished on a lead wheel), and few natural rubies contain inclusions that resemble the typical large flux inclusions.

Structural characteristics—such as the umbrella-shaped internal *d* growth zones (figure 15) or the near-colorless surface layers (figure 7)—cannot be expected in each sample. These properties are confined to the intermediate and outer growth areas, which would probably be at least partly removed by the bruting or cutting process. The characteristic twinning observed in tabular crystals is not present in cut stones from rhombohedral rough.

As demonstrated above, trace-element ratios may vary within a sample, depending on the orientation of the crystal measured. We usually found distinct amounts of Ti, Fe, and Ga, in addition to Cr, but V, if present, was below the detection limit of EDXRF.

Natural rubies usually have crystal faces different from those observed in the Douros synthetic ruby. They often show intercalated fine twin lamellae in one, two, or three spatial directions, with characteristic intersection lines. We did not see such structural features in the Douros material. Most Douros synthetic crystals did reveal growth planes confined to color zoning that do not occur in natural material in this form.

Even after heat treatment, mineral inclusions in ruby may exhibit crystal shapes that will help characterize the host stone as natural. Rutile needles, or the traces that remain after heat treatment, were not present in the Douros synthetic rubies we

examined. However, "veils" or fissures such as those shown in figure 20 could very well be confused with similar-appearing features that are commonly seen in natural ruby.

CONCLUSION

The Douros flux-grown synthetic ruby has been in the marketplace since January 1993. The manufacturers, John and Angelos Douros, report that they have been producing approximately 2,000 ct per month. The Douros product most closely resembles the Ramaura flux-grown synthetic ruby, with characteristics that are not seen in synthetic rubies by other manufacturers.

Most of the gemological properties of the Douros material overlap those of natural rubies. It is most easily identified as a synthetic when there

are large inclusions of flux, which are readily recognized by their coarseness, yellow color, crazed appearance, and bubbles. If no characteristic flux inclusions are seen, a combination of chemical analysis (to reveal the presence of Pb and compare the contents of V, Ti, Cr, Fe, and Ga with those typically encountered in natural rubies) and immersion microscopy (to reveal characteristic crystal-growth patterns and color zoning) should provide the evidence to distinguish this new synthetic ruby from its natural counterpart.

Acknowledgments: The authors are grateful to Prof. R. Guggenheim and Mr. D. Mathys, of the Laboratory for Scanning Electron Microscopy of Basel University, for their help in analyzing the flux. Dr. O. Medenbach, of the Institute for Mineralogy of Bochum University, helped with crystal drawings and X-ray diffraction analysis. Except where noted, all of the photomicrographs are by the authors.

REFERENCES

- Bosshart G. (1982) Distinction of natural and synthetic rubies by ultraviolet spectrophotometry. *Journal of Gemmology*, Vol. 8, pp. 145-160.
- Bosshart G. (1983) Ramaura—eine neue Rubinsynthese (erste Untersuchungsergebnisse). *Zeitschrift der Deutschen Gemmologischen Gesellschaft*, Vol. 32, pp. 164-171.
- Burch C.R. (1984) Some observations on a Kashan synthetic ruby. *Journal of Gemmology*, Vol. 19, pp. 54-61.
- Douros J., Douros A. (1993) Cultivated ruby from Greek production. *Chrysotechni*, Vol. 4, No. 45, p. 56.
- Dunn P. (1977) The use of the electron microprobe in gemology. *Journal of Gemmology*, Vol. 15, No. 5, pp. 248-258.
- Hänni H.A., Bosshart G. (1993) Flux synthetic ruby alleged European production. *ICA Early Warning Flash*, Laboratory Alert No. 71, June 8, 1993.
- Hänni H.A., Schmetzer K. (1993) First results on a new flux-grown synthetic ruby (Douros) produced in Greece. In *Abstracts of the 24th International Gemological Conference, Paris, France, 2-15 October 1993*, Association Française de Gemmologie, Paris, 1993.
- Kane R.E. (1983) The Ramaura synthetic ruby. *Gems & Gemology*, Vol. 19, No. 3, pp. 130-148.
- Kiefert L., Schmetzer K. (1991) The microscopic determination of structural properties for the characterization of optical uniaxial natural and synthetic gemstones. Part I: General considerations and description of the method. *Journal of Gemmology*, Vol. 22, pp. 344-354.
- Muhlmeister S., Devouard B. (1991) Determining the natural or synthetic origin of rubies using energy-dispersive X-ray fluorescence (EDXRF). In A. S. Keller, Ed., *Proceedings of the International Gemological Symposium 1991*, Gemological Institute of America, Santa Monica, CA, pp. 139-140.
- Schmetzer K. (1986a) *Natürliche und synthetische Rubine—Eigenschaften und Bestimmung*. Schweizerbart, Stuttgart.
- Schmetzer K. (1986b) An improved sample holder and its use in the distinction of natural and synthetic ruby as well as natural and synthetic amethyst. *Journal of Gemmology*, Vol. 20, pp. 20-33.
- Schmetzer K. (1987) On twinning in natural and synthetic flux-grown ruby. *Journal of Gemmology*, Vol. 20, pp. 294-305.
- Schmetzer K., Bank H. (1981): The color of natural corundum. *Neues Jahrbuch für Mineralogie Monatshefte*, Vol. 1981, pp. 59-68.
- Schmetzer K., Smith C.P., Bosshart G., Medenbach O. (1994) Twinning in Ramaura synthetic rubies. *Journal of Gemmology*, Vol. 24, pp. 87-93.
- Smith C.P., Bosshart G. (1993) New flux-grown synthetic rubies from Greece. *JewelSiam*, Vol. 4, No. 4, pp. 106-114; No. 5, p. 16.
- Stern W.B., Hänni H.A. (1982) Energy dispersive X-ray spectrometry: A non-destructive tool in gemology. *Journal of Gemmology*, Vol. 18, pp. 285-296.

BACK ISSUES OF

GEMS & GEMOLOGY

Limited quantities of these issues are still available

Spring 1987

"Modern" Jewelry: Retro to Abstract
Infrared Spectroscopy in Gem Identification
A Study of the General Electric Synthetic Jadeite
Iridescent Orthoamphibole from Greenland

Summer 1987

Gemstone Durability: Design to Display
Wessels Mine Sugilite
Three Notable Fancy-Color Diamonds
The Separation of Natural from Synthetic
Emeralds by Infrared Spectroscopy
The Rutilated Topaz Misnomer

Fall 1987

An Update on Color in Gems. Part I
The Lennix Synthetic Emerald
Kyocera Corp. Products that Show Play-of-Color
Man-Made Jewelry Malachite
Inamori Synthetic Cat's-Eye Alexandrite

Winter 1987

The De Beers Gem-Quality Synthetic Diamonds
Queen Conch "Pearls"
The Seven Types of Yellow Sapphire and Their
Stability to Light

Summer 1988

The Diamond Deposits of Kalimantan, Borneo
An Update on Color in Gems. Part 3
Pasek Pyropes
Three-Phase Inclusions in Sapphires from Sri Lanka

Fall 1988

An Economic Review of Diamonds
The Sapphires of Penglai, Hainan Island, China
Iridescent Orthoamphibole from Wyoming
Detection of Treatment in Two Green Diamonds

Winter 1988

Gemstone Irradiation and Radioactivity
Amethyst from Brazil
Opal from Opal Butte, Oregon
Kyocera's Synthetic Star Ruby

Spring 1989

The Sinkankas Library
The Gujjar Killi Emerald Deposit
Beryl Gem Nodules from the Bananal Mine
"Opalite": Plastic Imitation Opal

Summer 1989

Filled Diamonds
Synthetic Diamond Thin Films
Grading the Hope Diamond
Diamonds with Color-Zoned Pavilions

Fall 1989

Polynesian Black Pearls
The Capoeirana Emerald Deposit
Brazil-Twinned Synthetic Quartz
Thermal Alteration of Inclusions in Rutilated Topaz
Chicken-Blood Stone from China

Winter 1989

Emerald and Gold Treasures of the Atocha
Zircon from the Harts Range, Australia
Blue Pectolite
Reflectance Infrared Spectroscopy in Gemology
Mildly Radioactive Rhinestones and Synthetic
Spinel-and-Glass Triplets

Spring 1990

Gem Localities of the 1980s
Gemstone Enhancement and Its Detection
Synthetic Gem Materials of the 1980s
New Technologies of the 80s: Their Impact
in Gemology

Winter 1990

The Dresden Green Diamond
Identification of Kashmir Sapphires
A Suite of Black Diamond Jewelry
Emeraldolite

Spring 1991

Age, Origin, and Emplacement of Diamonds
Emeralds of Panjshir Valley, Afghanistan

Summer 1991

Fracture Filling of Emeralds: Opticon and "Oils"
Emeralds from the Ural Mountains, USSR
Treated Andamooka Matrix Opal

Fall 1991

Rubies and Fancy Sapphires from Vietnam
New Rubies from Morogoro, Tanzania
Bohemian Garnet—Today

Winter 1991

Marine Mining of Diamonds off Southern Africa
Sunstone Labradorite from the
Ponderosa Mine, Oregon
Nontraditional Gemstone Cutting
Nontransparent "CZ" from Russia

Spring 1992

Gem-Quality Green Zoisite
Kilbourne Hole Peridot
Fluid Inclusion Study of Querétaro Opal
Natural-Color Nonconductive
Gray-to-Blue Diamonds
Peridot as an Interplanetary Gemstone

Summer 1992

Gem Wealth of Tanzania
Gamma-Ray Spectroscopy to
Measure Radioactivity
Dyed Natural Corundum as a Ruby Imitation
An Update on Sumitomo Synthetic Diamonds

Fall 1992

Ruby and Sapphire Mining in Mogok
Bleached and Polymer-Impregnated Jadeite
Radiation-Induced Yellow-Green Color in
Grossular Garnet

Winter 1992

Determining the Gold Content of Jewelry Metals
Diamond Sources and Production
Sapphires from Changle, China

Spring 1993

Queensland Boulder Opal
Update on Diffusion-Treated Corundum:
Red and Other Colors
A New Gem Beryl Locality: Luumäki, Finland
De Beers Near Colorless-to-Blue Experimental
Gem-Quality Synthetic Diamonds

Summer 1993

Flux-Grown Synthetic Red and Blue Spinel
from Russia
Emeralds and Green Beryls of Upper Egypt
Reactor-Irradiated Green Topaz

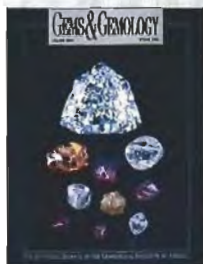
Fall 1993

Jewels of the Edwardians
A Prospectors' Guide Map to the Gem Deposits
of Sri Lanka
Two Treated-Color Synthetic Red Diamonds
Seen in the Trade
Two Near-Colorless General Electric Type IIa
Synthetic Diamond Crystals

Winter 1993
The Gemological Properties of Russian Gem-
Quality Synthetic Yellow Diamonds
Heat Treating the Sapphires of Rock Creek,
Montana
Garnets from Allay, China

Some issues from the 1984, 1985, and 1986
volume years are also available. Please call the
Subscriptions Office for details.

ORDER NOW!



Spring 1991



Spring 1992



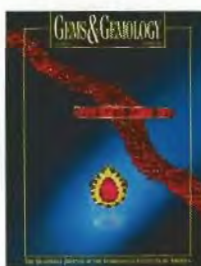
Spring 1993



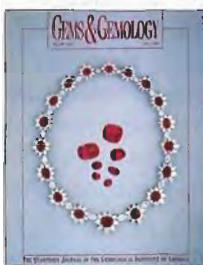
Summer 1991



Summer 1992



Summer 1993



Fall 1991



Fall 1992



Fall 1993



Winter 1991



Winter 1992



Winter 1993

Complete your back issues of Gems & Gemology NOW!

Single Issues* \$ 9.50 ea. U.S. \$ 13.00 ea. elsewhere

Complete Volumes:*

1986, 1987, 1989, \$ 34.00 ea. vol. U.S. \$ 44.00 ea. vol. elsewhere
1991, 1992, 1993

Three-year set \$ 95.00 U.S. \$120.00 elsewhere

Five-year set \$150.00 U.S. \$190.00 elsewhere

*10% discount for GIA Annual Fund donors at the Booster's Circle level and above.

**TO ORDER: Call toll free (800) 421-7250, ext. 394 or
(310) 829-2991, ext. 394**

**FAX (310) 453-4478 OR WRITE: Attn: G&G Subscriptions
GIA, 1660 Stewart Street, Santa Monica, CA 90404**

EMERALDS FROM THE MANANJARY REGION, MADAGASCAR: INTERNAL FEATURES

By Dietmar Schwarz

Inclusions in emeralds from the Mananjary region in the eastern part of the island nation of Madagascar are reported and compared with inclusions in emeralds from other, especially African, localities. Although most of these internal features are similar to those found in emeralds from other schist-type deposits, Mananjary emeralds usually can be separated from emeralds from other localities by means of associations of certain mineral inclusions (especially talc, carbonates, amphiboles, and quartz) with specific types of fluid inclusions.

ABOUT THE AUTHORS

Dr. Schwarz is a research gemologist with the Gübelin Gemmological Laboratory, Lucerne, Switzerland.

Acknowledgments: E. J. Petsch of Julius Petsch Jr., G. Becker of Friedrich August Becker, D. Th. Klein of Fritz Klein, K. Heringer of Kempfeld, L. Haag, and Stefan Kehl—all of Idar-Oberstein, Germany—provided samples, as did Dr. H. A. Hänni of SSEF, Zurich, Switzerland. Mr. Petsch, Mr. Haag, and Dr. Th. Eidt provided valuable information about Madagascar emeralds. J. I. Koivula of GIA, and G. Bosshart and C. Smith—both of the Gübelin lab—helped edit the original manuscript. Bettina Becker and Joachim Zang of the Department of Gemstone Research, Johannes Gutenberg University, Mainz, did some of the SEM and microprobe analyses. This study was part of a research project sponsored by the German Research Association (DFG) and carried out at the Johannes Gutenberg University of Mainz, Germany. All photomicrographs are by the author.

Gems & Gemology, Vol. 30, No. 2, pp. 88–101

© 1994 Gemological Institute of America

For many years, Africa has been one of the main producers of emeralds, with known schist-type deposits in Zambia, Zimbabwe, Mozambique, Tanzania, Egypt, and South Africa, as well as deposits formed in a special environment in central Nigeria. Significant quantities of fine emeralds (figure 1) have also been found in schists in the Mananjary region of Madagascar, a large island nation off the southeast coast of Africa (Schwarz and Henn, 1992). Until now, however, there has been little information in the gemological literature about the Mananjary emeralds and how their internal features compare with those of emeralds from schist-type deposits elsewhere.

According to knowledgeable sources (E. J. Petsch, Th. Eidt, W. Spattenstein, and H. Hänni, pers. comms., 1993), the Mananjary region was the only emerald-producing area in Madagascar until about two years ago, when mining began at a small deposit discovered in the southern region of Madagascar near the town of Benenitra (about 150 km east of the city of Toliara; see figure 2). However, this new deposit produces only small, dark crystals (E. J. Petsch, H. Hänni, and G. Spagnoli, pers. comms., 1993) and is not discussed further in this article.

The Mananjary region represents a mining area of considerable potential and size. Important mines within this region include an unnamed alluvial emerald occurrence, about 50 km west-southwest of Mananjary, near the town of Ifanadiana (Sinkankas, 1981); the Ankadilalana mine, near the town of Kianjavato (Hänni and Klein, 1982); and the Morafeno mine, about 30 km south of Mananjary (Schwarz and Henn, 1992). There are actually numerous operations throughout the region. In the general area of the Morafeno mine, for example, Thomas (1993) reports visiting nine mines: Ambodirofia, Ambodibonary, Ambadamanino, Ambodibakoly, Mororano, Ambodifandrika, Mohotsana II, Ambilanifitorana, and Ambodizainana.

Figure 1. Large quantities of emeralds have been mined from deposits in the Mananjary area of Madagascar. These eight faceted Mananjary stones range from 0.17 to 2.57 ct; the specimen measures approximately 35 × 20 × 15 mm. Stones courtesy of H. Hänni and John M. Bachman Inc.; photo © Harold & Erica Van Pelt.



The present article provides the first comprehensive description of the inclusion features of emeralds from the Mananjary region. It also compares these internal characteristics to those observed in emeralds from other localities. In many cases, these Madagascar emeralds can be distinguished from emeralds from other occurrences on the basis of their inclusions.

BACKGROUND

Emerald Occurrences in Madagascar. Beryl is one of the most important of the more than 50 gem minerals found on Madagascar (Chikayama, 1989). Aquamarine and other beryls from Madagascar have been known in Europe since French occupation of the island in 1883. Levat (1912) appears to have been the first to mention an occurrence of

emerald in Madagascar; Lacroix (1922) provided the first detailed survey account of occurrences—both primary and secondary (i.e., alluvial)—of gem-quality beryl there. However, the primary emerald occurrences that are in the vicinity of the coastal town of Mananjary have been known for only about 20 years. Sinkankas (1981) mentioned an emerald occurrence about 50 km west-southwest of Mananjary and about 250 km southeast of Tananarive (now named Antananarivo), the capital of Madagascar, near the town of Ifanadiana (again, see figure 2). In this alluvial deposit, small rounded emerald fragments have been found together with kyanite.

Hänni and Klein (1982) described emeralds from the Ankadilalana mine, near the town of Kianjavato. They reported that these emeralds,



Figure 2. Several emerald deposits have been identified on the island nation of Madagascar, which lies off the south-east coast of Africa. With the exception of the recent discovery at Benenitra, most lie within 50 km of the city of Mananjary. Mining operations include the deposit near Ifanadlana, the Ankadilalana mine, and the Morafeno mining region.

which originate from a mica schist, are similar to Zambian emeralds with respect to their blue-green color and optical properties. They described the emerald mining at that time as sporadic and carried out with primitive equipment.

Only during the last few years have the Morafeno occurrences, about 30 km southeast of the Ankadilalana deposit, been exploited commercially (figure 3). These deposits, which are also embedded in mica schists and subordinately in amphibole schists, are considered extensive and rich in emerald mineralization (Th. Eidt, pers. comm., 1993). At the beginning of the 1990s, the

worked area around Mananjary comprised at least 50 km² (E. J. Petsch, pers. comm., 1993; Thomas, 1993). Mining is performed by independent miners and a number of small mechanized operations (figure 4). Precise figures for the quantity or value of emeralds produced to date are not available; most crystals range from one to three carats, but low-quality crystals up to 1,000 grams have been reported (E. J. Petsch, pers. comm., 1993).

Compared to emeralds from the African mainland, many of the stones from the Mananjary region are somewhat light in color; others are a bluer green, similar to Zambian emeralds (again, see fig-



Figure 3. As this overview of one mining operation shows, some deposits in the Morafeno region have been worked extensively in recent years. Photo by E. Julius Petsch, of Julius Petsch Jr., Idar-Oberstein.

ure 1). The crystals range from opaque to transparent, and nice cabochons can be cut from translucent rough (figure 5). Generally, the emerald crystals are found embedded in the host mica or amphibole schist or in quartz (figure 6). Additional information on this locality, the material produced, and the gemological properties of these emeralds (which overlap those of Fe- and Cr-rich emeralds from other schist-type deposits) can be found in Schwarz and Henn (1992).

Previous Inclusion Studies. To date, the following mineral inclusions (see table 1) and other internal features have been reported for emeralds from Madagascar. In the stones from Ankadilalana, Hänni and Klein (1982) identified brown biotite, muscovite, apatite, hematite, goethite, quartz, ilmenite, tourmaline, liquid/gas two-phase inclusions, and color zoning. Campbell (1991) observed goethite and hematite, as well as limonite and phlogopite, in a cabochon-cut emerald from Madagascar that also showed color zoning and negative crystals. M. L. Delé-Lasir and J. P. Poirot (pers. comm., 1991) identified the following mineral inclusions in emeralds from Madagascar by means of Raman spectroscopy: carbonates (ankerite), quartz, phlogopite, apatite, flu-



Figure 4. At Morafeno, this mining company uses a backhoe to reach the emerald-bearing schists. Photo by E. Julius Petsch, of Julius Petsch Jr., Idar-Oberstein.

orite, pyrite, and pyrrhotite. Kleyenstüber (1991) also reported the internal features of Madagascar emerald from the same rough that yielded the sample described by Campbell: elongated hollow growth channels with a rectangular outline; a large hexagonal crystal with a distinct yellow-to-green pleochroism (possibly tourmaline or apatite); booklets of mica platelets (phlogopite and, probably, muscovite); negative crystals, usually filled with a liquid and gas; and minute to submicroscopic inclusions of a potassium feldspar (probably microcline) and quartz.

Thomas (1993) did not note any mineral inclusions in stones from Ankadilalana specifically, but only spiral stress fractures and numerous liquid-filled veil- and feather-like inclusions. He did list some mineral inclusions for emeralds from the Mananjary region (but did not indicate the methods by which he identified them). These include biotite platelets; euhedral transparent crystals of a colorless cubic mineral, possibly rhodizite; and small, well-formed black spinel crystals. Another group of Mananjary emeralds showed oriented "blocky" negative crystals and dense parallel groups of slender acicular negative crystals. In stones from Morafeno, Thomas described "Saturn-like" inclusions comprising a rather large, tabular negative crystal cavity surrounded by a partially healed liquid-and-gas stress halo; "fingerprints"; a few oriented, slender, rod-like inclusions; and small, transparent, cubic crystals (rhodizite?).

MATERIALS AND METHODS

More than 100 emerald crystals and crystal fragments (see, e.g., figure 7) were examined for this study. They were purchased in the Mananjary mining region by Idar-Oberstein gem dealers (some of whom are involved in the actual mining) and Dr.

Figure 5. Considerable cabochon-quality material, like the 4.88- and 3.42-ct emeralds shown here, has been recovered from deposits in the Mananjary region. Photo by Gerhard Becker.

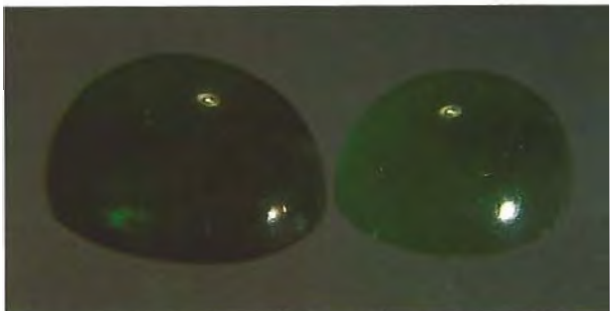


Figure 6. At Mananjary, emeralds are found embedded in a mica or amphibole schist (right) or in quartz (left). The larger specimen measures approximately 35 × 20 × 15 mm. Photo © GIA and Tino Hammid.

Thomas Eidt. They reportedly came from an area of at least 25 km² near the town of Morafeno and are representative of the emeralds recovered from the Mananjary deposits. Most of these samples ranged from 0.5 to 3 ct.

For this research project, the inclusions were first described and classified using a binocular Schneider immersion microscope with Zeiss optics. Then all of the different types of inclusions were photographed with the samples immersed in benzoic acid. Next, samples with mineral inclusions that appeared to be typical were polished down until the mineral inclusions to be analyzed were exposed at the surface. A Philips XL 30 scanning electron microscope fitted with an EDAX energy-dispersive X-ray spectrometer (SEM-EDS) was then used for chemical analysis of these inclusions.

Figure 7. These crystals, which average 2–3 ct, are representative of the Mananjary samples studied for this report. Photo by Gerhard Becker.



TABLE 1. Mineral inclusions in emeralds from the Mananjary region, Madagascar, and from some other localities.^a

Inclusions	In Mananjary emeralds as reported by	Also reported in emeralds from these other localities	Inclusions	In Mananjary emeralds as reported by	Also reported in emeralds from these other localities
Mica		Most African occurrences ^b	"Carbonates"		South Africa ^b
Biotite/ Phlogopite	Hänni and Klein (1982) Campbell (1991) Kleyenstüber (1991) Delé-Lasir and Poirot ^c Schwarz (this paper) Thomas (1993)	Most occurrences worldwide, e.g.; Austria (Grundmann, 1991; Schwarz, 1991b) Australia (Schwarz, 1991a) Brazil (Hänni et al., 1987; Schwarz et al., 1988a,b; Schwarz and Eidt, 1989; Schwarz, 1990; Schwarz et al., 1990) Russian Federation (Schwarz, 1991b)	Ankerite	Delé-Lasir and Poirot ^c	
			Calcite/Fe-Dolomite	Schwarz (this paper)	Zambia (Delé-Lasir and Poirot ^c)
Muscovite	Hänni and Klein (1982) Kleyenstüber (1991) ^d Schwarz (this paper)		Fluorite	Delé-Lasir and Poirot ^c	
Apatite	Hänni and Klein (1982) Delé-Lasir and Poirot ^c	Austria (Gübelin and Koivula, 1986)	Pyrite	Delé-Lasir and Poirot ^c Schwarz (this paper)	Austria (Grundmann, 1991) Brazil ^b (Schwarz and Eidt, 1989; Schwarz, 1990; Schwarz et al., 1990) Colombia ^b (Gübelin and Koivula, 1986) Mozambique (Delé-Lasir and Poirot ^c) Pakistan (Henn, 1988) South Africa (Van Eeden et al., 1939)
Hemalite	Hänni and Klein (1982) Campbell (1991) ^d	Zambia (Gübelin and Koivula, 1986)	Pyrrhotite	Delé-Lasir and Poirot ^c	
Goethite	Hänni and Klein (1982) Campbell (1991) ^d		Rhodizite ^b	Thomas (1993)	
Limonite ^d	Campbell (1991)		Spinel	Thomas (1993)	
Quartz	Hänni and Klein (1982) Kleyenstüber (1991) Delé-Lasir and Poirot ^c Schwarz (this paper)	Most African occurrences (Graziani et al., 1983; Bank and Gübelin, 1976; Delé-Lasir and Poirot ^c) Brazil (Hänni et al., 1987; Schwarz et al., 1988a)	Amphibole (actinolite/tremolite)	Schwarz (this paper)	African localities, including South Africa, Zambia, Zimbabwe ^b Austria (Schwarz, 1991b) Brazil ^b Russian Federation (Schwarz, 1991b)
Ilmenite	Hänni and Klein (1982)		Talc	Schwarz (this paper)	Brazil (Schwarz, 1990) Pakistan ^b Zimbabwe ^b
Tourmaline	Hänni and Klein (1982)	Austria (Grundmann, 1991) Brazil ^b Russian Federation ^b Zambia ^b (Koivula, 1992, 1984) Zimbabwe (Anderson, 1976)	Beryl	Schwarz (this paper)	Brazil (Hänni et al., 1987; Schwarz and Eidt, 1989; Schwarz, 1990; Schwarz et al., 1990) Colombia ^b Nigeria ^b Pakistan (Delé-Lasir and Poirot ^c)
Feldspar	Schwarz (this paper)	Austria (Schwarz, 1991b) Brazil (Hänni et al., 1987; Schwarz and Eidt, 1989; Schwarz et al., 1990) Colombia ^b Nigeria ^b Pakistan ^b Russian Federation (Schwarz, 1991b) Tanzania (Bank and Gübelin, 1976; Gübelin and Koivula, 1986; Delé-Lasir and Poirot ^c) Zimbabwe ^b	Chlorite	Schwarz (this paper)	Brazil ^b (Schwarz and Eidt, 1989; Schwarz et al., 1990) Pakistan (Gübelin, 1989) Zambia ^b Zimbabwe ^b
K-feldspar	Kleyenstüber (1991)		Molybdenite	Schwarz (this paper)	Austria (Grundmann, 1991) Brazil (Hänni et al., 1987; Schwarz et al., 1988b; Schwarz and Eidt, 1989; Schwarz et al., 1990) Pakistan (Henn, 1988) South Africa (Roulet, 1956; Gübelin, 1973)
Albite	Schwarz (this paper)		Barite	Schwarz (this paper)	Brazil (Mendes and Svisero, 1988) Colombia (Mendes and Svisero, 1988)
Other plagioclase	Schwarz (this paper)				

^aListed are all mineral inclusions attributed to Mananjary emeralds and the sources of these reports in the literature or the present paper. Also listed are some other localities that have produced emeralds in which similar mineral inclusions have been reported. Note that the "other localities" column refers only to the mineral species or group; specific minerals within a group are identified only for the Mananjary emeralds.

^bObserved by the author in the course of research.

^cPersonal communication, 1991.

^dIdentification uncertain.

OBSERVATIONS AND RESULTS

Many different mineral inclusions were identified. Most, but not all, also have been seen in emeralds from other localities in Africa and elsewhere. Table 1 lists the mineral inclusions seen in Mananjary emeralds and the reports on which the Madagascar identifications were based, as well as some other

countries that have produced emeralds with similar features (and the corresponding references). Some unusual fluid inclusions have also been seen in the Mananjary stones.

Quartz. About 35% of the samples contained one or more of the following four types of quartz inclu-

sions, which were categorized on the basis of their morphology and manner of occurrence:

1. Transparent, colorless, elongated, prismatic crystals oriented with their c-axis parallel to the c-axis of the host emerald, often associated with primary fluid inclusions. These occurred as isolated crystals, irregularly distributed throughout the host crystal, or dispersed over the planes of healing fissures. Some samples contained large numbers of these quartz inclusions in their central regions (figure 8).
2. Angular or somewhat rounded grains, some almost spherical (figure 9). These were less commonly associated with fluid inclusions than was the first type of quartz inclusion. Groups of such grains were concentrated in certain areas.
3. Irregularly rounded crystals, some of which had a badly corroded rough surface.
4. Isolated crystals that were probably daughter crystals of former fluid-filled cavities that were opened during sample preparation (figure 10).

These quartz crystals were often intergrown with other mineral inclusions, including talc, mica,

Figure 8. About a third of the Mananjary emerald crystals examined contained inclusions of quartz. Often, they occur as numerous colorless, transparent, elongated, prismatic crystals oriented in the direction of the c-axis of the host emerald. Many quartz crystals are associated—or intergrown—with growth tubes containing primary fluid inclusions. Immersion, magnified 20×.

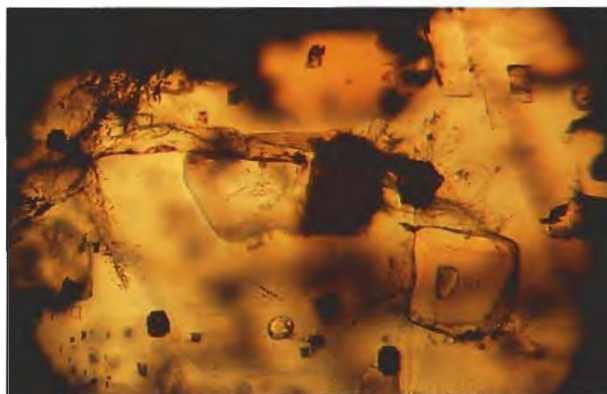
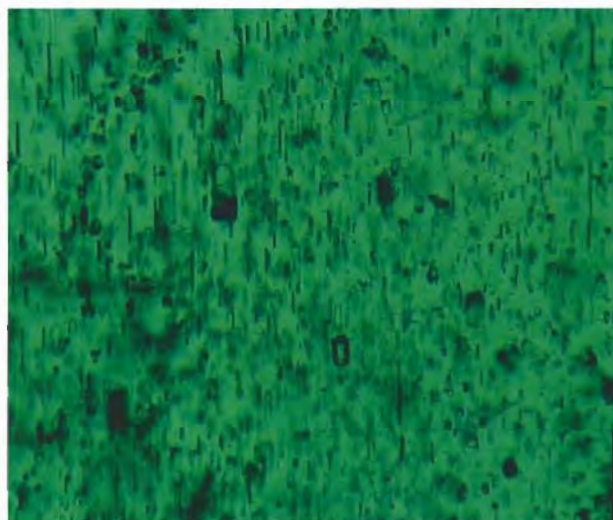


Figure 9. Other quartz inclusions in the Mananjary emeralds were angular or somewhat rounded. One of the large crystals shown here in a slice cut from one of the samples (the yellow color is from the immersion liquid) is partly covered by a substance that appears black in transmitted light; the other contains what appears to be a small secondary beryl crystal. Note the small, almost spherical quartz crystal toward the bottom of the photomicrograph. Magnified 70×.

amphibole, chlorite, carbonates (figure 11), and beryl. Such aggregates were often accompanied by unhealed tension fissures. In some cases, the quartz inclusions were covered by a substance that appeared black or opaque in transmitted light (again, see figure 9).

Quartz inclusions are mentioned in almost all

Figure 10. This scanning electron micrograph shows a quartz crystal as part of a fluid inclusion in a Mananjary emerald. When the host crystal was polished down and the cavity exposed at the surface, the other—gaseous and liquid—phases of the inclusion were lost. Magnified 500×.



reports on internal features of Madagascar emeralds, and they have been observed in emeralds from virtually all African localities (again, see table 1). Quartz-inclusion types 1 and 2 resemble features observed in many Brazilian emeralds from the Itabira/Nova Era mining region (compare Hänni et al., 1987; Schwarz et al., 1988a). Consequently, quartz inclusions are of little value in determining the locality of the host emerald.

Mica. The most common mineral group observed in the Mananjary emeralds, mica was seen in about half of the samples. In these emeralds, mica occurs mostly as randomly distributed transparent crystals that may appear dark brown in transmitted light. Usually somewhat rounded, they also may have an almost perfect (pseudo-) hexagonal outline (figure 12); they often appear as booklets of thin platelets (figure 13). Chemical analyses showed that most of the micas in the Mananjary emeralds belong to the biotite/phlogopite series (with about 15–20 wt.% MgO, 5–15 wt.% FeO, and 10–12 wt.% K₂O), although the Mg- and Fe-poor species muscovite was also identified.

Mica inclusions have been identified in all reports published to date on Madagascar emeralds, and by the author in emeralds from almost all African occurrences (Zambia, Zimbabwe, Tanzania, Mozambique, South Africa, and Egypt). Worldwide, most emerald deposits are related to mica schists. Consequently, biotite/phlogopite micas are the most common mineral inclusions in emeralds. They have been identified, for example, in emeralds

Figure 11. The intergrowth of quartz (black) and carbonate (white) inclusions in Mananjary emeralds is readily apparent in this scanning electron micrograph. Magnified 200×.

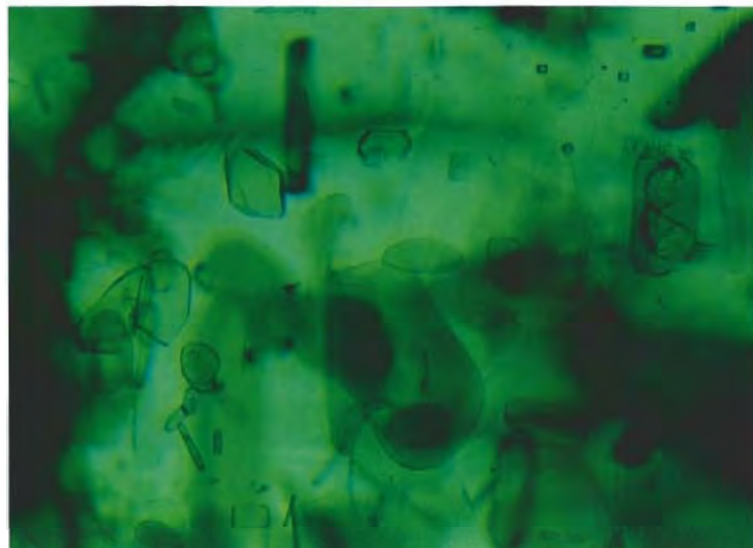
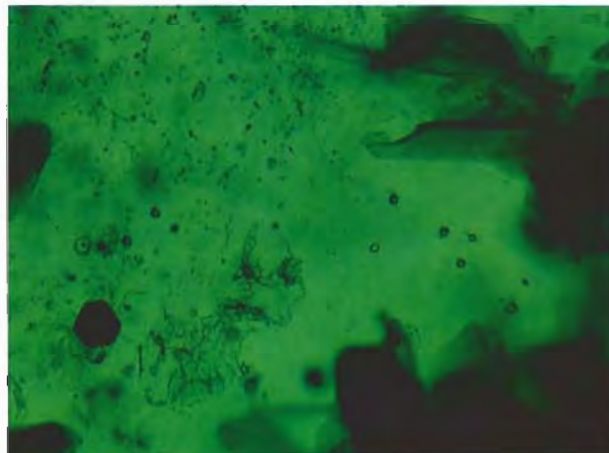


Figure 12. The most common inclusions in the Mananjary emeralds are these transparent, somewhat rounded or pseudo-hexagonal mica crystals (biotite/phlogopite), which are randomly distributed (i.e., without crystallographic orientation) in the host emerald. Immersion, magnified 50×.

from several localities in Brazil: the Belmont mine (see Hänni et al., 1987) and Capoeirana deposit (Schwarz et al., 1988a), in the state of Minas Gerais; the Fazenda Boa Esperança, Tauá, in Ceará (Schwarz et al., 1988b); the Carnaíba (Schwarz and Eid, 1989) and Socotó mining areas (Schwarz et al.,

Figure 13. In this Mananjary emerald are found mica booklets (e.g., the upper right); black-opaque appearing, six-sided molybdenite plates (lower left); and small, rounded fluid inclusions with a very strong relief (like gas bubbles). Immersion, magnified 35×.



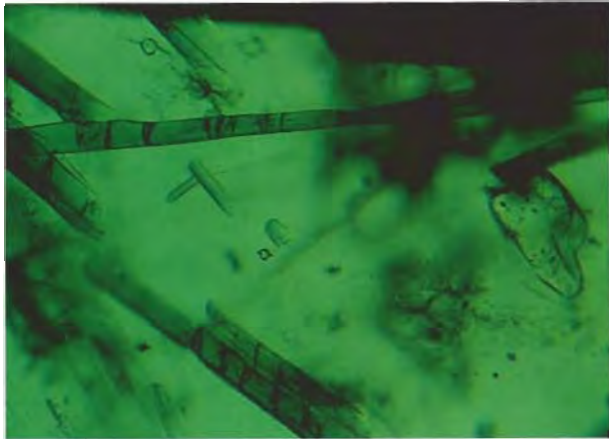


Figure 14. Many of the Mananjary emeralds examined contained long, prismatic, stalk-like, green amphibole (actinolite/tremolite) crystals with a system of fissures that run nearly parallel to the basal face. Note also in this inclusion scene the transparent, colorless, rounded quartz crystal on the far right. Immersion, magnified 50 \times .

1990), in Bahia; and the Santa Terezinha occurrence, in Goiás (Schwarz, 1990). Mica inclusions have also been described in emeralds from the Poona region and from Menzies in Western Australia (Schwarz, 1991a), from the Ural Mountains in the Russian Federation (Schwarz, 1991b), and from the Habach Valley (Habachtal) in Austria (Grundmann, 1991; Schwarz, 1991b).

Amphiboles. Until this study, minerals of the amphibole group had not been described as inclusions in Madagascar emeralds (see, e.g., Thomas, 1993). The author has seen them in emeralds from other African localities (the Sandawana/Machingwe mining area in Zimbabwe, the Ndola Rural district in Zambia, and the Leydsdorp district in South Africa), as well as the Carnaíba, Socotó, and Fazenda Boa Esperança mining areas in Brazil, among others. Although mica schists are the most common host rocks for emeralds, often these schists grade into amphibole-bearing or amphibole schists. This explains why amphiboles (mostly of the actinolite/tremolite series) are frequent inclusions in many emeralds and are sometimes the dominant inclusion mineral (as, for example, in emeralds from the Zeus claims in the Sandawana region of Zimbabwe).

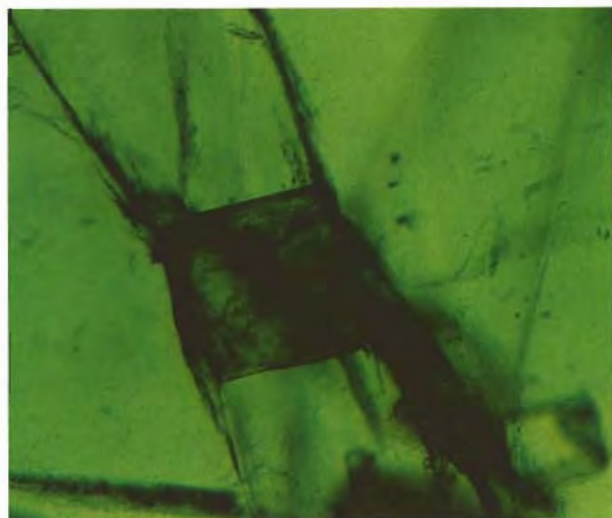
Amphibole crystals were seen in about 20% of the emeralds in this study. The amphibole crystals observed belong to the actinolite/tremolite series, with FeO and MgO each about 10–15 wt.%. The

sum (FeO_{tot} + MgO) in different crystals was found to be constant at about 26 wt.%. The actinolite/tremolite crystals are green, with a long, prismatic, stalky habit. Often they show systems of nearly parallel planes that are slightly inclined with respect to the main axis of the crystals (figure 14). This results in the bamboo-like appearance typical of actinolite/tremolite inclusions in emeralds from several other occurrences. The random distribution of these crystals and the fact that they are often broken at their extremities suggests that they are pro-togenetic, that is, that they formed before the host emerald.

The relative distribution of mica and amphibole crystals in the Mananjary emeralds is very irregular. Some emeralds contain many mica crystals and are practically free of amphiboles; others contain numerous amphibole crystals but practically no mica; and many contain amphibole and mica in almost equal quantities. This reflects the varying composition of the host rock in which the emeralds formed: a mica schist, an actinolite/tremolite schist, or a combination of both. It is likely that amphiboles were not reported in prior articles on inclusions in Mananjary emeralds because the samples studied were taken only from mica schists and not from amphibole schists.

Carbonates. About 15% of the samples contained carbonate inclusions, which are also relatively rare

Figure 15. Rhombohedral carbonate crystals were seen in many of the Mananjary emeralds. Although the crystal is actually colorless, it may appear brown in transmitted light because of corrosion at its surface. Immersion, magnified 70 \times .



in emeralds from other African localities. M. L. Delé-Lasir and J. P. Poirot (pers. comm., 1991) have identified carbonates in emeralds from the Transvaal in South Africa (as did Roulet, 1956), as well as from Zambia (dolomite, calcite) and Sandawana (dolomite, calcite).

Although some of the Mananjary-emerald carbonate inclusions were relatively well-developed rhombohedral crystals (figure 15), most were irregular or rounded grains; in general, they appeared transparent and colorless. The rare prismatic carbonate crystals observed usually appeared black or opaque in transmitted light because they contained numerous minute inclusions. Surface corrosion made some carbonate crystals appear slightly brown in transmitted light.

The carbonate inclusions are usually calcite crystals with small amounts (<1–2 wt.%) of manganese and/or iron. However, chemical analyses also identified Fe-dolomite and a calcite containing relatively high FeO and small amounts (<1%) of magnesium and manganese. Frequently, the carbonate crystals were intergrown with other mineral species (most commonly quartz and talc; again, see figure 11).

Feldspar. Feldspar crystals were identified in about 5% of the Mananjary emerald crystals. Surface corrosion and the presence of minute inclusions (of quartz, among other minerals) gave some of these typically transparent and colorless crystals a somewhat darker (sometimes brown) appearance in transmitted light. They were usually irregular in shape and often very rounded. The feldspars analyzed varied from almost pure albite (Na-feldspar) to a plagioclase containing about 5 wt.% Na₂O and 6–7 wt.% CaO. Sometimes, the feldspars were intergrown with quartz or mica. Kleyenstüber (1991) described a K-feldspar inclusion in a Madagascar emerald.

As table 1 indicates, feldspar inclusions also have been observed (by the author and others) in emeralds from Zimbabwe and Nigeria, as well as from Tanzania. Representatives of this mineral group are also known in emeralds from other occurrences, such as Colombia and the Swat region of Pakistan; the Belmont mine, Carnaíba, and Socotó, in Brazil; the Ural Mountains of the Russian Federation; and the Habach Valley of Austria.

Talc. Before this study, talc had not been reported as an inclusion in Madagascar emeralds. Talc inclusions were identified in about 20% of the samples.

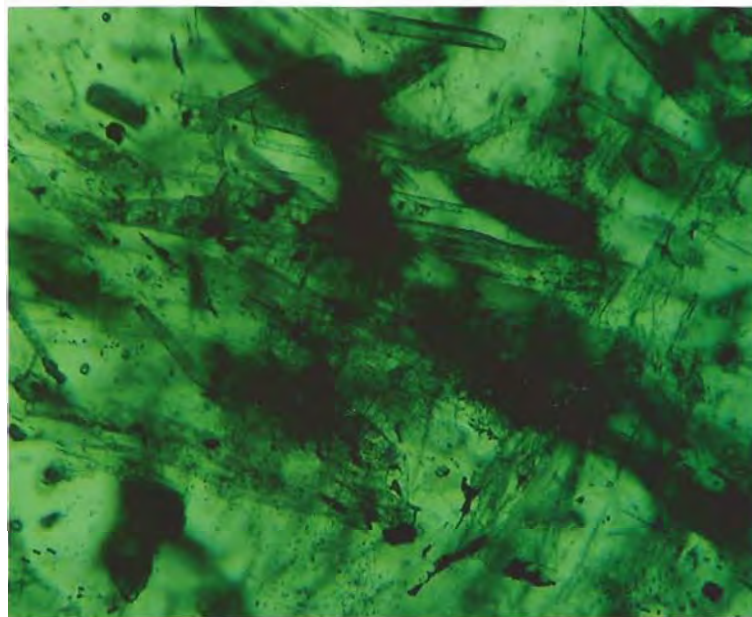


Figure 16. These fibrous aggregates are representative of the talc inclusions seen in Mananjary emeralds. Magnified 50x.

Normally light green, some were more brown. Chemical analysis revealed that the differences in color are related to iron substituting for magnesium in the crystal lattice. The FeO concentration in the analyzed crystals varied between 7 and 12 wt.%. Talc was observed in four different forms: (1) uncommonly, as fibrous aggregates, sometimes with a sheaf-like aspect (figure 16); (2) as irregular-shaped scales dispersed over fracture planes (possibly introduced in conjunction with an epigenetic filling process); (3) as pseudo-hexagonal transparent green platelets; and (4) intergrown with other inclusion minerals (e.g., quartz, pyrite).

The Sandawana/Machingwe (Zimbabwe) region is the only other place in Africa where talc crystals have been found in emeralds—and then only rarely. Therefore, the presence of talc (especially in its fibrous or sheaf-like form) may be useful in separating Mananjary emeralds from those from other African localities. However, the author has found that talc is one of the most common mineral inclusions in emeralds from the talc-carbonate schists of Santa Terezinha de Goiás, Brazil, and from the Swat region, Pakistan (see table 1).

Beryl. Inclusions of beryl typically occur either as colorless, irregular, strongly corroded crystals or as well-developed, heavily included prisms that appear white in darkfield illumination. In addition, some

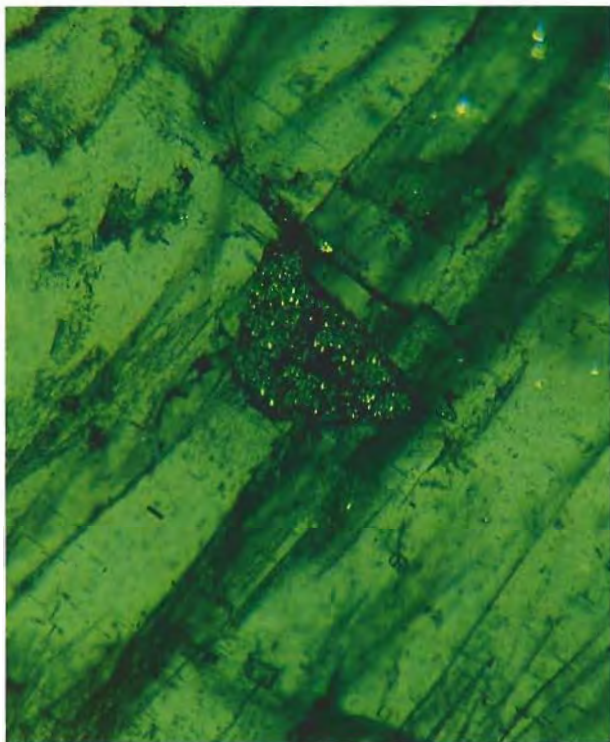


Figure 17. In reflected light, this pyrite grain in a Mananjary emerald shows the yellow color and metallic luster typical of this mineral. Immersion, magnified 50 \times .

beryl was observed as rounded grains in quartz inclusions (again, see figure 9), which indicates that at least two beryl "generations" (with different features) occurred in the area of the emerald mineralizations. Beryl and/or emerald crystals have been identified by the author and others as inclusions in emeralds from several occurrences (e.g., Colombia, Nigeria, Pakistan, and various localities in Brazil), so their presence is of little diagnostic value when determining the origin of an emerald.

Chlorite. Chlorite was observed in only a few samples, as small grains or platelets intergrown with quartz and/or mica. Although not previously reported in Madagascar emeralds, chlorite has been seen by the author in emeralds from Zambia, Zimbabwe, and the Itabira/Nova Era region in Minas Gerais, Brazil. Chlorite has also been seen in material from Pakistan and elsewhere in Brazil (Carnaíba and Socotó; see table 1).

Molybdenite. Identified in less than 5% of the Mananjary emeralds, molybdenite crystals occur as gray to silver platelets with a typical metallic lus-

ter. They may be slightly rounded or show a well-developed hexagonal outline (again, see figure 13).

Molybdenite is known as an inclusion in emeralds from many areas, such as the Transvaal in South Africa, various Brazilian deposits, the Habach Valley of Austria, and the Swat Valley of Pakistan (again, see table 1). Molybdenite has not been described before in emeralds from Madagascar.

Pyrite. Observed in less than 5% of the Mananjary samples, pyrite—as determined by X-ray diffraction analysis of a representative iron sulfide inclusion—appeared a typical metallic yellow under reflected light (figure 17). Most of the pyrite crystals were well developed. Chemical analyses revealed about 2 wt.% NiO and small amounts (<0.5 wt.%) ZnO.

M. L. Delé-Lasir and J. P. Poirot (pers. comm., 1991) have identified pyrite in emeralds from Mozambique as well as from Madagascar. Pyrite has been seen frequently by the author in emeralds from different types of occurrences, including Colombia, as well as the Santa Terezinha, Carnaíba, and Socotó deposits in Brazil. Pyrite has also been reported in emeralds from the Transvaal in South Africa, the Habach Valley of Austria, and the Swat Valley of Pakistan (see table 1).

Barite. Barite was observed in only two samples, as very small, colorless, transparent grains of irregular shape. Apparently a very rare inclusion in emerald, it has been reported in emeralds from only two other localities—Colombia and Santa Terezinha de Goiás, Brazil (Mendes and Svisero, 1988). It has not been reported for Madagascar emeralds before.

Tourmaline. Tourmaline was observed in less than 5% of the Mananjary emeralds. Those crystals seen were typical trigonal prisms, which chemical analysis showed to be members of the dravite-schorl series. Tourmaline inclusions, although by no means common in emerald, have been identified previously in Madagascar emeralds (Hänni and Klein, 1982) and by the author and others in emeralds from widely different occurrences elsewhere: Zambia and Zimbabwe in Africa, the Ural Mountains of the Russian Federation, Carnaíba and Socotó in Brazil, and the Habach Valley in Austria (see table 1).

Fluid Inclusions. One or more of the following types of fluid inclusions were observed in most of the Mananjary samples:

1. Numerous minute fluid inclusions (some associated with quartz—again, see figure 8—and others with an unidentified material) contained in healed to partly healed fissures.
2. Larger fluid or mineral inclusions accompanied by black-appearing spheres—actually clusters of numerous minute fluid inclusions (figure 18).
3. Primary fluid inclusions, often associated with quartz crystals. These inclusions were typically elongated—that is, within growth tubes—in a direction parallel to the c-axis of the host emerald (again, see figure 8). Most had well-developed rectangular or square outlines (negative crystals; figure 19); others were rounded and strongly resembled gas bubbles. Most of the fillings were two-phase (liquid and gas), but three-phase inclusions were also observed. These fluid inclusions may show unusually strong relief and, in transmitted light, often are so dark as to appear opaque.

When large numbers of primary fluid inclusions occur in fine, elongated cavities (figure 8), they are responsible for the so-called rain effect that gives a silk-like sheen to cabochon-cut emeralds. In some cases, they can even generate chatoyancy.

The fluid inclusions observed in the study samples resemble those in emeralds from the Ndola Rural district of Zambia, and from the Itabira/Nova Era mining region of Minas Gerais, Brazil (Belmont and Capoeirana; compare Hänni et al., 1987, and Schwarz et al., 1988a). However, in the Mananjary samples they do not display the impressive variety of their Brazilian counterparts.

Other Microscopic Features. Other internal features observed in the Mananjary emeralds include:

- Color zoning: normally a light core and a dark outer zone
- Growth striae parallel to the prism faces
- Concentrations of inclusions in certain areas of the host crystal (e.g., a central zone with numerous minute quartz crystals)
- Systems of essentially parallel fractures that are only partly healed
- Various types of fissures: delicate healed fissures with small fluid inclusions (often almost flat or slightly wavy, almost parallel to one another, and sometimes oriented parallel to the basal pinacoid of the host emerald); unoriented, unhealed fissures (partly filled with an unidentified material);

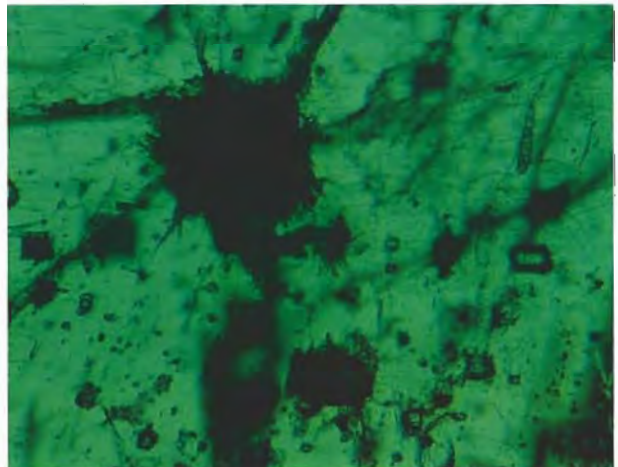
and unoriented, healed fissures with numerous minute "particles" (probably minute fluid inclusions)

DISCUSSION AND CONCLUSIONS

Although precise production figures for the emerald occurrences in the Mananjary region are not available, from the size of some of the mechanized operations it can be concluded that many thousands of carats have been mined. In addition, geologic conditions appear to favor the discovery of larger mineralization sites (Th. Eidt, pers. comm., 1993). Because the physical and chemical properties of Mananjary emeralds fall within the ranges for emeralds from most other localities, the emeralds of this region are best identified by their internal features.

Mananjary emeralds come from a geologic environment that is characterized by the association of different metamorphic schists (principally biotite/phlogopite schists and subordinately amphibole-bearing or amphibole schists) and pegmatite veins (that is, a "schist-type deposit," where pegmatites or pegmatoid veins are the primary source of the element beryllium). Thus, their inclusion features are very similar to those in most emeralds from other schist-type deposits (e.g., quartz, platelets of biotite/phlogopite mica, rods or needles of actinolite/tremolite, platelets or grains of chlorite, and feldspar crystals). These types of inclusions may occur, for example, in emeralds from Zambia

Figure 18. Spherical clusters of numerous fluid inclusions that appeared black in transmitted light were relatively common in the Mananjary emeralds but have not been reported in emeralds from many other localities. Immersion, magnified 50x.



(Ndola Rural district), Zimbabwe (Sandawana/Machingwe mining region), South Africa (Leyds dorp/Transvaal), and Brazil (e.g., Bahia and Minas Gerais). Other mineral inclusions—such as apatite, hematite, ilmenite, tourmaline, pyrite, or molybdenite—also can be seen in emeralds from other localities and different formation environments. However, they are so rare that they are of little diagnostic value.

Even with all of these restrictions, most Madagascar emeralds can be separated from those from other African localities. What is most characteristic is the association of certain mineral inclusions (especially talc, carbonates, amphiboles, and quartz) with specific types of fluid inclusions, such as: fluid inclusions with quartz crystals, in healing fissures; fluid inclusions in large numbers, forming spherical black clusters; and primary fluid inclusions that show very strong relief and appear almost opaque, or are rounded and resemble gas bubbles. Of the other African localities, only Zambian emeralds have fluid inclusions that are similar to the primary fluid inclusions, with well-developed rectangular or square outlines (negative crystals), seen in the Madagascar stones.

As previously mentioned, the fluid inclusions in emeralds from the Itabira/Nova Era region in Minas Gerais, Brazil (Belmont and Capoeirana mining fields), are similar to those observed in the Madagascar samples. Separating emeralds from these two sites could be very difficult. The presence of talc—especially when it appears in a fibrous or sheaf-like form—is a good diagnostic feature for Mananjary emeralds. So far it has been observed only very rarely in emeralds from one other African locality (the Sandawana/Machingwe mining area of Zimbabwe). Although talc is seen in

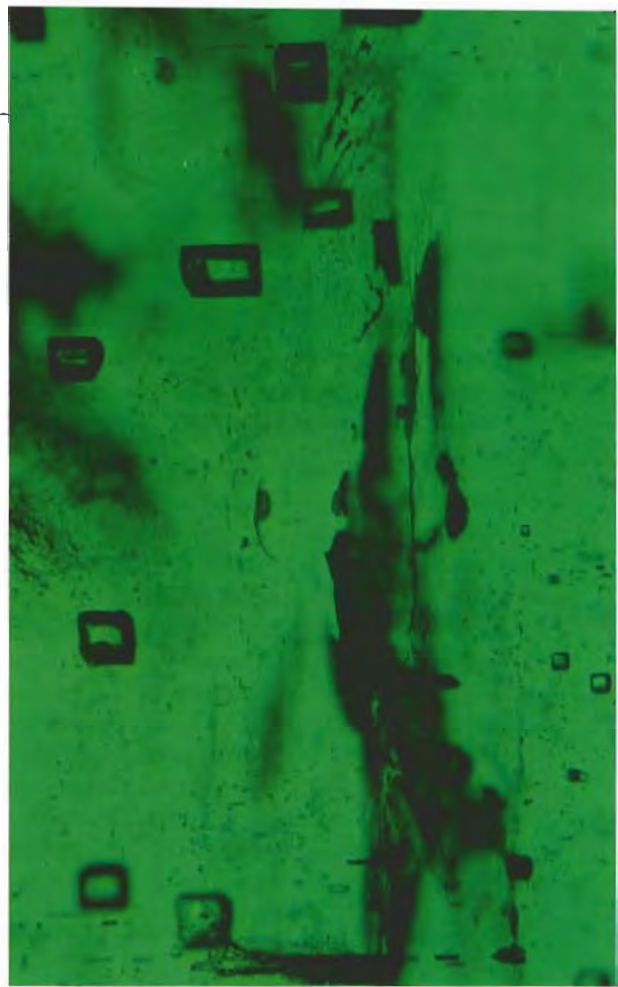


Figure 19. Fluid-filled negative crystals (usually with a gas phase as well) were common in the Mananjary emeralds examined. Note the well-developed rectangular or square outlines. Immersion, magnified 50 \times .

emeralds from other localities (e.g., Santa Terezinha de Goiás, Brazil, and the Swat region of Pakistan) the other internal features of these emeralds are so different that they are easily separated from Mananjary stones.

REFERENCES

- Anderson S.A. (1976) A note on the occurrence of emerald at Mayfield Farm, Fort Victoria, Rhodesia. *Journal of Gemmology*, Vol. 15, No. 2, pp. 80–82.
- Bank H., Gübelin E. (1976) Das Smaragd-Alexandritvorkommen von Lake Manyara/Tansania. *Zeitschrift der Deutschen Gemmologischen Gesellschaft*, Vol. 25, No. 3, pp. 130–147.
- Campbell C.C. (1991) A report on one of a number of emeralds from Madagascar. *South African Gemmologist*, Vol. 5, No. 1, pp. 8–15.
- Chikayama A. (1989) Gem localities in Madagascar. In *Abstracts of the 22nd International Gemmological Conference (IGC)*, Como/Milano, Italy.
- Graziani G., Gübelin E., Lucchesi S. (1983) The genesis of an emerald from the Kitwe district, Zambia. *Neues Jahrbuch für Mineralogie, Monatshefte*, Vol. 12, No. 4, pp. 175–186.
- Grundmann G. (1991) *Smaragd. Extra-LAPIS No. 1*. Christian Weise Verlag, Munich, Germany.
- Gübelin E. (1973) *Internal World of Gemstones*. ABC Edition, Zurich.
- Gübelin E. (1989) Gemological characteristics of Pakistani emeralds. In A. H. Kazmi and L. W. Snee, Eds., *Emeralds of Pakistan: Geology, Gemology, and Genesis*, Van Nostrand Reinhold, New York, pp. 75–91.
- Gübelin E., Koivula J.I. (1986) *Photoatlas of Inclusions in Gemstones*. ABC Edition, Zurich.
- Hänni H.A., Klein H.H. (1982) Ein Smaragd vorkommen in Madagaskar. *Zeitschrift der Deutschen Gemmologischen Gesellschaft*, Vol. 31, No. 1/2, pp. 71–77.
- Hänni H.A., Schwarz D., Fischer M. (1987) The emeralds of the Belmont Mine, Minas Gerais, Brazil. *Journal of Gemmology*,

- Vol. 20, No. 7/8, pp. 446–456.
- Henn U. (1988) Untersuchungen an Smaragden aus dem Swat-Tal, Pakistan. *Zeitschrift der Deutschen Gemmologischen Gesellschaft*, Vol. 37, No. 3/4, pp. 121–127
- Kleyenstüber A. (1991) Observation of inclusions in a Madagascar emerald and their possible implications. *South African Gemmologist*, Vol. 5, No. 2, pp. 4–9.
- Koivula J.I. (1982) Tourmaline as an inclusion in Zambian emeralds. *Gems & Gemology*, Vol. 18, No. 4, pp. 225–227.
- Koivula J.I. (1984) Mineral inclusions in Zambian emeralds. *Australian Gemmologist*, Vol. 15, No. 7, pp. 235–239.
- Lacroix A. (1922) *Minéralogie de Madagascar*. Augustin Challamel, Paris.
- Levat M.D. (1912) *Richesses Minérales de Madagascar*. Dunod & Pinat, Paris.
- Mendes J.C., Svisero D.P. (1988) As inclusões cristalinas e fluidas da esmeralda de Santa Terezinha de Goiás e seu significado geológico. *Anais do XXXV Congresso Brasileiro de Geologia, Belém, Pará*, Vol. 1, pp. 398–411.
- Roulet B. (1956) Métodos para determinação da procedencia de esmeraldas. *Gemologia* [Sao Paulo], No. 5, pp. 33–40.
- Schwarz D. (1987) *Esmeraldas*. Imprensa Universitária, Escola de Minas, Universidade Federal de Ouro Preto, Minas Gerais, Brazil.
- Schwarz D., Bank H., Henn U. (1988a) Neues Smaragd vorkommen in Brasilien entdeckt: Capoeirana bei Nova Era, Minas Gerais. *Zeitschrift der Deutschen Gemmologischen Gesellschaft*, Vol. 37, No. 3/4, pp. 146–147.
- Schwarz D., Hänni H.A., Martin F.L., Fischer M. (1988b) The emeralds of Fazenda Boa Esperança, Tauá, Ceará, Brazil: Occurrence and properties. *Journal of Gemmology*, Vol. 21, No. 1, pp. 168–177.
- Schwarz D., Eidt Th. (1989) The Brazilian emeralds and their occurrences: Carnaíba, Bahia. *Journal of Gemmology*, Vol. 21, No. 8, pp. 474–486.
- Schwarz D., Eidt Th., Couto P.A. (1990) The Brazilian emeralds and their occurrences: Socotó, Bahia. *Journal of Gemmology*, Vol. 22, No. 3, pp. 147–163.
- Schwarz D. (1990) Die brasilianischen Smaragde und ihre Vorkommen: Santa Terezinha de Goiás/GO. *Zeitschrift der Deutschen Gemmologischen Gesellschaft*, Vol. 39, No. 1, pp. 13–44.
- Schwarz D. (1991a) Die chemischen Eigenschaften der Smaragde II, Australien und Norwegen. *Zeitschrift der Deutschen Gemmologischen Gesellschaft*, Vol. 40, No. 1, pp. 39–66.
- Schwarz D. (1991b) Die chemischen Eigenschaften der Smaragde III. Habachtal/Österreich und Uralgebirge/UdSSR. *Zeitschrift der Deutschen Gemmologischen Gesellschaft*, Vol. 40, No. 2/3, pp. 103–143.
- Schwarz D., Henn U. (1992) Emeralds from Madagascar. *Journal of Gemmology*, Vol. 23, No. 3, pp. 140–149.
- Sinkankas J. (1981) *Emerald and Other Beryls*. Chilton Book Co., Radnor, PA.
- Thomas A. (1993) The emerald mines of Madagascar. *South African Gemmologist*, Vol. 7, No. 3, pp. 3–11.
- Van Eeden O.R., Partridge F.C., Kent L.E., Brandt J.W. (1939) *The Mineral Deposits of the Murchison Range, East of Leydsdorp*. Geological Survey of South Africa, Memoir No. 36, Pretoria.

The ultimate authority on diamonds and the diamond industry is now available for consultation.

Presenting

THE GIA DIAMOND DICTIONARY, 3rd EDITION

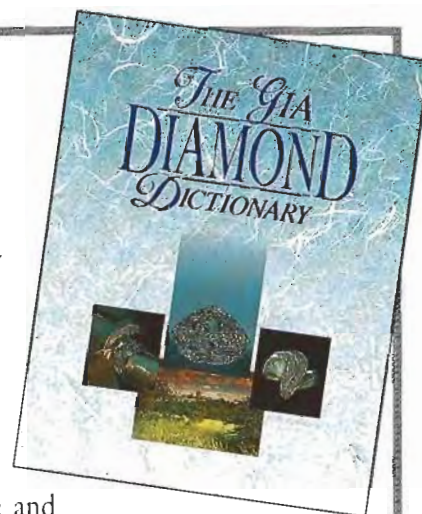
Completely revised and updated ♦ More full color photos, drawings and charts ♦ 100+ newly commissioned maps ♦ More facet diagrams ♦ More international in scope

The GIA Diamond Dictionary, 3rd Edition, contains the knowledge and expertise of an unprecedented team of industry leaders — gemologists, cutters, designers, bench jewelers, historians, geologists, physicists, and chemists from the South African grasslands to the Australian outback. It's the most detailed examination of the vast, complex and diverse world of diamonds ever published. No jewelry professional and/or student of gemology can afford to be without it.

To obtain your copy of *The GIA Diamond Dictionary, 3rd Edition*, for only \$99.50 (plus tax and shipping), call today toll-free:

(800) 421-7250, ext. 703, or FAX (310) 449-1161 ♦ **GIA Bookstore**

Price subject to publisher's change without notice



SYNTHETIC FORSTERITE AND SYNTHETIC PERIDOT

By Kurt Nassau

Large crystals of chromium-containing synthetic forsterite are being commercially manufactured for use as a laser material. Considerable color variation is possible, and some of this material resembles peridot, with which it could be confused. Synthetic peridot has been grown, but only experimentally. This material closely resembles natural peridot and might be difficult to distinguish if it were to appear in the gem market.

Recent research has led to two new products that are of potential interest, and concern, to gemologists: (1) a commercially available synthetic forsterite, MgSiO_4 , which contains chromium as both Cr^{3+} and Cr^{4+} ; and (2) a true synthetic peridot, $(\text{Mg}_{0.9}\text{Fe}_{0.1})_2\text{SiO}_4$, which currently is grown only on an experimental basis. Both forsterite and peridot are members of the olivine series.

Historically, synthetic gem materials usually emerged either indirectly from studies aimed at understanding mineralogical problems or directly from efforts to achieve the synthetic equivalent of a natural gem for jewelry use. In recent years, however, most new synthetics have been spin-offs of

research for solid-state technology, with laser research being the dominant contributor. This is the source of the recently developed synthetic forsterite (Nishide et al., 1985; Verdun et al., 1988), which is being investigated as a host material for a tunable near-infrared laser.

Chromium-doped synthetic forsterite crystals (figure 1) are currently being grown commercially using the Czochralski-pulling technique by K. Yamagishi, at the Ageo City Central Research Laboratory of the Mitsui Mining and Smelting Co., Tokyo. Studies of the optical properties and laser characteristics have been conducted in the Department of Physics and Electrical Engineering, City College of New York (Petricevic et al., 1988b-c, 1989a-c, 1990; Alfano et al., 1989); and by these researchers in cooperation with K. Yamagishi and coworkers (Petricevic et al., 1988a). They have demonstrated that this laser material is synthetic Mg_2SiO_4 , containing about 0.04 wt.% chromium. Under reducing conditions, all the chromium is Cr^{3+} , substituting simultaneously in both octahedral magnesium sites of this orthorhombic structure. When "standard" oxidizing conditions (i.e., ambient air) are used, there is also some Cr^{4+} present, substituting for silicon. It is this Cr^{4+} that provides the broad infrared fluorescence (680 to 1400 nm) that is used in the laser, which is tunable from 1167 to 1345 nm (note that in some of the

ABOUT THE AUTHOR

Dr. Nassau, retired from his position as Distinguished Scientist at AT&T Bell Laboratories, is now a freelance writer, consultant, and expert witness living in Lebanon, New Jersey.

Acknowledgments: The author thanks Y. Terashima, of Mitsui Mining and Smelting Co., and Dr. F. J. Ryerson, of Lawrence Livermore National Laboratory, for kindly supplying material for study. He also thanks the following personnel of the GIA Gem Trade Laboratory, New York: Dr. I. Reinitz for the absorption spectra of figure 6 and, with R. Crowningshield and former staff member D. Hargett, for checking gemological properties. Original manuscript received November 1992.

Gems & Gemology, Vol. 30, No. 2, pp. 102-108

© 1994 Gemological Institute of America

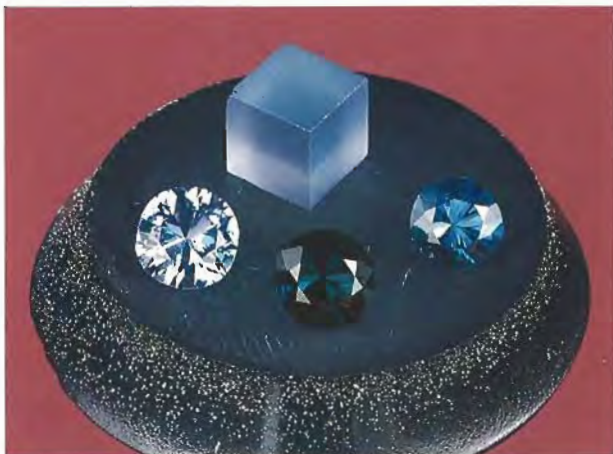


Figure 1. These samples of chromium-doped synthetic forsterite were manufactured by Mitsui Mining and Smelting Co. for laser use: a 2.7-cm-diameter slice, a 0.5-cm cube, and three faceted samples (1.18, 1.07, and 0.83 ct). Photo by N. DelRe.

early reports, the presence of Cr^{4+} had not yet been recognized). This is indeed the only laser material that uses Cr^{4+} . This variation in the valence state of chromium, as well as the differences in chromium concentration, combine with the pleochroism of olivine to produce a wide range of colors, including green, blue, pink, and purple. These hues could also be modified by heat treatment in different atmospheres.

According to a recent International Colored Gemstone Association (ICA) Laboratory Alert (Mican, 1992), green, chromium-containing synthetic forsterite is also being marketed for laser and jewelry use inappropriately labeled "chrysolite (olivine)" by Solix Co. of "Minsk, Republic of Byelarus." Mican examined some of this material, but he used the inappropriate designation "synthetic peridot" in his report. The older nomenclature is indeed confusing and is summarized, together with the modern usage, in box A.

BOX A: THE CHEMISTRY AND NOMENCLATURE OF THE OLIVINE SERIES

Forsterite is a member of the olivine group of minerals, which consists of the fayalite-forsterite solid-solution series with composition $(100-x)\text{Mg}_2\text{SiO}_4 \cdot x\text{Fe}_2\text{SiO}_4$, with iron in the divalent state. The designation forsterite applies to the end member Mg_2SiO_4 and traditionally also to the composition range $0 < x < 10$ (i.e., with as much as 10 mol.% fayalite), also designated Fo_{100} to $\text{Fo}_{90}\text{Fa}_{10}$, where Fo is forsterite and Fa is fayalite. The latter is the other end member, Fe_2SiO_4 , which has a traditional composition range of $90 < x < 100$ or $\text{Fo}_{10}\text{Fa}_{90}$ to Fa_{100} . Other traditional members of the olivine series are chrysolite, which covers the range $10 < x < 30$ or $\text{Fo}_{90}\text{Fa}_{10}$ to $\text{Fo}_{70}\text{Fa}_{30}$; hyaloserite, $30 < x < 50$; horttonolite, $50 < x < 70$; and ferrohorttonolite, $70 < x < 90$.

The modern approach is to drop all intermediate names—which, for example, are no longer listed as such in the *Glossary of Mineral Species* (Fleischer and Mandarino, 1991)—and simply to give Fo:Fa percentages. Details of the terminology, chemistry, structure, and other aspects of the olivines have been given by Deer et al. (1962) and by Brown (1982).

The gemologist knows olivine best as peridot, which is usually defined as the transparent to translucent yellowish green to greenish yellow to brownish green gem variety of olivine. The green derives from Fe^{2+} , whereas the yellow and brown components derive from the presence of some of the iron in the

Fe^{3+} state. The typical iron content has been reported as 9% (Bauer, 1904), 10% (Anderson, 1980), and 14% (Hanson et al., 1991), thus ranging in the traditional sense from the end of the forsterite field into the chrysolite field; the range of refractive indexes reported for peridot also brackets both of these fields (see also Bank, 1986). Thus, peridot is an olivine and belongs to both the iron-rich forsterite and the now-discontinued chrysolite mineral species. It does have significant structural iron content, not just at the color-causing impurity level.

The designation by Solix (Mican, 1992) of their chromium-containing forsterite product as "chrysolite (olivine)" is incorrect, because: (1) its composition does not belong to the chrysolite range; (2) even if it did, the term *chrysolite* is no longer used; and (3) while this material is indeed within the olivine series, it is not appropriate to use the series designation when dealing with end-member forsterite. In the opinion of the author, this material should also not be designated "synthetic peridot," as Mican (1992) does, because it contains a different color-causing impurity and also does not contain the necessary 10% or so of structural iron.

Pure (and thus colorless) forsterite has also been grown, both at Mitsui and elsewhere, but it was not available for examination. To a gemologist, such material is simply "colorless synthetic forsterite."

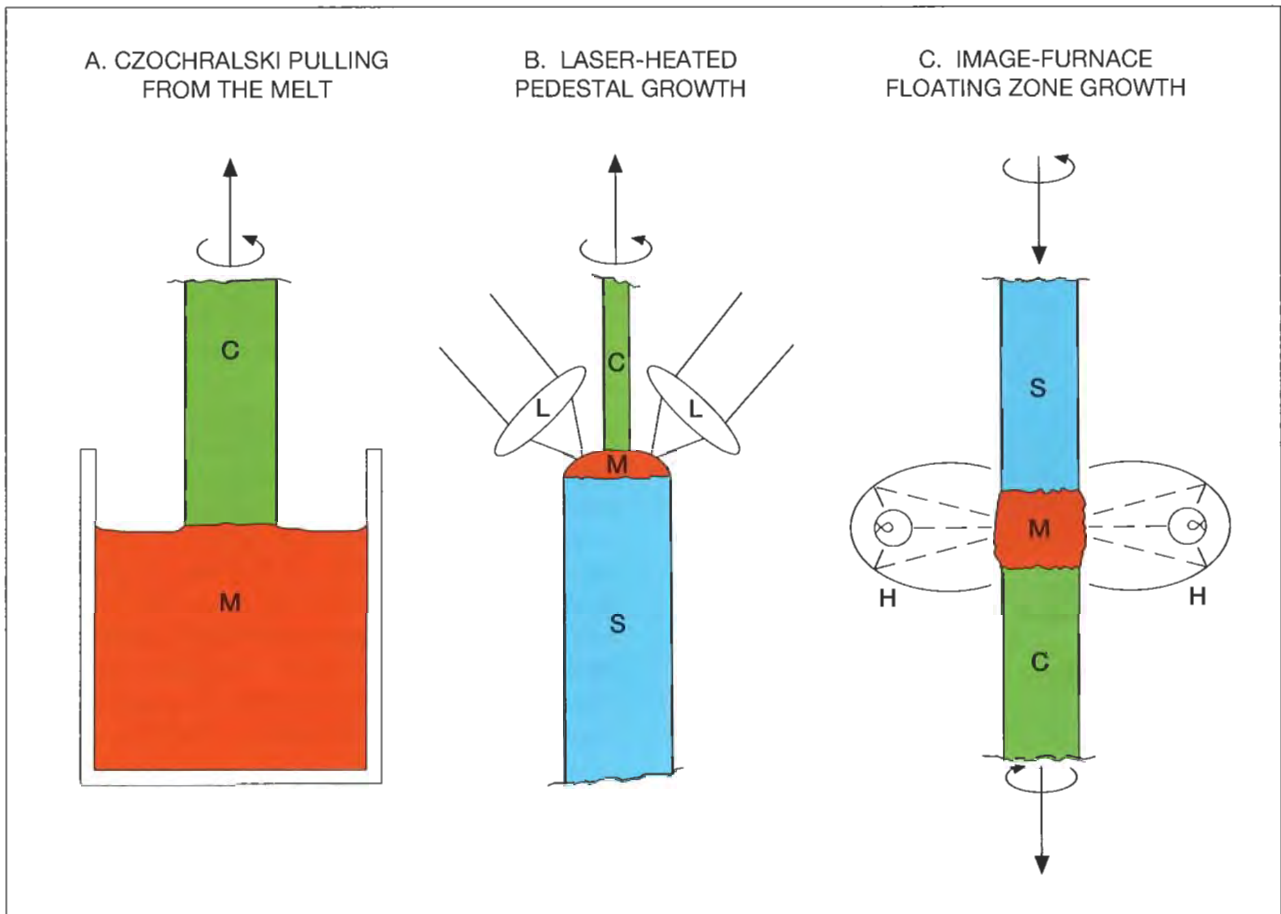


Figure 2. These three melt-growth techniques have been used to manufacture synthetic forsterite or synthetic peridot. The letters in each diagram refer to the following: M—melt, C—growing crystal, S—sintered ceramic, L—laser beam focused by a mirror and lens system (only partly illustrated), and H—halogen lamp focused by an ellipsoidal reflector. The arrows indicate motion.

True synthetic peridot has been grown as part of a study of the crystal growth of olivines at the Lawrence Livermore National Laboratory (LLNL), Livermore, California, as briefly outlined in box B. Experience has shown that any synthetic material, even if not intended for gem use, is likely to be faceted and would then become a real challenge to the unsuspecting gemologist. Accordingly, both the Mitsui synthetic forsterite and the LLNL synthetic peridot are described here.

CRYSTAL SYNTHESIS

Silicate compounds usually produce too viscous a melt to permit growth by techniques such as Czochralski pulling; rather, they require flux or hydrothermal growth as, for example, with synthetic emerald. However, forsterite and peridot appear to be exceptions, in that melt growth can be used if growth is slow and adequate care is taken.

Three melt-growth techniques have been used to produce laser-quality synthetic forsterite (SF)

and synthetic peridot (SP), as illustrated in figure 2: Czochralski pulling from the melt (for SF; Finch and Clark, 1971; Takei and Kobayashi, 1974; Nishide et al., 1985; also at Union Carbide and at the University of Marburg, Germany, as mentioned by Rager et al., 1991); laser-heated pedestal growth (for SF; Verdun et al., 1988; Jia et al., 1991); and image-furnace floating-zone growth (for SP; Hanson et al., 1991).

The Czochralski technique (figure 2A) is well known, and its use to grow synthetic forsterite is well documented (see, e.g., Peicong et al., 1992). In the pedestal technique (figure 2B), the intense light beam from a laser is used to melt the upper end of a vertical rod of sintered ceramic material; pulling is then performed upward out of this melt. In the floating-zone technique (figure 2C), the radiant energy from two 1.5-kW halogen light bulbs is focused onto a vertical sintered ceramic rod to melt a narrow zone which is then made to traverse the rod.

Earlier experiments to produce synthetic forsterite with the Verneuil flame-fusion technique (Shankland and Hemmenway, 1963) and the Bridgeman technique of directional solidification in a crucible (Jordan and Naughton, 1964) were successful, but they did not provide adequate quality or size.

Forsterite crystals over 2.5 cm in diameter and up to 20 cm long have been grown by Czochralski pulling. In North America, the Mitsui synthetic forsterite is marketed for laser use exclusively by Mediscience Technology Corp., Forsterite Division, of New York City. The Solix material (Mican, 1992) reportedly is also made by Czochralski pulling and is available as rods 2.5 cm in diameter and 12 cm long.

MATERIALS AND METHODS

The synthetic forsterite examined for this study was obtained from Mr. Y. Terashima of Mitsui's New York office. He provided a 15.85-ct slice (0.4 cm thick and 2.7 cm in diameter) and a 2.53-ct X-ray oriented cube (0.5 cm) for detailed study, as

well as three faceted samples (1.18-ct pale blue-green, 0.83-ct medium blue, and 1.07-ct dark blue) for brief examination (again, see figure 1). The pleochroic colors seen in the cube are shown in figure 3. Laser-grade material, by its nature, must be of the highest optical quality; the specimens available for study were of lower grade but still adequate for gem use.

A pale greenish yellow crystal of synthetic peridot (figures 4 and 5) was obtained from Dr. F. J. Ryerson of Lawrence Livermore National Laboratory. The 0.79-gram crystal was 0.6 cm in diameter and 1.8 cm long.

The properties given here for synthetic forsterite colored by chromium are based on precision scientific measurements (e.g., on polished prisms) reported by Alfano et al. (1989), Petricevic et al. (1988a-c, 1989a-c, 1990), in the Mitsui sales literature (no author, undated), and in the Solix literature as reproduced by Mican (1992). They are also based on gemological measurements made by the author and by staff members of the GIA Gem Trade Laboratory, New York, on the 15.85-ct slice and 2.53-ct cube.

BOX B: EXPERIMENTAL SYNTHETIC PERIDOT

True synthetic peridot—that is, a composition in the olivine series containing about 10 mol.% iron—has been produced as part of a research program at LLNL by Hanson, Young, and Ryerson (1991). This group has performed a detailed study on the crystal growth of synthetic olivines ranging from colorless pure synthetic forsterite Mg_2SiO_4 to a dark green $Fe_{0.67}Fa_{0.33}$ [that is $(Mg_{0.67}Fe_{0.33})_2SiO_4$], using the image-furnace floating-zone technique with an atmosphere of mixed carbon monoxide/carbon dioxide and a growth rate of about 0.2 cm per hour. When there was an oxygen leak, a brown peridot resulted, which also sometimes occurs in nature. Both cracking and bubble inclusions were problems, but these could be controlled by adjusting the shape of the crystal-melt interface with an afterheater. Crystals up to 1 cm in diameter and up to 7 cm long were grown without cracks and with only an occasional bubble.

The pale greenish yellow crystal studied was heavily included (see figures 4 and 5). Nevertheless, there were some clear areas. Good-quality and deeper green, higher-iron-composition crystals have been grown, but they were not available for this report as they were needed for technological studies. Although it is possible that such synthetic peridot could enter

the market as a lower-cost substitute for the natural material, the low demand for peridot relative to the current production of the natural material makes this scenario unlikely.

Because the clarity of the specimen examined was reduced by the many included gas bubbles, some with tails, only limited gemological data could be determined. A biaxial figure confirmed that the material was, like natural peridot, doubly refractive; other properties are listed in table 1. The pleochroism is light grayish green/light yellow, there was no reaction to U.V. radiation, and the hand spectroscope showed optical absorptions at about 453, 474, and 497 nm. All these data are consistent with values expected for a pale-colored natural peridot, as listed in the literature (e.g., Webster, 1983; GIA, 1988).

Since production to date has been experimental only, it is not possible to establish at this point what the distinguishing criteria between natural and a possible future commercial synthetic peridot might be. In view of the limited data available, conventional gemological testing will probably parallel that for many other synthetics, with the presence (or absence) of certain inclusions likely to be the significant distinguishing criterion.

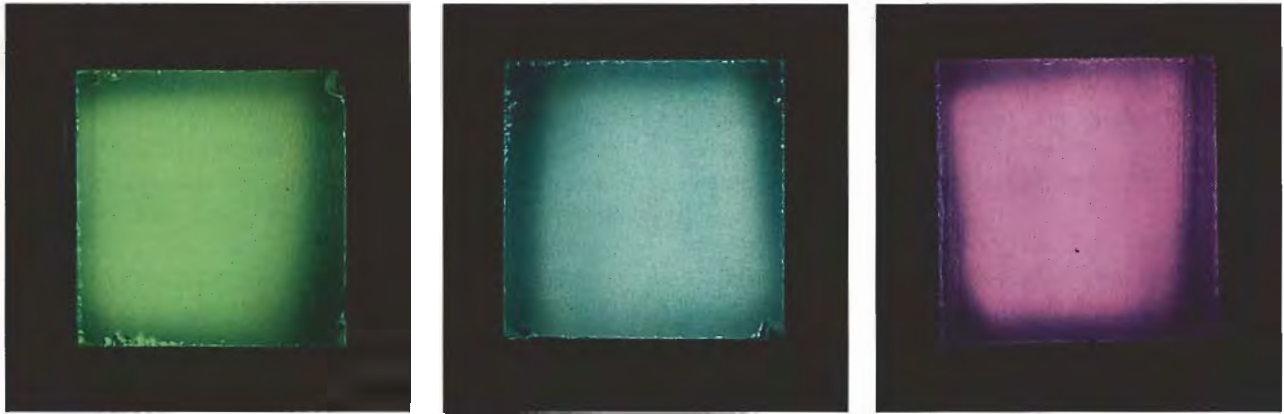


Figure 3. The 0.5-cm cube of chromium-doped synthetic forsterite in figure 1 is illustrated in three different orientations to show the pleochroism for the α , β , and γ spectra, respectively. Photos by N. DelRe.

We determined specific gravities by hydrostatic weighing and optical properties using a GIA-GEM Duplex II refractometer, a polariscope, a diffraction-grating hand spectroscope, and a dichroscope. Polarized absorption spectra were obtained from the 0.5-cm cube with a Hitachi U-4001 split-beam spectrophotometer with an integrating sphere detector.

GEMOLOGICAL PROPERTIES

The mechanical and optical properties of the slice and cube of synthetic forsterite and the crystal section of synthetic peridot are listed in table 1, together with comparative data for natural forsterite and peridot taken from the literature. Other observations on the synthetic forsterite are described below. The properties of the synthetic peridot specimen, which was not gem quality and was grown for experimental purposes only, are discussed and compared with those of natural peridot in box B.

Color. Chromium-containing synthetic forsterite varies from pale to deep blue to blue-green, green, pink, and purple. Since the precise pleochroic colors depend on the ratio of Cr^{3+} to Cr^{4+} and their concentrations, these colors may vary, including various shades of pale to deep yellow-green, green, blue-green, blue, and reddish purple (again, see figures 1 and 3).

Fluorescence. Like natural peridot, chromium-containing synthetic forsterite is inert to both short- and long-wave ultraviolet radiation. The red fluorescence of the chromium R line (present in all Cr^{3+} -containing materials, such as ruby and emerald) is seen only when the material is cooled to liquid-nitrogen temperature.

Absorption Spectra. In the hand spectroscope, there is an intense absorption up to 450 nm; a weak one (which is stronger when the color is intense) from there to 500 nm; a group of three bands at 530, 550,

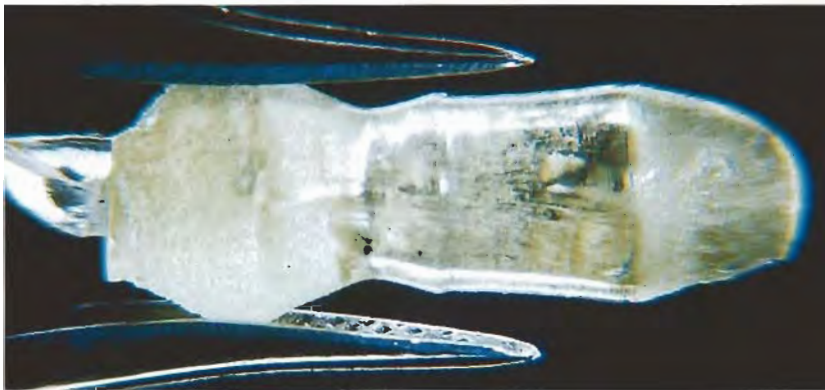


Figure 4. This 1.8-cm-long synthetic peridot crystal, shown viewed with darkfield illumination, was grown by the Lawrence Livermore National Laboratory for experimental purposes. Photo by N. DelRe.

and 580 nm; and a band at 690 nm. This spectrum is quite different from that caused by iron in peridot (GIA, 1988).

The polarized absorption spectra for the cube, shown in figure 6, are essentially the same as those reported by Petricevic et al. (1989a), Alfano et al. (1989), and Rager et al. (1991).

Inclusions. Laser-grade forsterite shows no inclusions at 10× magnification. The poorer-grade material we examined contained a number of white spicules and thin, thread-like inclusions or gas bubbles. The Solix forsterite was reported by Mican (1992) to contain gas bubbles as well as solid inclusions with tail-like hollow channels attached.

DISTINCTION OF SYNTHETIC FORSTERITE FROM NATURAL PERIDOT

While the color of chromium-containing synthetic forsterite usually differs from that of peridot, a peridot-like color is possible and there is sufficient overlap in the gemological properties to provide the possibility of confusion. However, both the refractive-index and specific-gravity values for synthetic forsterite are somewhat lower than those recorded for peridot (see table 1). In the absence of a careful specific-gravity determination or a detailed

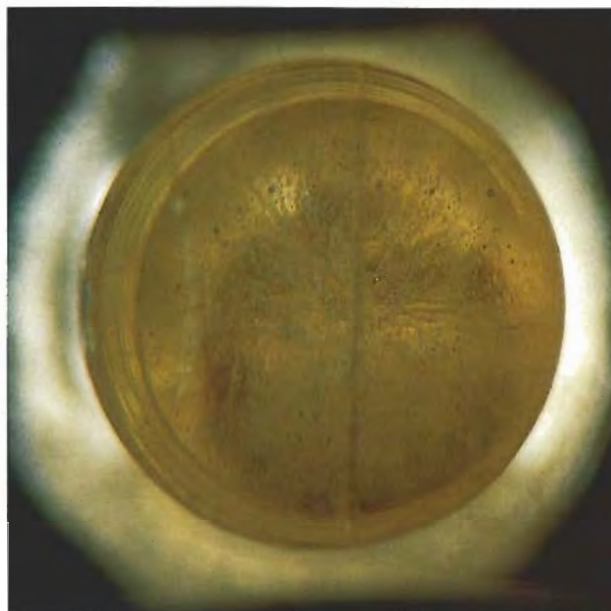


Figure 5. In this view of a cut and polished surface of the crystal in figure 4, one can see how heavily included it was in some areas. Photo by N. DelRe.

refractive-index study, the best distinction is given by the visible-range spectrum of the synthetic forsterite, which shows chromium-related features not found in natural peridot (or forsterite).

TABLE 1. Mechanical and optical properties of synthetic and natural forsterite and peridot.

Property	Forsterite			Peridot	
	Synthetic		Natural	Synthetic	Natural
	Literature ^a	Measured ^b	Literature ^c	Measured ^b	Literature ^d
Mechanical:					
Mohs hardness	6 ¹ / ₂ –7	7	7	7	6 ¹ / ₂ –7
Specific gravity	3.213–3.217	3.15	3.21–3.33	3.30	3.27–3.48
Fracture	Conchoidal with vitreous to subvitreous luster	Conchoidal with vitreous to subvitreous luster	Conchoidal with vitreous to subvitreous luster	Conchoidal with vitreous to subvitreous luster	Conchoidal with vitreous to subvitreous luster
Optical:					
Character	Biaxial positive	Biaxial	Biaxial positive	Biaxial	Biaxial positive
Refractive index	1.636–1.669	1.63–1.67	1.635–1.670	1.65–1.68	1.654–1.690
α	1.6359		1.635		1.654
β	1.6507		1.651		1.671
γ	1.6688		1.670		1.689
Birefringence	0.033–0.040	0.04	0.035	0.03	0.035–0.038

^aAfter Alfano et al. (1989), Petricevic et al. (1988a–c, 1989a–c, 1990), the Mitsui sales literature (no author, undated), and the Solix literature reproduced by Mican (1992).

^bMeasurements made by the author and GIA-GTL New York for this study on the five chromium-doped synthetic forsterites and one synthetic peridot described in this article.

^cAfter Roberts et al. (1974).

^dAfter the *Gem Reference Guide* (GIA, 1988) and Webster (1983).

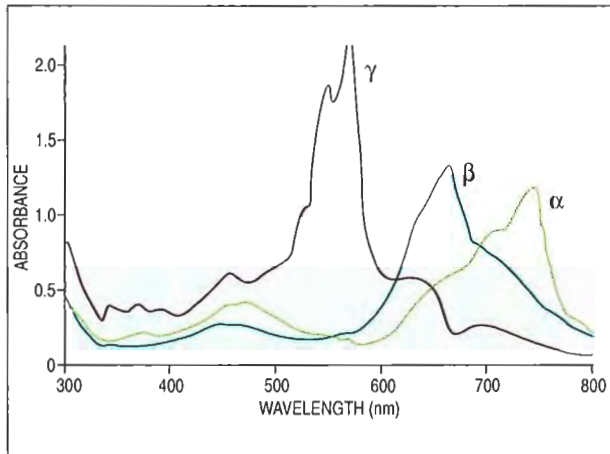


Figure 6. These absorption spectra were recorded from the three directions of the synthetic forsterite shown in figure 3: (α -spectrum E//b) greenish yellow direction, (β -spectrum E//c) bluish green direction, and (γ -spectrum E//a) purple direction.

CONCLUSIONS

Synthetic forsterite colored by chromium, which is being grown from a melt for laser use, is now commercially available in sizes up to 2.5 cm in diameter and 20 cm long. This material can vary somewhat in color because of variable Cr^{3+} and Cr^{4+} content; it is pleochroic—typically purple, bluish green, and greenish yellow. Although yellowish green to greenish yellow synthetic forsterite might be used as a substitute for natural peridot, the lower R.I. and S.G. values of the synthetic forsterite—due to the absence of a substantial amount of iron—help separate it from gem peridot. In addition, the visible absorption spectrum of the chromium-containing synthetic forsterite is significantly different from that of natural peridot.

The gemological properties of the experimental synthetic peridot examined are essentially the same as those of natural peridot. The only difference noted was in the inclusions.

REFERENCES

- Alfano R.R., Petricevic V., Seas A. (1989) Chromium doped forsterite laser. In F. Duarte, Ed., *Proceedings of the International Conference on Lasers '89*, Dec. 3–8, STS Press, McLean, VA, pp. 441–448.
- Anderson B.W. (1980) *Gem Testing*, 9th ed. Butterworths, Boston.
- Bank H. (1986) Hochlichtbrechende Olivine aus der Eifel. *Zeitschrift der Deutschen Gemmologischen Gesellschaft*, Vol. 35, pp. 185–186.
- Bauer M. (1904) *Precious Stones*. Reprinted by Dover Publications, New York, 1968.
- Brown G.E. (1982) Olivine and silicate spinels. In P. H. Ribbe, Ed., *Reviews of Mineralogy*, Vol. 5, Mineralogical Society of America, Washington, DC, pp. 275–381.
- Deer W.A., Howie R.A., Zussman J. (1962) Olivine group. In *Rock Forming Minerals*, Vol. 1, John Wiley & Sons, New York, pp. 1–33.
- Fleischer M., Mandarino J.A. (1991) *Glossary of Mineral Species 1991*. Mineralogical Record, Tucson, AZ.
- Finch C.B., Clark G.W. (1971) Czochralski growth of single crystal Mg_2SiO_4 [forsterite]. *Journal of Crystal Growth*, Vol. 8, pp. 307–308.
- Gemological Institute of America [GIA] (1988) *Gem Reference Guide*. Santa Monica, CA.
- Hanson D.R., Young M., Ryerson F.J. (1991) Growth and characterization of synthetic iron-bearing olivine. *Physics and Chemistry of Minerals*, Vol. 18, pp. 53–63.
- Jia W., Lu L., Tiddue B.M., Yen W.M. (1991) Valence and site occupation of chromium ions in single-crystal forsterite. *Journal of Crystal Growth*, Vol. 109, pp. 329–333.
- Jordan W., Naughton J.J. (1964) Growth of forsterite crystal in a reactive crucible. *American Mineralogist*, Vol. 49, pp. 806–808.
- Mican W. (1992) Synthetic peridot (Juwelia). In ICA Early Warning—Flash, Laboratory Alert No. 62, October 6, 1992.
- Nishide N., Segawa Y., Kim P.H., Namba S., Masuyama A. (1985) Optical Properties of Forsterite. *Reza Kagaku Kenkyu*, Vol. 7, pp. 89–91.
- Pcicong P., Hongbin Z., Shenhui Y., Yiao C., Siting W., Yinchun H. (1992) Distribution and valence of chromium in forsterite crystals grown by the Czochralski technique. *Journal of Crystal Growth*, Vol. 121, pp. 141–147.
- Petricevic V., Gayen S.K., Alfano R.R., Yamagishi K., Anzai H., Yamaguchi Y. (1988a) Laser action in chromium-doped forsterite. *Applied Physics Letters*, Vol. 52, No. 13, pp. 1040–1042.
- Petricevic V., Gayen S.K., Alfano R.R. (1988b) Laser action in chromium-activated forsterite for near infrared excitation. *Applied Optics*, Vol. 27, No. 20, pp. 4162–4163.
- (1988c) Laser action in chromium-activated forsterite for near infrared excitation: Is Cr^{4+} the lasing ion? *Applied Physics Letters*, Vol. 53, No. 26, pp. 2590–2592.
- (1989a) Chromium-activated forsterite laser. In M. L. Shand and H. P. Jensen, Eds., *Tunable Solid State Lasers*, Vol. 5, Proceedings Series of the Optical Society of America, Washington, DC, pp. 77–84.
- (1989b) Near infrared tunable operation of chromium doped forsterite laser. *Applied Optics*, Vol. 28, No. 9, pp. 1609–1611.
- (1989c) Continuous-wave laser operation of chromium-doped forsterite. *Optics Letters*, Vol. 14, No. 12, pp. 612–614.
- (1990) Forsterite laser tuncs in near-IR. *Laser Focus World*, November 1990, pp. 109–116.
- Rager H., Taran M., Khomenko V. (1991) Polarized optical absorption spectra of synthetic chromium-doped Mg_2SiO_4 [forsterite]. *Physics and Chemistry of Minerals*, Vol. 18, pp. 37–39.
- Roberts W.L., Rapp G.R. Jr., Weber J. (1974) *Encyclopedia of Minerals*. Van Nostrand Reinhold Co., New York.
- Shankland T.J., Hemmenway K. (1963) Synthesis of forsterite crystals. *American Mineralogist*, Vol. 48, p. 200.
- Takei H., Kobayashi T. (1974) Growth and properties of Mg_2SiO_4 single crystals. *Journal of Crystal Growth*, Vol. 23, pp. 121–124.
- Verdun H.R., Thomas L.M., Andrauskas D.M., McCollum T., Pinto A. (1988) Cr-containing forsterite. *Applied Physics Letters*, Vol. 53, p. 2593.
- Webster R. (1983) *Gems*, 4th ed. Rev. by B. W. Anderson, Butterworths, Boston.

UPDATE ON MINING RUBIES AND FANCY SAPPHIRES IN NORTHERN VIETNAM

By Robert C. Kammerling, Alice S. Keller, Kenneth V. Scarratt, and Saverio Repetto

Northern Vietnam began producing significant quantities of rubies and fancy sapphires in the late 1980s. Since then, mining has evolved at the two major producing areas: Luc Yen and Quy Chau. Heavy machinery is now used in both of these remote areas, but small-scale manual mining is ongoing. Efforts continue to establish organized cutting and distribution centers.

Vietnam is the site of some of the most significant gem deposits discovered in the last decade. Millions of carats of rubies and fancy sapphires have been produced since organized mining started in 1989 (see, e.g., figure 1). Although the United States' lifting of its 19-year-old trade embargo against Vietnam this past spring may not increase the number of gems that directly enter the U.S. from Vietnam (to date, most have come via Thailand), the potential for U.S. investment there could help increase gem production overall.

In 1991, Kane et al. published a comprehensive article on the gemological properties of rubies and fancy sapphires from northern Vietnam. At that

time, however, mining had just begun, and little detailed information was available on operations at the two main locations, Luc Yen (in Yen Bai Province) and Quy Chau (in Bu Khang District, Nghe An Province). Trips made by the present authors to these two areas in October and November of 1992, and January and November of 1993, provided the opportunity to see these mining activities firsthand and to update the extent of the operations. This article provides a brief review of our observations during these visits, as well as information on the current status of gem production at Luc Yen and Quy Chau as provided by mining company executives and local geologists.

LUC YEN DISTRICT

The first leg of the trip to Luc Yen from Hanoi is mostly over paved road, through fields of corn and tea, approximately 150 km northwest to the city of Yen Bai, the capital of Yen Bai Province (see map, Kane et al., 1991, p. 138). The town of Luc Yen is another 93 km north of Yen Bai, over rough, partially paved roads that are difficult to travel in the rainy season (May to November). During all visits, we had to present the proper documentation at military checkpoints before we were allowed to enter the mining area.

Gem-bearing gravels have been found just south of the town of Luc Yen, in valleys near and along the foothills of the Bac Bo Mountains, where marbleized limestone has weathered and left

ABOUT THE AUTHORS

Mr. Kammerling is director of identification and research, GIA Gem Trade Laboratory, Santa Monica, California; Ms. Keller is editor, *Gems & Gemology*, GIA, Santa Monica; Mr. Scarratt is director of Laboratory Services, Education, and Research at the Asian Institute of Gemological Sciences, Bangkok, Thailand; Saverio Repetto is general director, Gemological Institute of Vietnam, Hanoi.

Acknowledgments: The authors thank the following for providing information and access to the mining localities: Dr. Phan Truong Thi, Mineralogical Association of Vietnam, Hanoi; Boonsin Jatoorapreuk, managing director, B.H. Mining Co., Bangkok; Donato Cremaschi, FinGems, Chiasso, Switzerland; and Nguyen Duc Khai, senior expert, Council of Ministers, Government of Vietnam, Hanoi.

Gems & Gemology, Vol. 30, No. 2, pp. 109-114.

© 1994 Gemological Institute of America



Figure 1. These three gems (1.15–1.82 ct) are representative of the fine rubies and fancy sapphires that have been produced in Vietnam since mining commenced in 1989. The center stone shows some of the blue zoning commonly seen in Vietnamese material (see, e.g., Kane et al., 1991). Courtesy of Evan Caplan & Co., Los Angeles, CA; photo © GIA and Tino Hammid.

behind heavy minerals—including rubies, sapphires, and spinels—in potentially rich concentrations. The original engineering study on the Luc Yen area, by the Dutch firm Herinckx & Partners ("Mine plan revision . . .," 1990), identified 11 valleys in the Luc Yen area as having commercial gem potential: Lung Cay–Lang Chuong, "Area 298," Khoan Thong, Han Lo, Yen Thang, Yen The, Lieu Do, Da Doung–Ngoi Biet, Lang Thoc, Doong Boc, and "Area 606." As detailed in Kane et al. (1991), these valleys are often narrow, small depressions that are typically no more than 3 km²; small-scale working of the alluvial gravels in these and other areas has been ongoing since at least 1987, with organized mining since 1989.

At the time of our visits, the main mining activity at Luc Yen was a relatively sophisticated mechanized operation managed by a joint venture—established in August 1991 as "Viet-Thai Gems Company"—between the Thai firm B.H. Mining Co., the Vietnamese National Gems Company (Vinagemco), and the Industrial Geology Group of Yen Bai (formerly Hoang Lien Son) Province. The joint venture was granted a 12-year concession to exploit an area encompassing 81.7-hectares (200 acres). The concession area includes Khoan Thong Valley (five distinct prospects), Lung Cay, Lang Chuong, Nuoc Ngap, and Lieu Do ("The ruby project . . .," 1994).

Throughout the district, we also saw small "independent" operations. In all cases, we saw only mining of alluvial gravels, and we understand that no attempt has yet been made to mine rubies *in situ* (B. Jatooapreuk, pers. comm., 1994).

Mechanized Mining. We visited the first area exploited, Khoan Thong I, and one of the newest ones, Ngoc Ngap (1.5 km by road from Khoan Thong I). During our 1992 visits, Khoan Thong I was the only area being mined. Four electrically powered, high-pressure hydraulic cannons drew water from a nearby reservoir to wash the soil and gem-bearing gravels into a pit (figure 2). From the pit, this material was pumped to a nearby sluicing system for gravity concentration. The system consisted of a large (about 2 m in diameter) rotating drum and six vibrating jigs (four primary, two secondary); the resulting heavy concentrate was collected at the end of the sluicing system (figure 3) and taken to the mining camp to be sorted by hand (figure 4). Mine officials told us that approximately 155 people were involved in mining and processing at the time.

At Khoan Thong I, the joint venture processed about 250–300 m³ of soil and gravel daily, or about 8,000 m³ per month. According to the January 1994 B.H. Mining report ("The ruby project . . ."), from November 1991 to November 1992, this operation produced 88,329 grams (441,645 carats) of rough gem minerals, of which 5% was described as "ruby and pink sapphire," 0.04% as "blue sapphire," and 4% as "semi-precious" stones (including spinel). The balance was listed as "red corundum" (i.e., not gem quality).

By January 1993, the joint venture had greatly reduced activity at Khoan Thong I; by November 1993, mining had almost ceased (see figure 2, inset). During 1993, development started at Nuoc Ngap, using the same methods and equipment as



Figure 2. Khoan Thong I was the only deposit in Luc Yen being mined with heavy equipment during the authors' late-1992 visits. Here, high-pressure water cannons wash soil and gem-bearing gravels into a pit for subsequent processing. By November 1993 (inset), mining at Khoan Thong had almost ceased, and the original excavation had become an artificial lake not unlike the one at Mogok, Myanmar. Photos by Robert C. Kammerling.

we had seen used at Khoan Thong I earlier.

In July 1994, the managing director of B.H. Mining, Boonsin Jatoorapreuk, informed us that Khoan Thong I is now closed (the gravels completely worked out) and gem production at the concession has dropped off greatly in the last six months. Mining continues at Nuoc Ngap, but activities at the newest operation, Khoan Thong III, have been halted for reassessment because of poor production. The costs of building roads and bridges to bring equipment into this remote jungle area are high. Without an economic return like that from Khoan Thong I, Mr. Jatoorapreuk believes it may be more profitable for B.H. Mining to let the area revert to independent mining and simply set up a permanent buying office. Still, he remains optimistic about the gem potential of the area in general.

Independent Mining. Largely unsanctioned, independent mining has been ongoing in Luc Yen since

gems were first identified in the area. Two of the authors (RCK and ASK) saw one such operation high in the hills, where miners worked weathered material by hand in a small depression between an exposed marble pillar-like outcrop and the mountainside. Because there is no water in such venues, miners typically conduct a dry separation on site and then transport the gravels to lower-lying areas for washing. There are also small-scale operations working the valley gravels.

Marketing and Fashioning. Gems recovered by the joint venture are fashioned in their own factory in Hanoi, which became operational in November 1992. When one of the authors (KVS) visited this facility in January 1993, 48 faceting machines were being used to cut rubies, fancy sapphires, and other local gem materials. A cutting factory has also been built in Yen Bai, and training is expected to start soon (B. Jatoorapreuk, pers. comm., 1994).



Figure 3. From the pit shown in figure 2, the gem-bearing gravels were pumped to this large sluicing system that, at the time (November 1992), was about 30 m away. The heavy-mineral concentrate collected here, at the end of the system, was then taken to the mine headquarters. Photo by Robert C. Kammerling.

Independent miners can legally sell rough gems at a government-run market in the town of Luc Yen. This fenced-in compound accommodates about 40 to 50 small wooden tables at which the gem dealers sit (figure 5). On all our visits we saw thousands of carats of rough rubies and fancy sapphires. Most appeared to be typical "mine run," although we were told that higher-quality goods are available but not openly displayed. Most of the gem-quality rubies we saw were small (1 ct or less); there were also miscellaneous parcels of what appeared to be tourmaline, spinel (see, e.g., Koivula et al., 1993a), amethyst, and other varieties of quartz. The government receives a royalty of about 8%–12% on stones sold at this and the three other official gem markets (i.e., in Vinh, Hanoi, and Ho Chi Minh City).

All of the authors were offered stones outside the legal channels in all of the mining areas visited. Most of these "gems" were either of very poor quality or of synthetic origin, a recurring problem (see, e.g., Koivula et al., 1993b).

QUY CHAU (BU KHANG DISTRICT)

The Bu Khang District is located north-northwest of Vinh, the capital of Nghe An Province (again, refer to the map in Kane et al., 1991, p. 138). To reach the mining area from Vinh, we first traveled 50 km north on the road to Hanoi, then turned west onto the road to Quy Chau Village (63 km total, mostly partially paved or dirt road). As at Luc Yen, this mining region is difficult to access during the rainy season and entry is controlled by the military.

Mining started in the Bu Khang District only in late 1990. The area was worked by thousands of independent miners (see, e.g., Kane et al., 1991), who literally leveled hills in their search for the gem-bearing gravels. By late 1992, mining (all alluvial) of the area had been assigned to four specific "companies," which collectively controlled an area of approximately 300 hectares (741 acres).

Company No. 1. Located near the village of Quy Chau at a site known as "Billionaire Hill" because of the many gems early miners had found there, Company No. 1 is run by the Vietnamese Ministry of Heavy Industry. It began operation in May 1992 and was still active in July 1994 (P. T. Thi, pers. comm., 1994).

At the time of our November 1992 visit, this was a fairly typical mechanized open-pit operation.

Figure 4. Gem materials removed from Khoan Thong I concentrate were sorted at mine headquarters. Photo by Kenneth V. Scarratt.



A backhoe pushed the red lateritic soil and underlying gravels into a large depression filled with water transported by two diesel-powered pumps from a local stream. Here, the gravels were washed by a high-pressure water cannon and then pumped to a nearby sluice for processing. The heavy concentrate was examined and sorted on site by hand.

We were told by mine officials in November 1992 that the 120+-hectare concession employed 50 workers and had produced about 27 kg (135,000 carats) of rough rubies and fancy sapphires in the first six months of mechanized mining (May 7 to November 18, 1992). We were shown what was reportedly three days' production—a total of 239.80 carats from 240 m³ of gravels. The largest gem was 3.15 ct, but most of the crystals were extremely small, less than half a carat.

Traveling from Company No. 1 to Company No. 3, we saw dozens of independent miners still working in the area (figure 6). From these small (usually 2–3 m wide) pits, we could see that the top "soil" layer was anywhere from 2 to 5 m deep; it lay over a gravel layer (about 0.5–1 m deep) that contained abundant fragments of gray mica schist dispersed unevenly over a kaolin layer at least 1.5 m deep. Most ruby occurs in the gravel layer, and none had been found *in situ* in local outcrops. Spinel, garnet, and blue sapphire are also recovered (P. T. Thi, pers. comm., 1992).

Company No. 2. This small (about 40 hectares) operation, at a site known as "Millionaire Hill," is run by the local Quy Chau police in conjunction with the Nghe An provincial government. Although we saw a single diesel-powered water cannon working one small area, most of the miners used only shovels and buckets. Some pits were as large as 15 × 8 m and about 3–4 m deep (figure 7).

Companies No. 3 and 4. At the time of our visits, Company No. 3 had 120 hectares in the Ban Dung area near Quy Chau, with an operation similar to—but smaller than—that of Company No. 1. Of the 38 workers, 10 were guards. From July 1992 to November 1992, Company No. 3 reported producing only about 2 kg (10,000 carats) of ruby and fancy sapphire.

Company No. 4 was located at Quy Hop, only a few kilometers south of Quy Chau, and was not yet in production in November 1992. The equipment on site indicated that this would be a mechanized open-pit/sluice operation.

According to Professor P. T. Thi (pers. comm.,



Figure 5. At the official Luc Yen market, dealers offer a variety of rough rubies and sapphires, as well as other gem materials found in the Luc Yen area. Photo by Robert C. Kammerling.

1994), these two companies have since been dissolved and the areas turned over to the provincial tin-mining company. Now, "Military Division N." has begun a new mining operation on approximately 150 hectares near the area that Company No. 3 once occupied.

Distribution. The nearest government-sanctioned gem market is in the city of Vinh, where all gem materials are to be sold. Again, though, we were offered stones (both natural and synthetic) throughout the city and mining areas.

Our Vietnamese hosts pointed out numerous new homes throughout the Quy Chau and Luc Yen areas that they referred to as "ruby houses." These distinctive two-story buildings reportedly were constructed with money made in the gem trade. They were the most obvious signs of the new wealth the gem industry has brought to these regions.

FUTURE PROSPECTS

The future of gem mining in Vietnam will depend as much on developments in government policy and the foreign ventures who get involved as it will on the gem reserves available. In fact, the original engineering report on Luc Yen indicated reserves that at one locality could last 50 years ("Mine plan revision . . .," 1990). Although rules governing mining and trade in gemstones were promulgated in October 1993 ("Official regulations . . .," 1994), the situation continues to be both complicated and dif-

difficult for foreign investors. Since the discovery of gems in the Luc Yen area, only one company other than B.H. Mining has entered gem mining there—Metacom of Russia (since mid-1993). There are no foreign entities involved in mining in the Quy Chau area ("Gemstone joint ventures . . .," 1994).

Although at least six foreign ventures have been involved in gem processing, most have not been successful, according to one recent report ("What the Government Won't Tell You," 1994). In fact, this report maintains that as of June 1994 the State Committee for Cooperation in Investment (SCCI) had frozen the granting of new licenses to foreign firms pending an assessment of the ventures that had operated thus far. Prior to this move, however, the Vietnamese government did appoint New York-based Gemrusa as "advisor to the gem

Figure 6. Dozens of independent miners were working in the Quy Chau region in November 1992. Photo by Robert C. Kammerling.



Figure 7. Most of the mining operation of Company No. 2, located at Quy Chau's "Millionaire Hill," was being done by hand. Some of the miners reached the gem-bearing gravels by digging large pits like that shown here. Photo by Robert C. Kammerling.

and jewelry sector," to help guide and lead any potential investors on behalf of the government. This includes organizing the processing and distribution of all new and stockpiled gem materials. Gemrusa says that they are now consulting with Bulgari about establishing a jewelry-manufacturing operation using Vietnamese gems, and that they participated in the appointment of Sotheby's as the official auctioneer for future auction sales of Vietnam's rubies and fancy sapphires (M. I. Jabir, pers. comm., 1994). Although the situation in Vietnam remains fluid, there is promise of a more systematic, informed approach to the management of its gem riches.

REFERENCES

- Gemstone joint ventures travel a rocky road (1994). *JewelSiam*, Vol. 5, No. 3, pp. 50–52.
- Kane R.E., McClure S.F., Kammerling R.C., Khoa N.D., Mora C., Repetto S., Khai N.D., Koivula J.E. (1991) Rubies and fancy sapphires from Vietnam. *Gems & Gemology*, Vol. 27, No. 3, pp. 136–155.
- Koivula J.E., Kammerling R.C., Fritsch E. (1993a) Gem news: Spinel from Vietnam. *Gems & Gemology*, Vol. 29, No. 3, pp. 213–214.
- Koivula J.E., Kammerling R.C., Fritsch E. (1993b) Gem news: Glass imitating Vietnamese ruby. *Gems & Gemology*, Vol. 29, No. 3, p. 215.
- Mine plan revision, Luc Yen ruby mine, Vietnam (1990). Unpublished report prepared by Herinckx & Partners, project engineers.
- Official regulations of geological survey, mining, production and trade of gemstones (1994). *JewelSiam*, Vol. 5, No. 3, pp. 56–59.
- The ruby project in Vietnam (1994). Unpublished report prepared by B.H. Mining Co., January 1994.
- What the government won't tell you (1994). *JewelSiam*, Vol. 5, No. 3, pp. 54–55.

GEM TRADE LAB NOTES

EDITORS

Robert C. Kammerling and C. W. Fryer
GIA Gem Trade Laboratory, West Coast

CONTRIBUTING EDITORS

GIA Gem Trade Laboratory, East Coast
G. Robert Crowningshield •
Thomas Moses • Ilene Reinitz
GIA Gem Trade Laboratory, West Coast
Karin Hurwit • Mary L. Johnson •
Shane F. McClure

DIAMOND

Laser Drill Holes or Natural Inclusions?

Natural inclusions in diamond may resemble laser drill holes, and laser drill holes can have a very unusual appearance. Sometimes, only very careful observation with a microscope can reveal the inclusion's true identity. Recently, the East Coast laboratory encountered four such inclusions.

The first was in a 0.24-ct round brilliant-cut diamond. Our client's customer had returned the diamond on the grounds that apparent laser drilling had not been disclosed. However, examination at 63× magnification clearly revealed that the inclusion in question was actually a string of pinpoints (figure 1) connecting a small cloud and crystal to a larger cloud. The fact that this "string" did not break the surface of

Figure 1. Examination of this diamond at 63× magnification reveals that what appeared at low magnification to be a laser drill hole is actually a string of pinpoints connecting separate inclusions.



Figure 2. The squarish outline of the tube-like inclusions in this 4.03-ct fancy yellow diamond proved that they were etch channels. By comparison, the outlines of laser drill holes are typically round. Magnified 37×.

the stone proved that it could not be a laser drill hole. This is another instance where the client's use of a gemological microscope would have provided both more knowledge on the stone at hand as well as an opportunity to educate the customer as to the actual nature of the stone's internal characteristics.

Another diamond, a 4.03-ct fancy yellow cushion brilliant, had many angular tube-like inclusions. Unlike the coarse etch channels shown in the Fall and Winter 1992 Lab Notes sections, the channels in this stone were very thin and resembled laser drill holes. Nevertheless, magnification revealed that these inclusions had the squarish outlines of etch channels (figure 2), not the rounded outlines of laser drill holes. The angularity also indicated that these were natural inclusions.

Occasionally, however, we do see laser drill holes that are not



Figure 3. The somewhat irregular laser drill hole in this 4.69-ct diamond travels from the table to a crystal and feather inclusion. Note the cone-shaped opening. Magnified 27×.

entirely straight, such as the one in this 4.69-ct pear-shaped brilliant cut (figure 3), which starts at the table. As seen through the pavilion (figure 4), this laser drill hole wanders off line several times before reaching the inclusions, a crystal and a feather. The cone-shaped entry point of the

Figure 4. The unusual curvature of the laser drill hole shown in figure 3 is apparent when the diamond is viewed through the pavilion. Magnified 63×.



drill hole is an earmark of early laser technology, which was first noted in *Gems & Gemology* in the Fall 1970 issue (p. 224). Refinements in the laser-drilling process over the next few years led to laser drill holes without this cone-shaped point of entry.

The drill hole in figure 5, as viewed from the pavilion of this 1.15-ct round brilliant-cut diamond, is also atypical. As clearly seen in the image on the left, the main drill hole reaches a crystal-like inclusion, but also branches off to reach another inclusion, forming a "Y" shape. We spoke to a number of people who do laser drilling, but none of them could explain why these branching or curving phenomena occur.

Vincent Cracco

Diamond with Unusual Color Zoning

Diamonds with a yellow body color generally have fairly even color distribution throughout. When color zoning does occur, it is usually in the form of areas that are lighter and darker yellow, with indistinct boundaries. So, the West Coast lab staff were surprised to see the unusual color zoning evident in the 1.08-ct marquise brilliant shown in

Figure 5. This laser drill hole (seen doubled due to prism reflection) goes straight from the surface to one included crystal, but also branches to a second, deeper inclusion. Magnified 63 \times .



Figure 6. Parallel color banding is sharply defined in this 1.08-ct marquise brilliant-cut diamond, which measures 10.71 \times 5.25 \times 3.26 mm. Magnified 17 \times .

figure 6. Microscopic examination revealed two very distinct, parallel, dark yellow color bands in a stone of otherwise lighter yellow color. Running the length of the stone, the bands were more reminiscent of color distribution commonly seen in yellow sapphires.

With long-wave ultraviolet radiation and magnification, the banding was strikingly pronounced. It fluoresced a strong yellow that contrasted with the weaker blue fluorescence of the main body of the stone (figure 7). In fact, the orientation of the bands combined with the strength of their fluorescence to give the stone an overall yellow fluorescence when viewed faceup with the unaided eye.

This color distribution, obviously unrelated to the faceted shape, is an indication of natural color. Considering this and the fact that the diamond exhibited no distinct absorption lines that would be associated with laboratory irradiation, we concluded that the color was natural.

RCK and SFM

EMERALD, Trapiche from a New Locality

The locality in which a gem mineral occurs is often important to collectors and dealers alike. For some gem minerals, there is no question as to locality because they are found in only one or a few places. There are

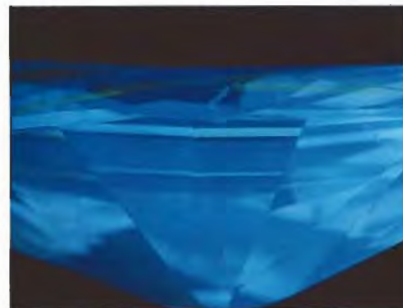


Figure 7. When the diamond in figure 6 was examined with long-wave U.V. radiation, the bands fluoresced yellow and the rest of the stone fluoresced blue. Magnified 17 \times .

times, however, when a new locality for the same type of material shows up. The GIA East Coast lab was fortunate enough to inspect such a specimen, a trapiche emerald that reportedly came from a locality other than Colombia. The dealer who submitted the pair of polished green hexagonal tablets in figure 8 (left) to the East Coast lab informed us that these were cut from a single crystal, which came from the state of Goiás, in Brazil. One weighed 4.62 ct and the other 4.21 ct; both measured approximately 9.85 \times 12.75 \times 3.50 mm.

On the basis of standard gemological tests and the distinctive appearance of the slices (see H. L. McKague, "Trapiche Emeralds from Colombia," *Gems & Gemology*, Fall 1964, pp. 210–213), we identified them as trapiche emeralds. (Discovered in Colombia, trapiche emeralds were named after the Spanish word for cane-crushing gears, which the Colombian type resembles—with its central green core and six black arms extending from the prism faces of the core [figure 8, right].) However, the refractive indices and specific gravity were found to be higher than those of the Colombian material: R.I., 1.583–1.589; S.G., taken hydrostatically, approximately 2.74. Trapiche emeralds from Colombia typically have R.I.'s of 1.563–1.569 and an S.G. of 2.65–2.69 [see J. Sinkankas, *Beryl*,

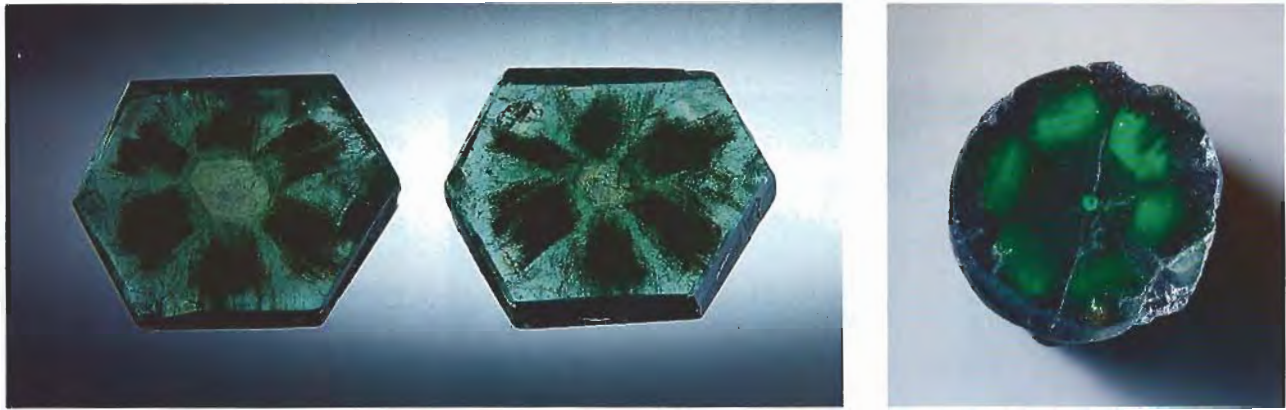


Figure 8. The trapiche emeralds on the left, which are reported to be from the state of Goiás in Brazil, are the first we have seen from a locality outside of Colombia. The two slices are approximately 12.75 mm on their longest dimension. On the right is a typical Colombian trapiche crystal; it measures 16 mm × 22 mm.

Butterworths, London, 1986, pp. 121–126).

In this Brazilian material, somewhat trapezoidal opaque dark areas extend inward to a hexagonal core from each of the six first-degree prism faces. Transparent green areas separate each of the opaque dark areas. However, the spoke pattern in these slices differs from that usually seen in gem-quality trapiche emeralds from Colombia. In the latter, thin black spokes radiate from the core and separate the usually saturated emerald green color into six areas (see again, figure 8, right). The newly submitted stones almost seem to be a photographic "negative" of the Colombian material.

Nicholas DelRe

JADEITE, with Metallic Inclusions

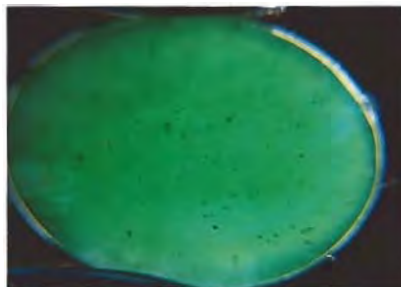
Until the recent concern with the bleaching and impregnation of jadeite (B jade), there appears to have been little interest in identifying or cataloguing inclusions in jadeite, possibly because they are encountered so rarely, at least in fashioned material. One of the few such references was a Spring 1973 Lab Note (p. 135), which described inclusions—in translucent jadeite—that had the appearance of pyrite.

Staff members at the East Coast lab recently examined an unusually translucent 8.60-ct green jadeite

cabochon (figure 9), which we determined to be untreated, that had inclusions reminiscent of those described in that earlier Lab Note. Because none of the inclusions reached the surface, the client kindly agreed to repolish the cabochon to expose several of them for further study. When viewed in reflected light, the inclusions appeared to be of two different minerals: One type seemed to be quite hard, with a brassy metallic luster; the other type had a brown appearance, undercut the surface markedly, and did not take a polish (figure 10).

Although the client did not want us to scrape the inclusions for X-ray diffraction analysis, he did agree to let us send the stone to Santa Monica for energy-dispersive X-ray fluorescence (EDXRF) analysis at GIA Research.

Figure 9. This highly translucent 8.60-ct jadeite cabochon has inclusions, something that is not often seen in jadeite. Magnified 10×.



Unfortunately, the size and position of the inclusions did not allow a definitive identification by this method. The project was further complicated by the general lack of data on trace elements in jadeite.

However, on the basis of luster, relative hardness, color, and appearance, it was concluded that the metallic inclusions are probably pyrite and the softer brown inclusions are probably pyrrhotite, which commonly occurs with pyrite. This opinion was substantiated by using polarized reflected light to observe a property that is called *bireflectance*. Specifically, the "pyrrhotite" inclusions appeared to shift in color as the cabochon (or polarizer) was rotated,

Figure 10. Some of the inclusions in the stone shown in figure 9, seen here with darkfield illumination, appear to be brown when viewed in reflected light. They may be pyrrhotite. Magnified 30×.





Figure 11. The 6.5- to 7-mm freshwater tissue-nucleated cultured pearls in this necklace are nearly round.

which indicates that the material is not isotropic; however, the color of the "pyrite" crystals did not vary with such a rotation, so they probably are isotropic. (Therefore, the soft material is not limonite, and the hard material is not marcasite.)

Although inclusions in jadeite are rare, the presence of some inclusions, such as sulfides, at the surface of a stone may indicate that the stone was not "bleached" by acid treatment, since some bleaching agents attack and may destroy certain inclusions, depending on the chemistry of the inclusion and the agent used.

GRC and Mary L. Johnson

Cultured PEARLS, Round and Near-Round Freshwater Tissue-Nucleated

With the tremendous (and still increasing) production of freshwater tissue-nucleated cultured pearls, and the greater attention to quality by cultured-pearl farmers in China, it is not surprising that some of these cultured pearls turn out nearly round or round, unlike the "rice-grain" types that dominated production up until the last few years. In fact, in late 1992 one staff member

of the East Coast lab was shown a 30-inch-long twisted rope of 12 strands of near-round 4- to 5-mm freshwater tissue-nucleated cultured pearls. Another staff member reported seeing many similar strands during a late-1993 trip to the Far East; he was told they were selling quite briskly.

In December 1993, however, a client showed us the largest freshwater tissue-nucleated cultured pearls we had seen to date—6.5 to 7 mm—in an 18-strand hank. Two of these strands were later used in the necklace shown in figure 11. Note that this is a popular size for saltwater bead-nucleated "Akoya" cultured pearls from Japan.

An X-radiograph of this necklace (figure 12) reveals an interesting potential problem: Many of the pearls do not show the void that would prove they are tissue-nucleated. This evidence may have been eliminated by the drill hole. Therefore, some freshwater tissue-nucleated cultured pearls may be indistinguishable from some freshwater natural pearls by X-radiography.

We have previously noted what we feel were efforts to drill away evidence of mantle-tissue nucleation

(*Gems & Gemology*, Spring 1986, pp. 51–52, and Summer 1986, p. 111). New information suggests that some "accidental" saltwater tissue-nucleated cultured pearls have been fraudulently substituted for natural pearls in old items of pearl jewelry. The perpetrators hoped that the oversized drill holes would eliminate the voids left by the tissue nuclei.

GRC

Glass-Coated QUARTZ

Two distinctly different treatments are typically used to produce a thin layer of surface color on gems: color coating and diffusion treatment. In the first, a colored layer is applied to the surface of the stone. Color-coated stones examined by the lab over the years have included diamonds coated with pink nail polish (Spring and Summer 1983 Lab Notes, pp. 43–44 and p. 112, respectively) and pale beryls coated with a green substance to imitate emerald (Spring 1983 and 1993 Lab Notes, pp. 44–45 and 46–47, respectively).

In another, newer type of coating, elemental gold is deposited on quartz and topaz gems, producing a greenish blue color with thin-film surface iridescence. This material is marketed under the trade name "Aqua Aura" (see *Gem News*, Winter 1988, p. 251, and Fall 1990, pp. 234–235).

Figure 12. An X-radiograph of the tissue-nucleated cultured pearls in figure 11 shows that in many instances evidence of the nucleus has been removed by the drill hole.



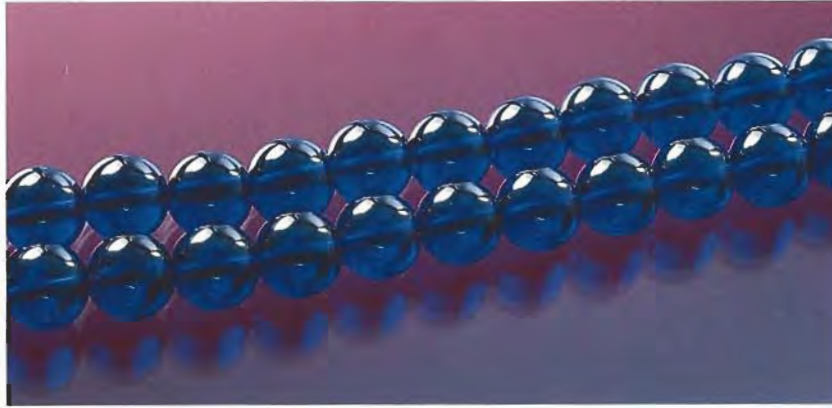


Figure 13. A glass-like coating is responsible for the apparent color of these 8- to 8.5-mm quartz beads.

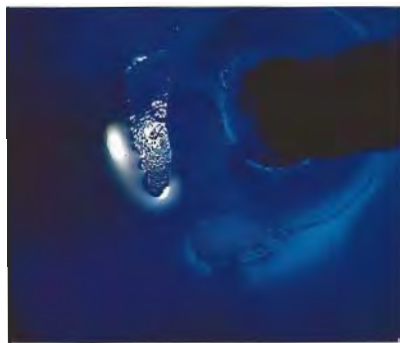
In diffusion treatment, coloring agents are diffused into the surface of the stone. To date, we have only examined gem corundums that have been color enhanced by this method (see related *Gems & Gemology* articles by Kane et al., Summer 1990, pp. 115–133, and by McClure et al., Spring 1993, pp. 16–28).

Recently, the West Coast lab received for identification a strand of 51 round beads (figure 13) about 8 to 8.5 mm in diameter. The transparent beads were dark violet-blue, reminiscent of cobalt-colored synthetic spinel or the rare cobalt-colored natural spinel. The client who submitted the beads knew that they had been treated, but not the method used.

Gemological testing revealed properties consistent with those of quartz, including a "spot" R.I. of 1.54, an S.G. of 2.65, and a "bull's-eye" optical interference figure. Magnification revealed that the color layer around some drill holes was thinner and lighter in tone than elsewhere on the beads. Some beads had dimple-like depressions in the surface layer, primarily near the drill holes, which exposed the underlying bead as colorless and with a rough-ground appearance (figure 14). Microscopic examination also revealed very little color in the drill holes. A small ridge with a concave side near the drill hole on many of the beads may have resulted from their having been treated while hanging on wire.

With the client's permission, we removed one bead and sawed a slice with surfaces perpendicular to the drill hole. This revealed that, away from the drill hole, the layer of surface color was actually fairly uniform (figure 15), approximately 0.07 to 0.10 mm thick, with a somewhat lower luster than that of the underlying colorless bead. The surface layer also "undercut" during preparation of the section, indicating a lower hardness than that of the bead itself. We determined a Mohs hardness of 5-6 for the coating on the sawn bead, softer than that of quartz (Mohs hardness of 7). The hardness test also revealed that the coating was very brittle, as it produced a succession of conchoidal chips. X-ray powder

Figure 14. These "dimples" seen in reflected light are areas of incomplete coating on some of the beads shown in figure 13. Magnified 20 \times .



diffraction analysis of a small scraping from the surface layer showed that it was amorphous. This is unlike the results we have obtained with diffusion-treated corundum, in which the surface layer is crystalline. Energy-dispersive X-ray fluorescence (EDXRF) analysis of the surface layer revealed large amounts of Si and Co, as well as smaller amounts of Pb, Na, Zn, Ti, and Fe.

From this testing, we concluded that the beads were quartz with a glass-like coating, possibly produced by an enameling process. If so, it would not be the first time enameling was used on quartz. In the rarely seen classic *en resille* enameling technique, rock crystal (or glass) was finely incised with lines that were subsequently overfilled with gold. The cells that formed were filled with enamel and then fired (see, e.g., Kenneth F. Bates's *Enameling Principles and Practice*, World Publishing Co., Cleveland and New York, pp. 138–140).

RCK and SFM

SYNTHETIC SAPPHIRE, with a Small Star

Almost all of the synthetic star corundums that we see exhibit not only uniform color and transparency, but also even distribution of the inclusions that cause the phenomenon. Some notable exceptions reported earlier include incomplete

Figure 15. A slice cut from one of the beads in figure 13 confirms the thin (0.07–0.10 mm) color layer on a colorless substrate. Magnified 40 \times .



stars in a synthetic star ruby (Summer 1982 Lab Notes, pp. 105–106) and a synthetic star sapphire (Winter 1991 Gem News, pp. 263–264).

Another variation on this theme was seen in an oval buff-top step-cut synthetic sapphire recently examined by the West Coast lab. The pinkish orange synthetic, measuring approximately $10.64 \times 8.91 \times 5.00$ mm and set in a yellow metal ring, was transparent except for a small area at the top of the dome. When examined with reflected light, this area displayed distinct six-rayed asterism. Magnification revealed the cause, a small localized plane of intersecting minute needle-like inclusions (figure 16). The gemological properties were consistent with corundum, and curved yellow color banding proved it to be synthetic. As the phenomenon was distinct, albeit confined to the apex, the item was identified as a synthetic star sapphire.

RCK

SAPPHIRES from Yogo Gulch, Montana

A group of crystals and faceted sapphires from Yogo Gulch, Montana—seen in the East Coast lab—provide an excellent example of how the shape of the rough often determines the final cut. Sapphires from this region crystallize mainly as short prisms, characterized by repeated

Figure 16. The inclusions causing the star in this pinkish orange synthetic star sapphire are confined to the whitish area at the apex of the cabochon. Magnified 20 \times .



Figure 17. In keeping with the typically "stunted" shape of the Yogo sapphire crystals (the largest, at the far right, is 6.60 ct), the 13.90-mm-long pear-shaped Yogo sapphire shown here is only 2.80 mm deep.

growth of a rhombohedral form, and are terminated by the basal pinacoid (figure 17; see S. E. Clabaugh, *Corundum Deposits of Montana*, U.S. Geological Survey Bulletin No. 983, 1952). For example, the blue 6.60-ct crystal in figure 17 measured about 15.70×13.00 mm, but was only 3.32 mm thick. Therefore, to retain weight, Yogo rough is typically cut into stones of shallow depth: The fine, and relatively large (for a Yogo sapphire), pear shape in figure 17 measures approximately 13.90×9.35 mm in outline. However, because of the shallow (2.80-mm) depth, it weighs only 3.59 ct.

In contrast, many sapphires from Sri Lanka crystallize as tapering hexagonal bipyramids (figure 18). The desire to retain weight from this type of rough typically results in native-cut stones with extremely deep pavilions.

Nicholas DelRe

TURQUOISE, Dyed and Impregnated

Seldom have staff members at the West Coast GIA Gem Trade Laboratory seen as interesting an example of dyed and impregnated turquoise as was presented by the slab (report-

edly a section cut from a nodule) shown in figure 19.

Gemological testing easily identified the sample as turquoise. Microscopic examination of the very irregular, darker blue periphery revealed concentrations of a dark blue material with a subvitreous luster; the material was readily indented by the point of a metal needle and reacted like a plastic to a thermal reaction tester. No further testing was needed to identify the turquoise as dyed and impregnated.

Of particular interest was the "before-and-after" effect illustrated

Figure 18. Because Sri Lankan sapphire crystals are typically bipyramidal, as shown here, they lend themselves to cut stones with deep pavilions.





Figure 19. This $7.90 \times 3.23 \times 0.90$ cm slab of dyed and impregnated natural turquoise clearly reveals the lighter blue color of the untreated material, in the center, where the treatment substance did not penetrate.

by the slab. The lighter portion clearly reveals the appearance of the turquoise before treatment.

RCK

Faceted VÄYRYNENITE

Among the many interesting materials we have the opportunity to examine in the laboratory are rare minerals that have been fashioned as collectors' stones. In past Gem Trade Lab Notes, we have reported on items such as augite (Spring 1989), clinohumite (Winter 1986), color-change diaspore (Spring 1987), lazulite (Spring 1993), phosgenite (Summer 1977), sapphirine (Summer 1987), stibiotantalite (Spring 1980), and triphylite (Fall 1988).

Recently, a colleague loaned the West Coast lab a 2.02-ct pinkish orange marquise step cut (figure 20) that was believed to be väyrynenite, a rare, monoclinic, beryllium-man-

ganese phosphate that occurs in lithium pegmatites. We determined the following gemological properties: refractive indices, 1.639–1.665; birefringence, 0.026; specific gravity, 3.23; biaxial optic character; trichroism of moderate strength in pinkish orange, pink, and yellowish orange; inert to both long- and short-wave

Figure 20. This 2.02-ct marquise step cut ($11.19 \times 5.20 \times 4.90$ mm) is a rare faceted example of the mineral väyrynenite.



U.V. radiation; a faint pink appearance through the Chelsea color filter; and absorption features including weak general absorptions at about 400–440 nm and about 660–700 nm, with a strong band centered at about 415 nm and a weaker band from about 540–560 nm. Examination with magnification revealed many partially healed fractures composed of one- and two-phase (fluid and fluid-and-gas) inclusions. These properties are all consistent with väyrynenite, a mineral with a Mohs hardness of 5. According to J. Arem's *Color Encyclopedia of Gemstones* (2nd ed., 1987, Van Nostrand Reinhold, New York, p. 198), faceted gems of this material are extremely rare and seldom exceed 0.5 ct. Cuttable material reportedly comes only from Pakistan, although the mineral was named after Finnish geologist Heikki Allan Väyrynen, who found the first deposit in Viitaniemi, Finland.

RCK

PHOTO CREDITS

Vincent Cracco took the photos in figures 1–5. Shane McClure provided figures 6, 13–15, 19, and 20. Nicholas DelRe supplied the pictures used in figures 8 (left), 9, 11, and 17. The X-radiograph in figure 12 was taken by Bob Crowningshield. The photomicrographs in figures 7 and 10 are by John I. Koivula. The photo used in figure 16 was furnished by Maha DeMaggio. Michael Havslad took the photo in figure 18. Figure 8 (right) is © Harold & Erica Van Pell.

Editor's note: The initials at the end of each item identify the contributing editor who provided that item.

Gems & Gemology, Vol. 30, No. 2, pp. 115–121

© 1994 Gemological Institute of America



GEM NEWS

JOHN I. KOIVULA, ROBERT C. KAMMERLING, AND EMMANUEL FRITSCH, EDITORS

MARY L. JOHNSON AND DINO G. DEGHIONNO, CONTRIBUTORS

DIAMONDS

Argyle upgrades operation. A second major upgrade will soon be completed at the Argyle mine, according to a statement by the CRA-Ashton Mining joint venture in early 1994. The purpose of the upgrade, which includes installation of a second high-pressure crusher plus additional screening units and conveyors, is to help maintain diamond production over the remaining seven-year life of the open-pit operation. Although the current ore horizon consistently produces 6 ct per ton, the yield is expected to decline eventually to 4 ct per ton.

Production for 1994 is projected to be about 39 million carats. Although only 5% of output is typically gem quality, this 5% generates about 50% of the mine's revenue. The pink diamonds, for which Argyle is so well known, account for less than 0.001% of total production. (*Mining Journal*, March 25, 1994, p. 223)

De Beers's rough diamond sales up. Sales of rough diamonds by De Beers's Central Selling Organisation (CSO) for the first six months of 1994 were US\$2,580 million, 1.5% higher than the same period last year and 41.5% higher than the second half of 1993. The CSO reports their sales of rough diamonds from 1984 to 1994 (in millions of US\$) as follows:

Year	First half	Second half	Total
1984	US\$ 945 m	US\$ 668 m	US\$1,613 m
1985	837	986	1,823
1986	1,214	1,343	2,557
1987	1,560	1,515	3,075
1988	2,201	1,971	4,172
1989	2,317	1,769	4,086
1990	2,477	1,690	4,167
1991	2,084	1,843	3,927
1992	1,787	1,630	3,417
1993	2,543	1,823	4,366
1994	2,580	—	—

The CSO reduced supplies to the market in the second quarter, following a buildup of stocks in the cutting centers and continued concerns about cutting-center profitability.

Demand for retail jewelry remained weak in Europe and Japan, high in East Asia, and stable in the United States. Any significant improvement in sales of rough diamonds depends on improved Japanese and European markets and on CSO clients being in a position to increase their levels of profitability, said De Beers.

Discussions continue between De Beers and the Russian diamond authorities about future contractual relationships. Although the present contract runs out at the end of 1995, the Russians have made it clear that they support market stability. Both sides have agreed to issue only joint public comments on their negotiations, according to the CSO.

Diamond pipes located outside Canada's "Corridor of Hope." Ashton Mining of Canada's recent discovery of a diamondiferous kimberlite pipe at Cross Lake, in the Northwest Territories, has proved the existence of such pipes outside the northwest/southeast-trending zone aptly named the "Corridor of Hope" by diamond geologist Ed Schiller. This 50-km-wide zone, which extends from Yamba Lake in the north to Artillery Lake in the south, is delineated by a set of parallel diabase dikes that are quite noticeable on regional aeromagnetic maps. Several diamondiferous pipes—including those located in the Lac de Gras area by BHP/Dia Met and DHK/Kennecott—have been found within this zone. The Ashton find, 200 km to the west of the zone, offers great encouragement to other companies who hold claims outside the Corridor of Hope. The pipe was discovered by a combination of till sampling for indicator minerals and aeromagnetic surveys. The claims on which the Cross Lake pipe is located are held by Tenajon Resources and Pure Gold Resources, in a joint venture with Ashton Mining of Canada. (*Northern Miner*, April 4 and May 16, 1994, both on p. 2; courtesy of Bram Janse)

More evidence that Wisconsin diamonds come from Canadian pipes. A significantly diamondiferous kimberlite pipe found in the Hudson Bay-James Bay Lowlands region of northern Ontario, Canada, reaffirms the possibility that the diamonds found in the terminal moraines of southern Wisconsin may have been transported there from the northern Ontario region by glaciers. This idea was first proposed by Hobbs (*Journal of Geology*, Vol. 7,

1899, pp. 375–388) to explain the late-19th-century finds of large (up to 21.25 ct) diamonds by farmers and well diggers in the area.

Discoveries since the late 1970s of at least 20 kimberlite pipes in the Upper Peninsula of Michigan had suggested a closer source for the Wisconsin diamonds. However, detailed investigations have shown that these kimberlites are virtually barren.

The northern Ontario find was made by KWG Resources, of Montreal, Quebec, on the basis of drilling of selected aeromagnetic anomalies. As the new pipe has only been intersected by one drill hole, no firm data are available on the shape or size of the pipe, or the grade or quality of the diamonds. However, one 29-kg section of kimberlite drill core contained six small diamonds (larger than 0.5 mm in two dimensions) and 63 microdiamonds (smaller than 0.5 mm). (*Northern Miner*, May 23 and June 20, 1994, both p. 2; courtesy of Bram Janse)

Update on Ghana production. Shallow alluvial reserves at the Ghana Consolidated Diamond Mines (GCD) operation at Akwatia are reportedly nearing exhaustion; annual output is now barely 200,000 carats (1992 production was 214,155 carats). However, there are substantial deep alluvial deposits in stream gravels of the Birim River Valley, which GCD is actively mining. Diamond production at other small and medium-sized mines in Ghana totalled 479,874 carats in 1992. (*Mining Journal*, November 26, 1993, p. 366; *Mining Magazine*, January 1994, p. 20; *Mining Annual Review* 1993, p. 188)

Russia offers rough for sale . . . In mid-March, Komdragmet, the Committee on Precious Metals and Gems of the Russian Federation, put up for sale approximately 114,000 carats of rough. This is part of an "open tender" that Russia is permitted to hold under the terms of its marketing agreement with De Beers. Per-carat estimates suggest that the overall value of the goods is in the US\$10–11 million range. Although this amount is significantly larger than past such auctions—which were typically in the \$500,000–\$2 million range—the increase is seen merely as a "catching-up" exercise and is still within the amounts permitted under the De Beers agreement. In November 1993, authority to conduct these independent sales in Russia was transferred from Almazjuvelirexport, then a part of the mining group Almazly Rossii-Sakha, to Komdragmet, which controls the Russian stockpile. (*Diamantaire*, No. 21, April 1994)

. . . and develops diamond-cutting equipment. To double the output of its domestic polishing industry by late 1995, the Russian government has directed several machinery manufacturers to speed development of diamond-fashioning equipment. Newly available equipment includes a bruting lathe that permits two diamonds of equal weight and diameter to be bruted without the use of diamond tools. This product of Precision Machine



Figure 1. This 0.42-ct near-colorless synthetic diamond crystal was produced in Russia by means of a belt apparatus. Courtesy of Chatham Created Gems; photo by Shane F. McClure.

Works, St. Petersburg, has reportedly been tested successfully at the Kristall polishing factory. In late 1993, SKTB Kristall, of Smolensk, introduced a work station that includes five sawing units with automatic heads and consoles to control the heads. (*Diamant*, No. 371, January–February 1994, p. 28)

Production plant upgrade for Zimbabwe. The recovery plant at the River Ranch diamond mine in Zimbabwe will be upgraded with the goal of increasing annual production from 130,000 carats to more than 300,000 carats. Proven reserves should allow for continuous operation of the mine for at least 15 more years. (*Mining Journal*, February 18, 1994, p. 121)

Near-colorless Russian synthetic diamond examined. This past May, GIA Research examined a 0.42-ct near-colorless synthetic diamond crystal from Russia (figure 1). It was grown using a "belt" apparatus, not the split-sphere (or "BARS") technology the Russians use to produce their yellow synthetic diamonds, according to Tom Chatham, Chatham Created Gems, San Francisco, California, who loaned the crystal to GIA. (For more on Russian synthetic yellow diamonds, see the article by Shigley et al., *Gems & Gemology*, Winter 1993, pp. 228–247.)

The features most useful in identifying this near-colorless cuboctahedral crystal as synthetic are its large metallic inclusions and yellow fluorescence to short-wave ultraviolet radiation only.

The metallic inclusions appear predominantly brown when viewed in reflected light. They were sufficiently large and numerous that the crystal adhered to a simple magnet. Energy-dispersive X-ray fluorescence chemical analysis confirmed that the inclusions contained iron. No graining, and only very weak anomalous birefringence ("strain"), was noted.

The crystal did not fluoresce to long-wave U.V., and it only fluoresced weak yellow to short-wave U.V. The fluorescence appeared evenly distributed. When the short-wave U.V. lamp was turned off, the crystal phosphoresced yellow for 30 to 45 seconds.

These and other features observed were consistent with those of other near-colorless synthetic diamonds examined by GIA Research. The crystal was slightly electrically conductive, with the degree of conductivity varying considerably depending on which pair of crystal faces was tested. No absorption bands were seen with a handheld spectroscope. The absorption spectrum recorded at liquid-nitrogen temperature with the spectrophotometer revealed no absorption in the visible range. The mid-infrared spectrum identified this synthetic diamond as type IIa. GIA researchers could not record an infrared spectrum that had features associated with type-IIb diamond to confirm the measurements of electrical conductivity, presumably because the metallic inclusions interfered with recording a spectrum in the direction in which the type-IIb character would most likely be seen.

COLORED STONES

Amber marketed with photomicrography. As noted in the Spring 1994 Gem News, amber was well represented at the February 1994 Tucson shows. In that item, we mentioned one Russian dealer who provided customers with small note cards describing the type of insect in each of his specimens. Another amber dealer at Tucson—Dan McAuley of the Berkeley Amber Group, a firm based in California—took this marketing/educational approach one step further by providing each buyer with a photomicrograph of the actual inclusion in the specimen. Working with Mr. McAuley was Pat Craig, who identified and then photographed the inclusions. Mr. Craig, who has been studying amber for more than 20 years, produced the photomicrographs using a video camera and a digital thermal printer. The end result was an "instant" color photomicrograph with good resolution (see, e.g., figure 2). Although magnification in most of the photographs ranged from 1:1 to about 20 \times , theoretically it is limited only by the microscope used. The system also included a standard Sony color monitor, so visitors to the booth could easily watch Mr. Craig work.

Packages being offered at the show included the piece of amber, the photo of its inclusion, and a certificate giving the inclusion's identity. The advantage of such a package for retailers is that the picture can be displayed with the specimen, permitting prospective customers to "examine" inclusions without a microscope or

hand lens—and the corresponding help of a salesperson.

Mr. Craig noted that a standard video-cassette recorder could be added to the system to save images and print them at a later date.

Basel Fair Highlights. For the second year in a row, *Gems & Gemology* and other GIA representatives attended the European Watch, Clock and Jewellery Fair, held in Basel, Switzerland, from April 13 to 21. Although our representatives were veterans of numerous trade shows and more than 20 years of Tucson shows, they found the 1994 Basel Fair to be a superb experience for the gem enthusiast.

Buyers from all over the world (fair organizers reported total attendance of 83,000) explored the four large buildings in which diamonds, colored stones, jewelry in a variety of metals and bold designs, watches, and machinery were displayed by more than 2,133 exhibitors from 24 countries. Among the many high-quality gem materials offered were large numbers of cabochon-cut as well as faceted emeralds, rubies, and sapphires; significant quantities of Paraíba tourmaline; several large (5-ct plus) alexandrites; numerous important Polynesian cultured pearls from Tahiti, as well as fine large carvings and carvings set in jewelry. Of particular interest were the new Design Hall and Prestige Room. The latter—set up in a warm, sophisticated environment on the bottom floor of Building 2—featured gem-set jewelry by some of the finest jewelers in the world, including Carrera y Carrera, Damiani, Henry Dunay, Hammerman, Nova Stylings, and La Nouvelle Bague. One of the most unusual colored-stone pieces on display was a rhodochrosite brooch by Henry Dunay (figure 3).

The 1995 Basel Fair will be held April 26–May 3.

Figure 2. This photomicrograph of an approximately 3-mm-long Tertiary pseudoscorpion in Dominican amber was taken by video camera and "instantly" printed by a digital thermal printer. Photo by Pat Craig.





Figure 3. The 1994 Basel Fair showcased many fine, as well as unusual, colored gems. This unique brooch features a 115.13-ct rhodochrosite "rosette" set in 18k gold with 2.80 ct of diamonds. Courtesy of Henry Dunay Inc., New York.

Fluorite from California. Some green fluorite of very high clarity has been found at the Felix fluorite mine, a deposit in the hills above Azusa in Los Angeles County, California, that has been known for many decades. In October 1993, mineral collector Robert Housley led a group to a pocket that he had discovered. One member of the group, Tish Hunter, picked up some broken pieces of fluorite rough after the others had finished collecting mineral specimens. She later asked Michael Gray, of Coast-to-Coast Rare Stones, Missoula, Montana, to facet one. The result was a 30.67-ct round modified brilliant (figure 4) that was subsequently donated to the San Bernardino County Museum.

Mr. Gray estimated that a few hundred carats of fluorite came from the pocket; some has entered the trade. Although southern California is known for its important gem deposits, including tourmaline, spessartine garnet, and the original occurrence of kunzite, the densely populated Los Angeles basin is not usually thought of as a source of gem material.

Gem artistry knows no boundaries. Although gem carvings and pieces inlaid with gem materials have been valued as art objects for thousands of years, "conceptual gemologist" John Nels Hatleberg, of New York City, has

extended the concept of gem artistry to new arenas. Best known for his success at fashioning replicas of famous diamonds (including the Hope, the Portuguese, and the Guinea Star) by taking silicon molds from the actual diamonds and casting them in a custom-formulated resin, Mr. Hatleberg has also developed a unique line of jewelry known as "Gold Body Gems"—temporary tattoos fashioned of 23k gold that are modelled after famous diamonds.

Last year, he completed a unique "painting" fashioned of gems and minerals. The large-scale (14.5 × 16 cm; 36 × 40 inches) picture, titled "Woo," uses pearl, tourmaline, and chiastolite placed on a pyrite mirror set in a frame of quartz crystals cast in gold leaf (figure 5). Note that the "corn cobs" are made of natural corn cob with Chinese freshwater pearls strung on gold wire. He is currently working on a number of other projects that mix gems with other natural materials, such as a delicate nest of blond hair in which egg-shaped South Seas pearls have been laid.

Green gems from Australia. Chrysoprase chalcedony, an attractive gem in its own right, is often used as a jade simulant. The misnomer "Queensland jade," for example, describes chrysoprase chalcedony from an important deposit discovered in 1965 near Marlborough Creek (see Webster's *Gems*, 4th. ed., 1983, p. 220). We saw considerable quantities of this gem material at the February Tucson shows. Particularly interesting were fine, intense yellowish green cabochons in calibrated sizes ranging from 6 × 4 mm to 28 × 20 mm (see, e.g., figure 6) and strands of well-matched beads from 3 to 11 mm in diameter. Offered by Po Yuen Gems Company of Hong Kong, this chrysoprase reportedly came from their mine in

Figure 4. This 30.67-ct fluorite was faceted from material recovered from the Felix fluorite mine in Los Angeles County, California. Photo by Shane F. McClure.

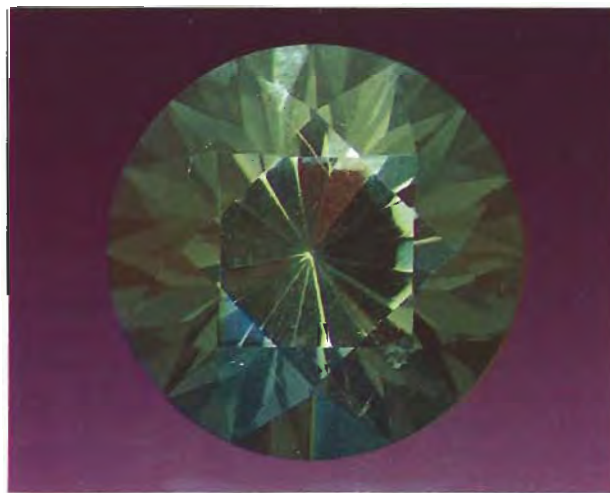




Figure 5. This gem "painting" (14.5 × 16 cm) was fashioned by gem artist John Nels Hatleberg from pearls, tourmaline, and chiastolite—with other natural materials—placed on a pyrite "mirror" and set into a frame of gold-cast quartz crystals. Photo by Durston Saylor.

Queensland. Similar rough and fashioned Queensland chrysoprase—including carvings with Oriental motifs—was offered by Kajar-USA of Montclair, California.

A second major chrysoprase-producing area represented at Tucson is the Yerilla District in Western Australia. As of November 1993, annual production from a mine operated by the Gembank Group was projected to be 100 tons (see the article by R. W. Jones, *Lapidary Journal*, February 1994, pp. 71–79).

Another green ornamental gem from Australia was offered at Tucson under the trade name "Allura" (again, see figure 6). Vendor Martin Rosser, of Munich, Germany, reported that this gem material is actually the mineral gaspeite, a nickel, magnesium, and iron carbonate $[(Ni,Mg,Fe)CO_3]$, which comes from a site in Western Australia about 300 km southeast of Perth.

We recorded the following gemological properties on a 3.15-ct cabochon of "Allura": diaphaneity—opaque; R.I.—1.62 to over-the-limits (noted with a "birefringence blink"); inert to both long- and short-wave U.V. radiation; no reaction to the Chelsea color filter (i.e., it appeared green); S.G.—3.51. These properties are consistent with

those reported in the mineralogical literature for gaspeite, although the S.G. is somewhat lower than the reported 3.71. This may be partly explained by the matrix in the test sample, a predominantly brown veining. The lower S.G. value may also be due to the presence of some magnesite (S.G. 3.0–3.1), since gaspeite forms a solid-solution series with both that magnesium carbonate ($MgCO_3$) and the iron carbonate siderite ($FeCO_3$).

Myanmar liberalizes gem trading. For the first time in three decades, Myanmar (Burma) will let foreigners purchase privately owned gems, jade, and jewelry year-round with few restrictions, according to a May 2 press release from Myanmar VES Joint Venture Company, Yangon. Any Myanmar citizen or company can sell for export. All such export transactions must be made through one of six Gem Trade Centers: Yangon, Mandalay, Taunggyi (Shan State), Tachileik (on the border across from Mae Sai, Thailand), Muse (on the Chinese border), or Kaw Thauung (on the southern border with Thailand).

All sales are to be made in U.S. dollars or other approved foreign currencies. Each sale is subject to a 15% tax: 5% is a commission paid to the Myanmar Gems Enterprise (MGE); the remaining 10% consolidates all income, commercial, and other taxes that might otherwise be applicable.

Under the new provisions, any business registered with the MGE may sell finished jewelry up to US\$30,000 as long as MGE-supplied sales receipts are used. Sales of rough and fashioned jade and other gems up to \$30,000 must be made under MGE supervision at one of the Gem Trade Centers, where MGE will issue the receipt. Sales of \$30,000 or more are permitted as long as they are referred to the MGE headquarters in Yangon, which will issue the receipt. These receipts are the only documents accepted or required by the Myanmar Customs Department to allow purchasers to export gems or jewelry.

Figure 6. The cabochon on the left (2.65 ct, 8 × 10 mm) is chrysoprase chalcedony from Queensland, Australia; the other (3.15 ct, 8.22 × 10.13 mm) is gaspeite, a nickel ferrous carbonate mined in Western Australia. Photo by Maha DeMaggio.



The new regulations will be in effect for a one-year trial period, after which they will be reviewed. The Ministry of Mines is optimistic that the program will markedly promote free trade and discourage illegal gem trading. More than 200 firms registered with the MGE in the first two weeks of the program's implementation.

Freshwater pearls from Bangladesh. One pleasure of attending the Tucson shows is seeing gem materials from countries not usually considered gem producers. This year, we noticed a parcel of seven very attractive seed pearls, labeled "from Bangladesh," at a booth specializing in South Asian gems.

The pearls (figure 7) were oval to button shaped and ranged up to 3.8 mm in longest dimension. Body colors were white to pink, and all exhibited a very strong pink overtone. The luster was exceptional, being almost metallic. X-radiography and X-ray fluorescence together confirmed that they are natural freshwater pearls. All were purchased in Bombay, India, according to a representative of the vendor Ruedisili, of Sylvania, Ohio.

Tiger's-eye quartz production record in South Africa. South Africa set a new record for tiger's-eye quartz production in 1992, the most recent year for which complete figures are available. At 620.8 tons, this was an increase of 22% over the previous year. Demand for this gem material is primarily from the Far East, Europe, and the United States; demand for material with a strong yellow to red color component comes mainly from the first two areas. (*Diamond News and S.A. Jeweller*, No. 11, November 1993, p. 21)

Cat's-eye sillimanite from Orissa, India. In both the Summer and Winter 1993 Gem News sections, we reported on cat's-eye sillimanite from the state of Orissa, India. This gem material, sometimes called cat's-eye fibrolite because of its fibrous structure, was one of the more readily available phenomenal gems at the 1994 Tucson shows. When cut *en cabochon*, these gems invariably exhibit very distinct, sharp chatoyant bands that are noticeable with even weak overhead lighting. Body colors that ranged from near-colorless to gray, with white chatoyant bands, were most common at Tucson; these stones often had high transparency. Also seen were medium to very dark brown stones with light yellow-brown cat's-eyes. A representative of Orissa Gems reported that brown sillimanites with pink chatoyant bands would soon be in the trade.

The gray body-color material seemed almost visually identical to some of the fiber-optic chatoyant glass marketed under such names as "Catseyte," "Cathaystone," and "Fiber Eye" (see figure 8). The two materials also share the ability to "project" type down the length of their fibers when placed over type on a book or other publication (as does the fibrous mineral ulexite; see the Summer 1991

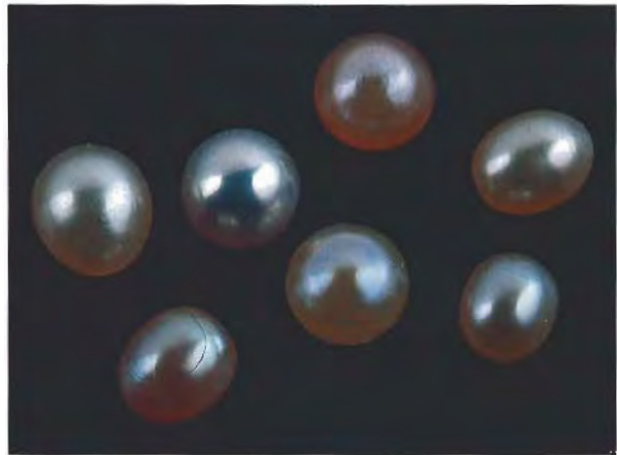


Figure 7. These natural freshwater pearls, ranging up to 3.8 mm in longest dimension, reportedly came from Bangladesh. Photo by Maha DeMaggio.

Gem News, p. 123, for more on this effect in fiber-optic glass). When examined down the length of its fibers, however, the fiber-optic glass revealed the hexagonal packing of its optical fibers; no similar effect was seen in the cat's-eye sillimanite. With magnification, we saw some fibers in the sillimanite at one or two different orientations to the main acicular crystals; we have not seen this in any chatoyant glass. Also, the chatoyant glass is opaque when examined perpendicular to the fibers; the sillimanite ranges from almost transparent to translucent.

At Tucson, we also saw a few cat's-eye sillimanites from Sri Lanka, which has produced this gem material in small quantities over the years; these stones are typically

Figure 8. Glass or sillimanite? A 1.78-ct cat's-eye sillimanite from the relatively new source of Orissa is on the left. The other, 1.72-ct cabochon is chatoyant fiber-optic glass. Photo by Shane F. McClure.

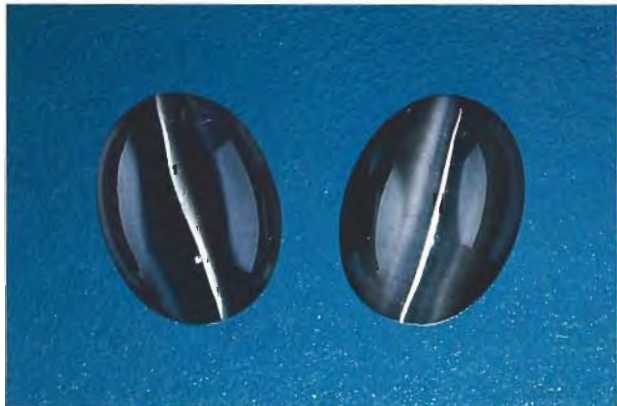




Figure 9. This 2.02-ct tanzanite ($6.92 \times 7.09 \times 6.44$ mm) is a most unusual example of a faceted gem with a reflecting "pinwheel" inclusion. Courtesy of Kaufman Enterprises; photo by Shane F. McClure.

gray and nearly opaque. Before the Indian material appeared on the market, chatoyant sillimanite was considered fairly rare. This is no longer the case.

"Wagon wheel" tanzanite. Both gemologically and aesthetically, some of the most interesting inclusions are those that are positioned in fashioning so as to become integral components of the gemstone's faceup appearance. Among the most familiar examples of this are the acicular inclusions that produce asterism and chatoyancy. Another interesting, if less common, use of acicular inclusions is in the fashioning of "wagon wheel" gemstones, where a single needle-like inclusion is positioned so that it runs from the culet to the center of the table facet. The result is a symmetric pattern of spoke-like reflections, reminiscent of a wagon wheel. Most such gems seen by the editors have been fashioned from rock crystal quartz containing a tourmaline or rutile needle (see, e.g., Gem News, Summer 1986, p. 115).

This spring, the editors saw a very unusual example of this "phenomenon": a 2.02-ct tanzanite that the cutter, Mark A. Kaufman of San Diego, California, calls a "pinwheel" (figure 9). The editors did not have the opportunity to conclusively identify the reflector inclusion, which was very dark with a somewhat granular appearance. It may actually be a growth tube that has filled epigenetically with foreign mineral matter.

Bicolored topaz. Some gem materials, such as tourmaline, frequently occur as color-zoned crystals that can be

cut to show the different zones in a fashioned stone. Other gems, including topaz, rarely display such pronounced color zoning (for an exception, see Lab Notes, Summer 1987, p. 110).

Mark Herschede, of Turмали & Herschede, Sanibel, Florida, reports that rough suitable for cutting intentionally color-zoned topaz (figure 10) is now coming from several locations in western Russia and the Ukraine (the latter producing the finest quality). Mr. Herschede has seen crystals (with small areas of cutting quality) as large as 8 kg, with one faceted stone exceeding 1,000 ct. He maintains, though, that total annual production from all localities is only 30 to 50 kg and that less than 10% of the total production is "facet grade."

The crystals are predominantly lighter shades of blue and pink (see, e.g., figure 11). Some particolored crystals show alternating color zones, such as: blue, pink, blue, brownish pink, and blue.

"Zebra" stones from Australia. At Tucson this year, the editors came across two distinctly different ornamental gem materials that were being offered as "zebra" stones because of their banding. Both are of Australian origin.

"Zebra marble" (figure 12, left) is aptly named for its irregular black-and-white banding. A spot R.I. reading taken on a 547.77-ct sphere gave values of approximately 1.51 to 1.67 with a "birefringence blink." These R.I. values are in the ranges of calcite and dolomite, both carbonates. When exposed to long-wave U.V. radiation, the white areas fluoresced a strong, chalky white and phosphoresced a weak green-white; with short-wave U.V., the reactions were the same colors although the fluorescence was weaker and the phosphorescence stronger. The black areas were inert to both wavelengths. X-ray diffraction analyses of both the black and the white areas

Figure 10. The rough from which this 11.32-ct bicolored topaz ($18.69 \times 8.66 \times 7.35$ mm) was fashioned reportedly came from western Russia or the Ukraine. Courtesy of Turмали & Herschede; photo by Maha DeMaggio.



produced patterns matching a standard for dolomite. We concluded that the material is a dolomitic marble.

The source rock was probably a gray or dark-colored stromatolite ooze (formed from algal reefs) that has been recrystallized. If its origins are similar to that of "zebra dolomite" from Leadville, Colorado, the white bands formed when dolomite dissolved and re-precipitated from formation water (e.g., groundwater) during cave-forming events in the massive dolomite (Horton, 1989, Geological Society of America, *Abstracts with Programs*, Vol. 21, No. 5, p. 95). Although attractive, the material is probably not the best choice for a durable jewelry stone because of its 3.5–4 Mohs hardness. However, material cut as hearts was being offered for use as pendants.

The second ornamental gem material, offered as "zebra rock," consists of alternating parallel layers that are medium-dark reddish brown and tan (figure 12, right). It was described first by Trainer in 1931 (*American Mineralogist*, Vol. 16, No. 5, pp. 221–225) and more recently by Bracewell (*Australian Gemmologist*, Vol. 17, No. 11, 1991, pp. 454–456). This "zebra rock" is from an Upper Proterozoic or Precambrian deposit in the East Kimberley region of Western Australia. It is reported to be a fine-grained siliceous argillite, which is a clay- or mud-containing sedimentary rock that has reacted with silica-rich fluids to form a harder material; Trainer (1931) confirmed quartz and chlorite as visible components.

A triangular tablet of "zebra rock" gave a spot R.I. value of 1.525, although this value could be attributed to a colorless lacquer surface coating (Bracewell, 1991). Such a coating is detectable by an acrid odor produced when it is touched by a thermal reaction tester ("hot point") and by the presence of minute gas bubbles noted with magnification. Microscopic examination also revealed a texture

Figure 11. This 1,644-ct parti-colored topaz is the termination from an 8-kg crystal. Courtesy of Turмали @ Herschede; photo by Maha DeMaggio.



Figure 12. Although both are promoted as "zebra" rocks, the 547.77-ct sphere is a dolomitic marble and the 28.79-ct triangular tablet is a fine-grained siliceous argillite. Photo by Maha DeMaggio.

consistent with fine-grained silt subjected to later cementation. The darker bands are colored by the presence of hematite. These bands, however, do not correspond to the original bedding planes of the siltstone, and there are secondary concentrations of brownish material in the widest tan areas. Although we do not know the cause of color banding in this material, the type of zoning is typical of material that has been colored by rhythmic chemical precipitation, a phenomenon that causes repeated circular features—known as *Liesegang rings*—within fluid-saturated rocks (see, e.g., R.A. Ball, *Australian Gemmologist*, Vol. 12, No. 3, 1974, pp. 89–91).

ENHANCEMENTS

New emerald treatment/polishing systems from Israel.

The Spring 1993 Gem News section (pp. 62–63) described LubriGem, a system produced in Israel that was being commercially promoted for the fracture filling of emeralds. The report mentioned that the system was available in two sizes, one that permitted treatment of several "cups" of stones at a time and a second, smaller unit, that accommodated a single cup. Zvi Domb, developer and manufacturer of LubriGem, has advised us that his company is now offering a mid-size unit, which has a capacity of 400 stones (as compared to 50 and 1,000, respectively, for the small and large units offered originally). All of the units have been designed so that they can be used with a vacuum pump, to remove air and moisture from fractures before they are filled under pressure.

Another Israeli manufacturer, Colgem-Zamrot of Ramat Gan, is now also offering fracture-filling equipment. Two new electrically powered items are for filling fractures in emeralds and other colored stones. The larger unit, called the VPO ("Vacuum and Pressure Oiling System"), reportedly can treat "thousands" of stones in a

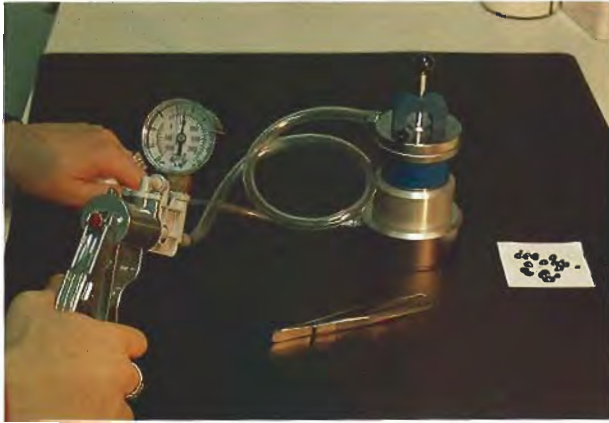


Figure 13. The "Mini Oiler" uses a hand-operated vacuum pump, first to remove air and moisture from fractures and then to carry out fracture filling under pressure. Photo courtesy of Colgem-Zamrot.

few hours with any of a wide range of filling substances, including natural and synthetic oils and resins. It basically consists of two chambers. In one chamber, the stones are first warmed in a vacuum—as above, to remove air and moisture from the fractures. In the second, the filling substance is warmed to reduce viscosity before it is transferred to the chamber that has the prepared stones. To help the filler penetrate the stones, the first chamber can be pressurized up to eight atmospheres.

The other unit, called the Mini Oiler (figure 13), has a single electrically heated chamber. A hand-operated pump creates the vacuum in which the stones are first heated in a small basket at the top of the sealed chamber. They are held there by an ingenious magnet system while the filler is warmed below. Releasing the magnet causes the stone-filled basket to drop into the heated filler. The pump can then be used to pressurize the chamber. Additional filler chambers are available for both systems to permit rapid substitution of different types of fillers.

The third unit, a Rotary Cleaning Machine, has been designed for one specific application: cleaning and buffing stones after fracture filling. Using a circular motion, the machine first cleans the stones for about 30 seconds with soft cloths. The cloths are then replaced with a chamois for a 30-second buffing. The system reportedly can clean "thousands" of stones per hour.

SYNTHETICS AND SIMULANTS

New emerald imitation. D. Swarovski & Co., from Wattens, Tirol, Austria, provided us with a new material—"Swarogreen"—that they designed to imitate emerald. We tested seven small (0.08–0.42 ct) faceted samples (figure 14) and one large (223-ct) parallel-windows sample made to our specifications.

We determined an R.I. range of 1.608–1.612 for this

green, isotropic material (Swarovski had reported 1.605–1.615). All of the faceted samples sank in 3.05-S.G. liquid and floated in 2.67 liquid, which is consistent with the 2.88–2.94 range reported by the manufacturer. Our samples of "Swarogreen" fluoresced a weak green to short-wave ultraviolet radiation and a weak-to-faint yellowish green to greenish yellow to long-wave U.V. With the handheld spectroscope, we noted a strong, broad doublet at about 442 and 448 nm; a triplet of increasing intensity at 466, 472, and 483 nm; and a moderate, broad band centered at about 590 nm. There was no color-filter reaction (i.e., the material appeared green). The faceted samples were all inclusion-free, although we saw some bubbles in the larger sample. We were later told by a company representative that faceted stones containing bubbles are discarded at the factory. Swarovski product literature reports the dispersion at about 0.030, and a Mohs hardness of approximately 6.5.

EDXRF analysis at GIA Research confirmed Swarovski reports that the material is a calcium-aluminum silicate. We also detected praseodymium (Pr) and copper (Cu). X-ray diffraction analysis demonstrated that the material is amorphous. U.V.-visible absorption spectrophotometry confirmed the peaks noted above, and also showed a broad, strong absorption extending from the near-infrared into the visible range to approximately 570 nm. The green color is due to the transmission window formed by the Pr³⁺ (with the 442 to 483 nm peaks) and the Cu²⁺ absorptions starting at about 570 nm.

We concluded that "Swarogreen" is a glass with a relatively high R.I.; it is also significantly harder than most commercial glasses (which have an average Mohs hardness of about 5.5). The higher-than-usual R.I. is due to the presence of both calcium and aluminum.

Although this material is an attractive emerald simulant, it is easily separated from natural emerald because almost all of the gemological properties are different.

Kimberley expands product line. New York-based Kimberley Created Emeralds, which has an exclusive

Figure 14. These faceted examples of "Swarogreen," a new glass imitation of emerald, range from 0.08 to 0.42 ct. Photo by Maha DeMaggio.





Figure 15. These 1.15-mm synthetic spinel triplets are representative of some of the tiny synthetics and simulants now being fashioned with robotic cutting. Photo by John I. Koivula.

agreement to market Australian-produced Biron hydrothermal synthetic emerald in North America, has expanded its product line to include Czochralski-pulled synthetic rubies and blue sapphires. Pulled synthetic alexandrite will also be available soon, according to Kimberley president Leonard Kramer. All these new pulled synthetics are produced in the United States.

Minute "machine-cut" synthetics. Robotic cutting is used to fashion various natural colored stones rapidly and uniformly. This technology is also used to fashion synthetics and simulants. At the 1994 Tucson shows, Golay Buchel had colorless cubic zirconia, flame-fusion synthetic rubies, and synthetic sapphires. All had been robotically cut at the firm's Swiss facilities in calibrated sizes ranging from 1 to 6 mm in diameter. Stones larger than 6 mm are cut by hand, according to Johnny Wong of the firm's California subsidiary.

What we found most interesting is that, to fill out their line of colored stones and provide an emerald simulant, the firm also commercially produces green synthetic spinel triplets (figure 15) in sizes as small as 1 mm in diameter. In such tiny sizes, the central color layer is proportionately a much higher percentage of the entire stone than it is in larger triplets (figure 16).

All of these small stones can present quite an identification challenge to gemologists, especially if set in jewelry.

Faceted synthetic opal. Because most opal with white, gray, or black body color is translucent to opaque, it is typically fashioned as cabochons. Similarly, the synthetic counterparts of white and black opal are almost always fashioned as cabochons.

Some of the more transparent types of natural opal, however, may be faceted. These include the orange to red fire opals, colorless crystal opal, and some of the slightly less transparent milky-appearing material. This year at Tucson, one firm had faceted synthetic material—10 × 5 mm marquises and "roll-top" cuts in 8 × 6 and

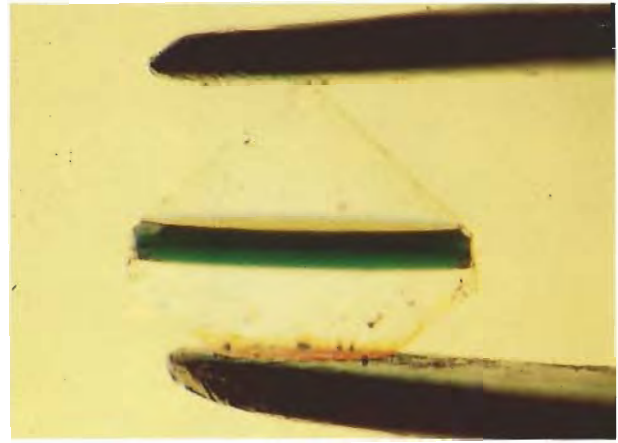


Figure 16. As seen parallel to the girdle when immersed in methylene iodide, the central color layer of this 2-mm-diameter synthetic spinel triplet represents an unusually large proportion of the stone. Photomicrograph by John I. Koivula.

10 × 8 mm sizes (see, e.g., figure 17). This Gilson synthetic opal was semitransparent and near-colorless, that is, with a slightly milky body color. It exhibited a full range of hues in its play-of-color, with green usually predominating.

When examined face-up, most pieces displayed a "streaky" pattern to the play-of-color, something we have noted in the past with synthetic opal cabochons that have been fashioned with their bases oriented at right angles or at a very oblique angle to the direction of sedimentation of their silica spheres. Because of the orientation in fashioning, the diagnostic "chicken-wire" structural patterns were seen when the stones were examined through their sides rather than face-up; this is typically the case with synthetic opal cabochons cut to display a "harlequin" pattern to their play-of-color.

Bright yellow "pulled" synthetic sapphires. A number of Czochralski-pulled synthetic gem materials have been in the trade for some years. These include synthetic alexandrite and yttrium aluminum garnet (YAG) in various colors, as well as synthetic ruby and blue, green, and pink synthetic sapphires. At Tucson this year, Manning International, of New York, offered what appears to be a new color of Czochralski-produced synthetic sapphire—a highly saturated, slightly greenish yellow (figure 18). Although the color was unlike that of most natural or flame-fusion synthetic yellow sapphires (which usually have a secondary orange-to-brown component), it resembled that of some golden beryls.

EDXRF analysis of two specimens revealed the presence of nickel, but no other chromophores in significant amounts. Although nickel has long been used to produce yellow in flame-fusion synthetic sapphires, these typically also contained other elements. For example, chromium and/or iron moderate the "nickel yellow" to a more natural-appearing tint (see, e.g. "Naturally-Coloured and Treated Yellow and Orange-Brown Sapphires," by



Figure 17. Like some natural crystal opal and other transparent-to-translucent types, these Gilson synthetic opals (0.70–1.96 ct) have been faceted rather than cut en cabochon. Courtesy of Manning International, New York; photo by Robert Weldon.

Schmetzer et al., *Journal of Gemmology*, Vol. 18, No. 7, 1983, pp. 607–622). In fact, with the desk-model spectroscope, we did resolve a faint 690-nm emission ("fluorescent") line—which commonly denotes the presence of chromium in flame-fusion synthetics—in three samples tested gemologically. All three also fluoresced a faint orange to short-wave U.V. radiation; one of the three had a similar reaction to long-wave U.V.

Magnification revealed a few pinpoint inclusions, possibly gas bubbles, in one of the three specimens. Using immersion, brightfield illumination, and a blue contrast filter, we saw curved growth features in all three stones. In one sample, these consisted of curved yellow color banding, like that noted in some flame-fusion yellow synthetic sapphires. Each of the other two pieces appeared evenly colored except for one curved colorless band. With the possible exception of this band and the atypical color, there were no features that would clearly distinguish this product from flame-fusion synthetic yellow sapphires.

ANNOUNCEMENTS

"Cutting Edge" winners start tour. Winning entries in the 1994 Cutting Edge Gemstone Competition debuted at



Figure 18. Nickel is the primary coloring agent in these three synthetic sapphires (1.66, 2.91, and 1.66 ct) produced by the Czochralski-pulling method. Courtesy of Manning International; photo by Maha DeMaggio.

the June JCK Show in Las Vegas, starting a year-long tour of North American museums, trade shows and retail stores. The 47 winners were chosen from 290 entries in 24 categories.

The gemstone-fashioning competition now includes two divisions. Division 1, the International Gemstone Showcase, is open to natural gemstones fashioned in any country by any cutter, even if the identity of the cutter is not known (collectors and dealers, as well as cutters, can submit entries). Division 2, the North American Gem Design Competition, is limited to natural gemstones cut in North America by professional lapidary artists.

Winners were chosen April 17 at the Dallas headquarters of the American Gem Trade Association (AGTA), which created the competition in 1991. Sites where the winning entries can be viewed include the New Mexico Museum of Natural History, Albuquerque, October 19–31; the William Weinmann Mineral Museum, Cartersville, Georgia, November 7–22; and the AGTA GemFair in Tucson, Arizona, February 1–6, 1995 (winners will be honored there at an awards reception on February 1, 1995).

Rare colored diamonds displayed. "Exceedingly rare" is how Joel Bartsch, curator of gems and minerals for the Houston Museum of Natural Science, describes a collection of 162 colored diamonds on display at that museum through December 31. Only one or two diamonds in 10,000 can be considered fancy color, according to the museum in Houston, Texas. Billed as the Butterfly Collection, the diamonds are on loan from Aurora Gems and weigh up to 3 ct.

THE PROFESSIONAL'S GUIDE TO JEWELRY INSURANCE APPRAISING

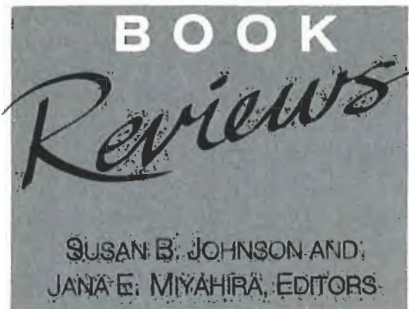
By Patti J. Geolat, C. Van Northrup,
and David Federman, 167 pp., illus.,
Vance Publishing Corp., Lincoln-
shire, IL, 1994. US\$95.00.*

Geolat, Northrup, and Federman announce the mission of their seminal text early in the introduction: to provide "a beginner's book on the discipline of appraising as well as a specific guide to jewelry insurance appraising . . . to make the precepts of replacement value appraisals both accessible and understandable to both jewelry and insurance industries." Because of this ambitious mission, we are exposed to the basics of two separate but interrelated subjects: jewelry appraising and jewelry insurance.

As befits a beginner's text on the discipline of appraising, the authors lay their foundation without presuming that the reader has had any prior appraisal education. In addition, as the title suggests, they narrowly limit their focus to issues consistent with *insurance* appraisal. However, an experienced jewelry appraiser will find provocative and valuable ideas.

Three chapters address appraisal issues that are both timeless and current, often probing controversial topics that clearly merit examination. Two examples—chapters titled "The Probity Principle" and "The Law of Objectivity"—are well thought out and presented in an interesting fashion. They emphasize the essential elements of ethical appraisal practice. Particularly important, and unique among appraisal texts, is the concise explanation of the insurance contract options available for jewelry protection. Most appraisers, neophyte and veteran, should find these chapters stimulating reading and a wise investment of their time.

Four chapters on basic gemology comprise almost half the book. Although it is written for the novice gemologist, this portion of the text does contain important and timely



information about diamonds, colored stones, and jewelry-fabrication techniques. For example, the chapter on "Finished Jewelry" presents excellent reference charts as well as color photographs detailing the features that identify whether metalwork has been poorly or correctly crafted.

A comprehensive case study concludes the text. This study examines and explains a thorny appraisal assignment, probing the "market data" method of valuation. It effectively embodies the book's main thrust and drives home the practical necessity of adhering to responsible professional standards, both technical and ethical.

This well-written text leaves little to criticize. My greatest disappointment, and the book's principal weakness, is its lack of a bibliography. In addition, chapter two contains a laborious historical excursion that is of questionable value. Finally, because the authors' treatment of professional ethics and valuation methodology advances important yet controversial precepts, greater depth of discussion would have been most welcome.

SHARON WAKEFIELD

*Wakefield Gemological Laboratory
Boise, Idaho*

JEWELRY AND METALWORK IN THE ARTS AND CRAFTS TRADITION

By Elyse Zorn Karlin, 272 pp., illus.,
publ. by Schiffer Publishing, Atglen,
PA, 1993. US\$69.95*

The Arts and Crafts movement was started in mid-19th century England

as a reaction against the dehumanizing effects that the Industrial Revolution was having on the arts. Movement leaders believed that by returning to the craft guild system of the Renaissance era, artisans would regain a sense of pride in their work. Guilds were formed by small groups of artists who produced goods of simple design and affordable materials that were predominantly handmade. Many of these artists also taught at schools that were set up specifically to provide training in the decorative arts. Within a short period, Arts and Crafts-inspired movements spread throughout the Western world.

This book is an excellent reference for the jewelry produced as part of the Arts and Crafts movement. The author not only describes how the movement was manifested in different countries, but she also demonstrates how it has evolved up to the present day. Each chapter begins with the chronological development of the style in that country or group of countries, followed by short biographical details for the artists and artisans; sidebars show the typical materials, techniques, and motifs used, as well as provide descriptions of the makers' marks when known. The text is lavishly illustrated with photographs and drawings of jewelry and metalwork by the craftsmen described. In addition, references are indicated in the text, with full bibliographic details given at the end of each chapter.

The bulk of the book focuses on England, where the movement began and where it had its greatest following. Ms. Karlin has included every name she could find that was connected with English Arts and Crafts, although the amount of information for each person varies considerably. Her reasoning is that more information may come in time, and at least each contributor is noted. For artists such as Charles Robert Asbee, how-

*This book is available for purchase at the GIA Bookstore, 1660 Stewart Street, Santa Monica, CA 90404. Telephone (800) 421-7250, ext. 282.

ever, the mini-biographies fill several pages. These biographies are followed by historical details for guilds, schools, and leading jewelry firms.

In general, the same format is continued for each chapter throughout the book, although where there was little manifestation of the style, or little information to be had, the chapters are very brief (as is the case with Ireland and Australia). "France and Beyond" tackles the question of how to distinguish Arts and Crafts pieces from those in the contemporaneous Art Nouveau style. Essentially, Arts and Crafts is more staid in subject matter, with an emphasis on simplicity of line and materials; Art Nouveau is more passionate and figurative, and humble materials such as horn and glass are frequently combined with more expensive gemstones and gold. This chapter also addresses the jewelry from Belgium, Spain, Italy, and Russia—countries that produced more pieces in the Art Nouveau style than in Arts and Crafts. Subsequent chapters cover the Jugendstil in Germany, the Secessionsstil in Austria, Scandinavia's contribution, and Arts and Crafts in the United States.

The book closes with a series of appendices that include a brief glossary of terms, a list of hallmarks, and lists of dealers, auction houses, and museums that specialize in—or have collections of—Arts and Crafts jewelry. Also provided is a value reference for some of the jewels illustrated in the book, a particularly useful feature for appraisers. Finally, there is an extensive bibliography and an equally extensive index.

Even though there are currently several other books that go into more detail on specific artists, or on the general movement in particular countries, this is the best overall reference on the subject to appear so far. If the quality of the photographs is sometimes deplorable, they are nevertheless important illustrations for the text and thus can be forgiven. The text itself is very readable, and the author's organization of this

sprawling subject is commendable. Considering the amount of information contained in this solid work, it is well priced and should be a welcome addition to the library of all antique-jewelry enthusiasts.

ELISE B. MISIOROWSKI

Research Librarian

Richard T. Liddicoat Library

and Information Center

Gemological Institute of America

Santa Monica, California

THE LAST EMPIRE: DE BEERS, DIAMONDS, AND THE WORLD

*By Stefan Kanfer, 409 pp., illus.,
publ. by Farrar, Straus & Giroux,
New York, 1993. US\$25.00**

Good news doesn't make good "news." Most of us feel that, as a result, sensationalist writers emphasize the "bad" to lure the interest of readers. To those of us in the gem and jewelry industry, this book will have little appeal because it is a rehash of a story that's been told before. It's another tale about business—albeit the excitement of the diamond business. Mr. Kanfer questions the enduring power of De Beers Consolidated Mines and whether it is a credit to the leadership of the company as well as to the industry it serves. "A benevolent monopoly" is the description of De Beers commonly used throughout the diamond industry to reply to this query.

Mr. Kanfer is a veteran writer who weaves his sometimes rambling story from the discovery of diamonds in South Africa in the late 1800s, up to present-day warnings of a crisis in the industry. Given the situation in South Africa at this time, any prediction of future events would necessarily have to be fraught with trepidation.

The author describes the fantastic development of the De Beers organization and how it has thrived notwithstanding wars, political upheavals, economic depressions, American antitrust efforts, African liberation, and a host of other challenges.

The main source of De Beers's wealth has been diamonds. Their strategy is, as it has been, to make diamonds more valuable by keeping them rare—hence the formation of the Diamond Trading Company (DTC). Mr. Kanfer describes in detail the formation of the DTC and discusses the beneficiaries of its development. He mentions the heavy Jewish influence in the diamond trade, which resulted because many Jews were denied opportunities elsewhere. The amalgamation of diamond miners by Cecil Rhodes and its subsequent development by the Oppenheimer family is also clearly described, including the ritual of sightholders receiving their allocations of rough stones in "cigar boxes." For people not in the industry, these anecdotes are quite interesting. However, the author goes on to suggest that De Beers acted improperly during World War II in their handling of the stockpile of industrial diamonds needed for the war effort. I find this attack completely untrue. De Beers operated under wartime supervision by the British government, and the British government dictated policy. This type of sensationalistic distortion and the suggestions of impropriety certainly sour the book for those of us in the industry who are aware of the positive role that the De Beers organization played in the United States' wartime effort.

Worldwide, the development of natural resources has often been tough and brutal. However, capitalism flourishes. As distinguished American jurist, Judge Learned Hand, noted earlier this century, it was proper to arrange one's affairs to pay the least taxes. And many of our major industrial companies have grown on the "backs of others." These practices are not new. Following these lines, Mr. Kanfer's book would have benefited from a sturdier formation of purpose.

HOWARD HERZOG

Gueits, Adams, Herzog & Cohen

Newport Beach, California

GEMOLOGICAL ABSTRACTS

C. W. FRYER, EDITOR

REVIEW BOARD

Andrew Christie
GIA, Santa Monica
Jo Ellen Cole
GIA, Santa Monica
Nanette D. Colomb
GIA, Santa Monica
Maha DeMaggio
GIA, Santa Monica
Emmanuel Fritsch
GIA, Santa Monica

Juli Cook-Golden
Royal Oak, Michigan
Michael Gray
Missoula, Montana
Patricia A. S. Gray
Missoula, Montana
Professor R. A. Howie
*Royal Holloway University of London
United Kingdom*
Karin N. Hurwit
GIA Gem Trade Lab, Santa Monica

Robert C. Kammerling
GIA Gem Trade Lab, Santa Monica
Loretta B. Loeb
Visalia, California
Elise B. Misiowski
GIA, Santa Monica
Gary A. Roskin
*European Gemological Laboratory
Los Angeles, California*
Jana E. Miyahira
GIA, Santa Monica

James E. Shigley
GIA, Santa Monica
Christopher P. Smith
*Gübelin Gemmological Laboratory
Lucerne, Switzerland*
Carol M. Stockton
Los Angeles, California
Rolf Tatje
*Duisburg University
Duisburg, Germany*
Robert Weldon
Radnor, Pennsylvania

COLORÉD STONES AND ORGANIC MATERIALS

Communicating colour in gemmology. G. Brown, *Australian Gemmologist*, Vol. 18, No. 6, 1993, pp. 187-190.

This report, Dr. Brown's presidential address to the Gemmological Association of Australia on May 7, 1993, begins by briefly reviewing the importance of color in gemology and contrasting that with the often poor color-communication skills of many gemology students and practicing gemologists. He then asks rhetorically if the Gemmological Association of Australia (GAA) should not put more emphasis on color communication in its training.

After next summarizing the physiology of color perception, Dr. Brown looks at factors involved in quantifying and describing gemstone colors. The accuracy and reproducibility of a color-match system depends on: (1) the composition and structure of the color standards used (e.g., GIA's ColorMaster and commercially printed color-grading systems such as Gem Color Dialogue, Gem Dialogue, and Gem Color Scan) and their respective limitations, as well as the lighting chosen; (2) the training, experience, and practice of the grader; (3) the lack of any color-perception deficiency of the grader; and (4) the absence of confounding optical effects (e.g., negative after image) from the grading environment.

Next described are three admittedly broad levels of color communication used in the gemstone industry. Level 1 communication uses the simplest descriptive terms, such as "pink tourmaline" and "Burmese ruby." Level 2 employs somewhat more detailed (yet still sub-

jective) descriptions, for example, "light grayish blue aquamarine" or "vivid medium-dark slightly bluish green Zambian emerald." Level 3 uses specific instrument-based descriptions, such as the Gem Technology Systems GTS-4000X computer-generated certificates. However, this technology, Dr. Brown points out, is not available to many gemologists.

He then proposes that color science be taught as an integral part of GAA's Diploma in Gemmology. Some specific components of this proposed training are then provided. RCK

Cultured pearl grading. A. J. Clark, *Australian Gemmologist*, Vol. 18, No. 7, 1993, pp. 214-215.

Concern about cultured pearls that have very thin nacre coatings led the British Association of Cultured Pearl Importers in 1990 to approach the Gemmological Association and Gem Testing Laboratory of Great

This section is designed to provide as complete a record as practical of the recent literature on gems and gemology. Articles are selected for abstracting solely at the discretion of the section editor and his reviewers, and space limitations may require that we include only those articles that we feel will be of greatest interest to our readership.

Inquiries for reprints of articles abstracted must be addressed to the author or publisher of the original material.

The reviewer of each article is identified by his or her initials at the end of each abstract. Guest reviewers are identified by their full names. Opinions expressed in an abstract belong to the abstractor and in no way reflect the position of Gems & Gemology or GIA.

© 1994 Gemological Institute of America

Britain (GAGTL-GB) for help in designing a system for grading nacre thickness. This article describes the system developed by the GAGTL-GB in conjunction with the British Jewellers Association.

The first step in grading is production of a standard X-radiograph. Nacre thickness is measured on the X-radiograph using a 10× corrected lens with a built-in millimeter graticule. The measurements are taken on each pearl in a necklace, at a point on the film perpendicular to the drill hole, as this is the area subjected to the greatest wear. An average thickness is then calculated and a grade assigned, based on a five-tier system. Any pearl with less than an 0.15-mm nacre thickness must be replaced before the GAGTL-GB will issue a grading report on the necklace. RCK

The first occurrence of musgravite as a faceted gemstone. F. Demartin, T. Pilati, M. Gramaccioli, and V. de Michele, *Journal of Gemmology*, Vol. 23, No. 8, 1993, pp. 482–485.

Until this time, musgravite has not been known to occur in qualities suitable for faceting. The authors describe how they identified as musgravite two stones that had been represented as taaffeite. These two specimens are noticeably lighter in color than is typical for taaffeite, but they are otherwise indistinguishable from taaffeite on the basis of routine gemological testing. Refractive indices, density, optical spectra, fluorescence, and inclusions are essentially the same for both musgravite and taaffeite. In addition, chemical distinction depends on stoichiometry rather than on elemental differences, so chemical analysis does not readily provide a clear separation either. The authors made their determinations on the basis of X-ray diffraction analysis, which does give positive proof of identity, and the exact data are given in the article. The two minerals are easily distinguished when in crystal form, since their habits are distinct: rhombohedral and doubly terminated for musgravite, versus pyramidal with polar symmetry for taaffeite. It remains to be seen how the gem market—given the collector value of taaffeite and the apparently greater rarity of gem musgravite—will react to this discovery. Either way, gemologists should be aware of the distinction. It is hoped that additional means of separation, such as infrared spectrometry, will be explored by these or other researchers. CMS

An intriguing black necklace. G. Brown and S. M. B. Kelly, *Australian Gemmologist*, Vol. 18, No. 6, 1993, pp. 200–202.

This Gemmology Study Club Report addresses the authors' examination of an incomplete necklace, with the appearance of jet, that was submitted for identification. The components of the necklace were black in thick section and brownish red or purplish red in thin section, with a resinous luster like that of amber. However, gemological testing eliminated the possibility

that it was jet. The fracture was smooth, with a somewhat granular surface. The material chipped on peeling (also like amber), had a Mohs hardness of 2, and had a black streak. It was not noticeably softened by the application of volatile organic solvents, ether and toluene, and it melted when touched with a hot point. Other properties determined were an S.G. of 1.15, a vague 1.5+ R.I., and no reaction to either ultraviolet wavelength.

Based on these data, the authors hypothesize—tenuously—that the necklace may have been constructed from albertite, a rare "mineral asphalt" (asphaltic pyrobitumen) with a jet-like appearance that occurs in veins in the Albert Shale of Albert County, New Brunswick, Canada. The authors invite informed comment about the possible identity of the material. RCK

Unusually dark red tourmaline of the dravite-schorl series. U. Henn and H. Bank, *Neues Jahrbuch für Mineralogie, Monatshefte*, No. 9, 1991, pp. 408–412.

This article gives the chemical composition, determined by electron microprobe analysis, and the polarized optical absorption spectra of a dark red tourmaline from a location about 80 km north of Lusaka, Zambia. The data fall within the range of those from similar dark red dravites from Kenya and Zambia. The tourmaline examined is definitely a dravite-rich member of the dravite-schorl series, and shows dark red and brownish red pleochroism. Its color is caused by iron. RT

DIAMONDS

Can diamonds be dead bacteria? E. G. Nisbet, D. P. Matthey, and D. Lowry, *Nature*, Vol. 367, February 24, 1994, p. 694.

In this letter to the Scientific Correspondence section of *Nature*, the authors suggest that organic materials from hydrothermal-ridge communities may be the source of carbon for some diamonds from eclogites. The ¹³C isotope ratios in eclogitic diamond are very light, and carbon from living organisms is the main terrestrial material that contains such light isotopes. Because of this, previous authors had suggested that the carbon in some diamonds originally came from organic-rich sediments.

Communities of living creatures have been found growing near hydrothermal plumes that are associated with oceanic crust presently forming at mid-ocean ridges. Methanogenic bacteria thriving in these communities not only have extremely light carbon isotopes, but they also produce sulfur with sulfur isotopic ratios that are consistent with those found in sulphide inclusions in eclogitic diamonds. The high manganese content of some diamondiferous eclogites is also consistent with a mid-ocean-ridge hydrothermal source.

Oceanic crust formed at mid-ocean ridges is recycled into the Earth's mantle through subduction. This explains how carbon-rich sediments from hydrothermal plumes can end up at diamond-forming depths. The

methane-forming bacteria at these plumes have not changed since late Precambrian times, and some authors have suggested that these bacteria may have been the first life on Earth, from which all other life evolved. Thus, as metamorphosed fossil bacteria, eclogitic diamonds may be the physical remains of our earliest ancestors.

Mary L. Johnson

Diamond replicas—possible but just. R. Willmott, *Journal of Gemmology*, Vol. 23, No. 8, 1993, pp. 486–490.

Mr. Willmott describes the problems and issues encountered in making replicas of famous diamonds, beginning with a description of the differences between a replica and a model. The latter is a dimensionally very precise match, usually of a rough diamond, created to explore cutting options. This is now usually done on a computer, but a variety of materials have been used, including lead. A replica is usually made from a finished gem and is designed to appear as much as possible like the original diamond, including color and transparency as well as size and cut; however, its dimensional accuracy is less than that of a model. This article explains why.

Following a brief review of the history of diamond replicas, the author describes the many problems that the replicator might encounter, as well as some good sources of information. One of the most common problems is that the original is rarely available for study. Either the diamond's whereabouts are unknown, or it is in a private collection. Even data collected by reputable laboratories is often confidential. When a certificate or report actually is available, it is invariably inadequate. Photographs, such as those in sales catalogs, provide useful information about design details of cuts and are often published "actual size," but determination of facet angles is difficult. Sometimes casts were made of historic diamonds and may still be available, although their accuracy will depend on the immutability of the cast's material. Although few gemologists will ever face these issues, this is an interesting and very readable short article. CMS

Gemmological properties of type Ia diamonds with an unusually high hydrogen content. E. Fritsch and K. Scarratt, *Journal of Gemmology*, Vol. 23, No. 8, 1993, pp. 451–460.

The best-known impurities in diamond are nitrogen (type-I diamonds) and boron (type IIb), but hydrogen has recently emerged as a third common impurity (in type-Ia diamonds). This article provides some insight into how hydrogen may influence the optical properties of gem diamonds. One hundred and thirty-nine hydrogen-rich type-Ia diamonds were studied, plus 31 treated specimens, as identified on the basis of infrared features reported by previous researchers. This collection includes 78 yellow, gray, or brown diamonds; six bluish gray to grayish violet diamonds; eight white ("opalescent") diamonds; 47 blue or green diamonds, plus the 31 green, blue, or yellow

treated stones. The testing procedures included microscopic examination, exposure to U.V. radiation, and optical and infrared spectroscopy. Only rarely did a handheld spectroscope indicate the presence of H, with a line at about 545 or 563 nm. Infrared and U.V.-visible spectroscopy revealed features typical of H-rich diamonds, and further showed that all of the diamonds in the collection were type Ia, with characteristic features in their optical spectra. The researchers also observed H-related features not previously reported. Some of the features are related to color, such as a correlation noted between the 3235 cm^{-1} band and the gray-to-violet color range. Most notably, H-rich diamonds include grayish blue stones that resemble type-IIb diamonds and stones that exhibit chameleon behavior. Observations also show that H-rich diamonds have both octahedral and cuboid growth sectors. No distinctions between H features in natural and treated specimens are mentioned. Spectral graphs and color photographs well illustrate the features discussed.

CMS

It's not us flooding the market. C. Even-Zohar, *Mazal U'Bracha*, Vol. 10, No. 56, 1994, pp. 33–40.

Editor Chaim Even-Zohar interviewed Russian "diamond czar" Evgeny Bychkov when Bychkov was in Israel to negotiate the opening of an Israeli office of Komdragmet, the Committee on Precious Stones and Metals of the Russian Federation.

As chairman of Komdragmet, Bychkov has lately been engaged in a war of words with De Beers's Central Selling Organisation (CSO) over the issue of large parcels of Russian diamonds allegedly turning up on the market, and whether Russia has been violating its sales agreement with the CSO and selling its diamond rough outside the De Beers network. Bychkov, while claiming that Russia can get 20% to 30% more for its diamonds on the open market than De Beers is paying, denies the charge. At several points in the interview, Bychkov maintains that the stones in question are not Russian at all, and that the only diamonds Russia sells outside the network are industrial diamonds that De Beers declined to purchase. Russian gem-quality diamonds are turning up in the market simply because the rough that Russia has sold to De Beers is now being sold off by sightholders, he says.

According to Bychkov, De Beers is simply upset because Russia has changed its diamond policy so that its diamonds are now sold through a commercial organization representing the interests of Yakutia and Russia, as well as through the state organization to which De Beers is accustomed.

Bychkov confirms that Russia and De Beers are discussing a Moscow diamond sight as well as an offer to Komdragmet by De Beers for seats on its board, stock shares, and cash in exchange for control of the Russian diamond stockpile (which, he says, is "somewhat lower" than the interviewer's estimate of 200 million carats worth \$7 billion).

AC

GEM LOCALITIES

On the colour and pleochroism of Cu-bearing green and blue tourmalines from Paraíba, Brazil. U. Henn and H. Bank, *Neues Jahrbuch für Mineralogie, Monatshefte*, No. 6, 1990, pp. 280–288.

After a short review of the composition and the causes of color in other blue and green tourmalines, Henn and Bank discuss the microprobe analyses and absorption spectra in the 1,400–200 nm range carried out on polished and oriented sections of Paraíba tourmalines. The microprobe analyses revealed very low Fe contents and no Ti, V, and Cr, but distinct concentrations of Cu and Mn. The absorption spectra showed absorption bands at 700 nm and 520 nm in blue stones, but only the 700-nm band in green stones. While blue and green in other tourmalines can be linked to charge-transfer processes of Fe, Cr, and V, Henn and Bank believe that the blue in these tourmalines is caused mainly by the absorption of Mn^{3+} with influence by Cu^{2+} , whereas the green color and pleochroism are caused by Cu^{2+} alone. RT

Leopardwood mosaic opal. M. Sawicki and G. Brown, *Australian Gemmologist*, Vol. 18, No. 6, 1993, pp. 195–196.

This brief report describes some opal diggings in far southwest Queensland. The Leopardwood mine, located in the Blackgate opal field, about 800 km (500 miles) west of Brisbane, is one of several localities that produce small ironstone "nuts" and boulders that contain opal "in-filling" shrinkage fractures and central cavities. This ironstone occurs in "remnant" deeply weathered sediments of the Cretaceous Winton Formation. At the Leopardwood mine, the opal level—1 to 2 m underground—typically consists of a conglomerate that overlies a water-retentive clay and underlies soil and sandstone.

While the ironstone "nuts" and larger boulders are relatively easy to find at the mine, locating those that contain opal with play-of-color is much more difficult and requires some machinery, hand mining, and a lot of luck. Gems cut from this material usually contain both matrix and opal, and are referred to as opal matrix, or mosaic opal. Photos of some attractive matrix gems accompany the report, as does a good map of the area.

Also mentioned is the senior author's Ben Hur mine. Unfortunately, only 5% of the opal from this mine is suitable for cutting, as the ironstone backing is very brittle and often causes the opal to crack during shaping and polishing. Some material from this mine also suffers from rapid dehydration. RCK

Myanmar and its gems—an update. R. C. Kammerling, K. Scarratt, G. Bosshart, E. A. Jobbins, R. E. Kane, E. J. Gübelin, A. A. Levinson, *Journal of Gemmology*, Vol. 24, No. 1, 1994, pp. 3–41.

Comprising most of the issue, this article updates the 1992 *Gems & Gemology* article on the Mogok ruby and

sapphire deposits. The scope of this new article is much broader; it encompasses the wide range of materials found in Myanmar, including corundum, jadeite, peridot, spinel, beryl, lapis lazuli, topaz, tourmaline, zircon, pearls, and a host of unusual gem and collectors' minerals. The article reviews the general geology of the region, as well as the various mining localities, illustrated by several maps. Many color photographs accompany the text, which concludes with a discussion of the current marketing situation. This article should be of interest to all gemologists, as it covers one of the world's great gem sources. CMS

Rhodonite from Upper Coomera—S.E. Queensland. G. Brown and H. Bracewell, *Australian Gemmologist*, Vol. 18, No. 6, 1993, pp. 197–199.

After reviewing rhodonite's mineralogy, the authors describe two gem deposits in the Upper Coomera district of southeast Queensland. One, a commercially operated fossicking (collecting) area known as the Jasper Farm, is located 7 km west of Helensvale, a small town 70 km south of Brisbane. This site produces a low-manganese-content pinkish to reddish jasper.

The other site, also producing a pinkish to reddish ornamental gem material, lies approximately 2 km southwest of the Jasper Farm, on the eastern slope of Tambourine Mountain. Specimens from this locality, which is called the Old Gold Mine because gold was commercially mined there in the 1930s, were examined by the authors. They determined the following properties: color—reddish pink, extensively veined by black manganese oxide and whitish quartz; [Mohs] hardness—6; fracture—low conchoidal; S.G.—3.32 to 3.49; spot R.I.—two distinct readings, at 1.56/1.55 and 1.72/1.73; diaphaneity—translucent to opaque; polish luster—waxy; pleochroism—very indistinct shades of red; and absorption spectrum—not diagnostic.

On the basis of these properties and criteria in unpublished research from the Queensland Mines Department, the authors identified this ornamental gem material as a quartz-rich rhodonite-quartz intergrowth. The material is illustrated both macroscopically and microscopically, and a locality map is included. RCK

Role of aluminium in the structure of Brazilian opals. F. Bartoli, D. Bittencourt Rosa, M. Doirisse, R. Meyer, R. Philippy, and J.-C. Samama, *European Journal of Mineralogy*, Vol. 2, No. 5, 1990, pp. 611–619.

The authors studied more than 120 opals from the Pedro II mine in Piauí, Brazil. Opals there occur in "recent" fractures that crosscut contacts of sandstones, claystones, and dolerites. Most of the article details the testing methods used—chemical analysis, thermal analysis, infrared spectroscopy, and X-ray diffraction analysis—and how results of that testing link the outward appearance of the Brazilian opals to their respective host rocks

and Al content. Opal in sandstone was "white-yellow" to dark yellow, Al poor, and had a relatively well-ordered silica-sphere structure. Opal in claystone had blue iridescence, less-densely packed silica spheres, and was Al rich. Opal in dolerite was blue to dark blue with violet and blue iridescence and was Al poor. Aluminum appears to influence the order and packing structure of the silica spheres. Rehydration was more complete with Al-rich opals than with those that are Al poor. The opals differ clearly in water and trace-element content. The authors also compare their results to earlier studies of both Piauí and Australian opals. RT

INSTRUMENTS AND TECHNIQUES

Fluorescence excitation-emission spectra of chromium-containing gems: An explanation for the effectiveness of the crossed filter method. D. B. Hoover and A. F. Theisen, *Australian Gemmologist*, Vol. 18, No. 7, 1993, pp. 182–187.

Emission of red light induced by absorption of blue or green light is the basis for the crossed-filter method of gem testing in chromium-containing stones such as rubies and emeralds.

The authors looked at 25 specimens of 10 different chromium-bearing gem species, using an automated Perkin-Elmer MPF-448 fluorescence spectrophotometer. Emission spectra were measured for each specimen for excitation wavelengths from 270 nm (ultraviolet) to 600 nm (orange). They discuss in detail their results for ruby, emerald, red spinel, and jadeite; they mention alexandrite, kyanite, chrome tourmaline, and pink topaz. In general, light emission by these materials is more efficient for excitation by blue or green light than by ultraviolet light.

Verneuil (flame-fusion) synthetic rubies and natural rubies from Burma (Myanmar) show sharp emission at 692 nm for all excitation wavelengths, although the emission is least efficient for excitation at 310 nm. Iron quenches chromium fluorescence, so Thai rubies—for example—emit no light for excitation below 350 nm, and they emit only about 1% as much light as Fe-free rubies for excitations at longer wavelengths.

The maximum emission wavelength for emerald is beyond 700 nm in the infrared region, although there is appreciable emission at 700 nm. Synthetic stones show the strongest emission spectra; emission efficiency decreases sharply as iron content increases. Emission is strongest for wavelengths of light that are best absorbed by the stone (i.e., bands seen in the absorption spectrum of emerald at 400–460 nm and 560–600 nm). Emerald, red spinel, and jadeite emit almost no light for excitation wavelengths below 350 nm. The maximum emission for red spinel is at 685 nm; for jadeite it is somewhere in the infrared (which is why fine chrome jadeites do not show a red response to the Chelsea filter).

The crossed-filter method does not require a spectrophotometer, only a strong incandescent light source and a pair of filters: one that transmits only high-energy

(blue or green) light, and one that absorbs high-energy light and only transmits red light). When observed between the filters, stones with significant chromium content (if not quenched by iron) will appear to glow red against a black background. The authors note that this test will not provide conclusive proof of natural versus synthetic rubies, since many synthetics now contain iron. Mary L. Johnson

JEWELRY HISTORY

Fruit salad à la Deco. E. Blauer, *Lapidary Journal*, Vol. 47, No. 11, February 1994, pp. 50–54

This article makes a strong case that the style of jewelry popularly known as "fruit salad" or "tutti-frutti" owes its origin to India. The style was popular from the mid-1920s to mid-30s, though imitations are produced even today. Tracing the Mughal empire in India, with its attendant mix of cultures, Ms. Blauer explains how strictures of the Moslem religion prohibited some motifs. Besides India, gems came from nearby Burma (Myanmar) and Ceylon (Sri Lanka). The enamels of Jaipur and Lucknow echoed the colors of ruby, sapphire, and emerald. It seems more than mere coincidence that Jacques Cartier first visited the area in 1911, and pieces of jewelry employing the distinctive style—although much more refined—were subsequently produced by his studio. The Cartier Museum now has perhaps the largest collection of "fruit salad" jewelry—more than 1,000 pieces. Three color photos accompany the article. PASG

PRECIOUS METALS

Gold sales soar 8% for 1993, WGC reports. G. Beres, *National Jeweler*, Vol. 38, No. 8, April 16, 1994, pp. 4, 28.

The World Gold Council (WGC) reported a 10.6% increase in gold jewelry sales last December, capping an impressive year in which total sales increased 8%, to \$9.65 billion. Last year's success, which included the highest single-month increase since WGC began tracking retail sales of gold in 1988, comes on the heels of a 5% increase for 1992.

All classes of trade that were measured showed a profitable 1993. Discount stores, with an 11% share of the gold jewelry market, saw dollar sales increase 24.6%; department stores, representing 21% of sales, were up 7.1%; chain jewelers, 29% of the market, posted a 5.3% gain; catalog showrooms, with a 15% share, finished the year with a 4.2% increase; and independent jewelers recorded a 6.7% rise.

Gold jewelry was a top performer in all merchandise categories last year, and neck chains, representing 43% of overall business, led the way, growing 8.4% in 1993. For the fifth straight year, the average price paid for a piece of gold jewelry remained at \$88. Although all retail channels sold at a higher average price in 1993, the tremendous sales growth of the discount sector flattened out the overall average price. MD

SYNTHETICS AND SIMULANTS

Opalite triplets—new imitations of opal. K. Scarratt, R. C. Kammerling, and J. I. Koivula, *Journal of Gemmology*, Vol. 23, No. 8, 1993, pp. 473–481.

Although the plastic simulant of opal called "Opalite" was first commercially available in the 1970s, it only now seems to be reaching the market in significant quantities. This new production includes doublets, triplets, and mosaic triplets, as well as solid Opalite. The new production does not differ from that described previously—except for the triplets, which may be difficult to distinguish from natural-opal triplets, and so are targeted specifically by this article.

Six triplets and two mosaic triplets of Opalite were examined. All had clear domes made of a material (probably glass) similar to that used for natural-opal triplets. Useful identifying characteristics of the Opalite triplets include the lack of matrix material in the opal-like layer, a greater-than-usual thickness of the clear cap, and the hot-point reaction of the wax-like base. In the mosaic triplets, the Opalite pieces did not phosphoresce, while their adhesive did—a reversal of what was found in a natural-opal mosaic triplet. Also, the Opalite mosaic consisted of triangular pieces, whereas the natural-opal mosaics are composed of irregularly shaped pieces. The authors warn gemologists that the materials used to manufacture triplets often vary, and thus other Opalite samples may differ significantly from the samples that they describe. They close with an additional warning to use great care in the identification of triplets, especially those in closed-back bezel settings. This article is exceptionally well illustrated with color macro- and micro-photographs. CMS

Unusual twinning in natural and synthetic amethyst. U. Henn, *Australian Gemmologist*, Vol. 18, No. 7, 1993, pp. 222–224.

Natural amethyst almost universally exhibits Brazil-law twinning, whereas hydrothermal synthetic amethyst is almost always untwinned. Therefore, gemologists typically separate synthetic and natural amethyst based on the presence or absence of twinning. After laying this background, the author proceeds to describe and illustrate three cases in which this general rule does not apply.

The first such material is natural amethyst from Pau d'Arco, Brazil. According to the author, these stones only rarely show polysynthetic twinning on the Brazil law. Instead, they generally display small areas of twinning with unusual zigzag or undulating structures. Other samples exhibit the twin boundary only in the area below the negative rhombohedron.

The other two exceptions to the general rule are synthetic amethysts. One of these, from Russia, exhibits strong color zoning and twinning structures very similar

to those seen in natural amethyst. The other synthetic amethyst, of Japanese manufacture, includes tiny metallic (copper?) platelets, with acute-angled twinned areas extending from the inclusions.

The author ends by cautioning readers that the above exceptions make the separation of natural from synthetic amethyst more difficult. He suggests that infrared spectroscopy be used as an additional test. RCK

The role of fashioning in effective gemstone substitutes. R. C. Kammerling and J. I. Koivula, *South African Gemmologist*, Vol. 7, No. 3, 1993, pp. 19–27.

This article lists materials used to create imitation rough and cut gem materials. Details that can help make these materials more effective imitations include color, transparency, and even simulated matrix glued to the surface for that "just mined" appearance. The morphology and texture of rough crystals can also be effectively imitated.

Also, the crystal morphology of the authentic gem generally dictates the final cut of both the real stone and its imitations. For example, because of the shape (long, thin) of green tourmaline crystals, long and thin emerald cuts are often popular. Therefore, suitably colored glass imitations of green tourmaline are often elongated emerald cuts. One indication of a possible deception might be a particularly expensive gem material that has been given an unusual cut. JEC

MISCELLANEOUS

Notes from the Gem and Pearl Testing Laboratory, Bahrain—3. A. Bubshait and N. Sturman, *Journal of Gemmology*, Vol. 24, No. 1, 1994, pp. 42–44.

Three notes on fillings in natural and synthetic rubies provide some important information for gemologists plagued with detecting this persistent problem, including the occurrence of color flashes similar to those seen in filled emeralds and diamonds. In addition, an unusual lot of pearls—submitted by Bahrain's Customs and Ports Directorate—is described. The lot included natural pearls, non-nucleated cultured pearls, and a few nucleated cultured pearls. Among these were some partially nacreous and completely non-nacreous specimens. X-ray fluorescence reactions were varied. Since the intent of the testing was to comply with Bahraini customs requirements that all incoming pearls be natural, this lot normally would have been returned to its source. However, circumstances were far from normal. These pearls were destined to be crushed and used for their "medicinal" properties—supposedly to help treat eye problems, cystitis, and impotency. Because the lot was not destined for the jewelry trade, customs okayed it and allowed it into the country (after visiting the importer and verifying that the pearls would indeed be crushed). CMS